FIRE IN THE RAINFOREST: FIRE HISTORY AND CARBON POOLS IN SOUTHWESTERN BORNEO'S TROPICAL RAINFOREST

by

LAUREN B. HENDRICKS

A DISSERTATION

Presented to the Department of Geography
and the Graduate School of the University of Oregon
in partial fulfillment of the requirements
for the degree of
Doctor of Philosophy

June 2020

DISSERTATION APPROVAL PAGE

Student: Lauren B. Hendricks

Title: Fire in the Rainforest: Fire History and Carbon Pools in Southwestern Borneo's Tropical Rainforest

This dissertation has been accepted and approved in partial fulfillment of the requirements for the Doctor of Philosophy degree in the Department of Geography by:

Daniel Gavin	Chairperson
Patrick Bartlein	Core Member
Lucas de Carvalho Ramos Silva	Core Member
Alison Carter	Institutional Representative

and

Kate Mondloch	Interim Vice Provost and Dean of the Graduate School

Original approval signatures are on file with the University of Oregon Graduate School.

Degree awarded June 2020

DISSERTATION ABSTRACT

Lauren B. Hendricks

Doctor of Philosophy

Department of Geography

June 2020

Title: Fire in the Rainforest: Fire History and Carbon Pools in Southwestern Borneo's Tropical Rainforest

Tropical rainforests are globally important resources for carbon storage as well as biodiversity. Despite high precipitation, fires now occur on an annual basis in Southeast Asia's forests. Fire in the rainforest is not totally unprecedented; many paleorecords show evidence of fire throughout the Holocene. Humans have been using fire in these environments for millennia, but some fires cannot be clearly attributed to human influence. Furthermore, we do not have a good understanding of the prevalence or spatial pattern of these fires earlier in the Holocene, nor how they have altered terrestrial carbon stocks. Here, I investigate the late Holocene fire history in a primary rainforest located in southwestern Borneo and its imprint in carbon pools.

This work begins with the task of understanding the pattern of fire through the last 3,200 years at Cabang Panti Research Station (CPRS; West Kalimantan, Indonesia). I use ^{14}C dating of soil charcoal and its relative abundance across forest types to assess the role that humans played in fire occurrence in this primary rainforest. Using a natural gradient of fire susceptibility, I find that fire activity across the site peaked ca. 1500 CE. This coincides with both regional drought and increased human pressure in Southeast Asia. I conclude that humans likely supplied ignitions, but drought allowed fire to spread throughout the study

area. In the third and fourth chapters I quantify soil carbon pools at the study site with a particular focus on the contribution of pyrogenic carbon (PyC). I show that a simple, inexpensive chemical oxidation method using only standard laboratory equipment and reagents consistently and accurately quantifies PyC in soil samples when the pyrogenic carbon is produced in fires >400°C. Using this method, I find that PyC makes up a non-negligible portion of carbon pools at Gunung Palung National Park (approximately 5%), and thus should be considered separately in future models of carbon stocks and cycling at the site due to its potential to persist for hundreds to thousands of years. This work expands our understanding of fire in tropical rainforest and the role humans have played throughout history.

This dissertation includes previously unpublished co-authored material.

CURRICULUM VITAE

NAME OF AUTHOR: Lauren B. Hendricks

GRADUATE AND UNDERGRADUATE SCHOOLS ATTENDED:

University of Oregon, Eugene
Thayer School of Engineering at Dartmouth College
Colby College

DEGREES AWARDED:

Doctor of Philosophy, Geography, 2020, University of Oregon
Master of Science, Environmental Studies, 2016, University of Oregon
Bachelor of Engineering, 2012, Thayer School of Engineering at Dartmouth College
Bachelor of Arts, Environmental Studies, 2011, Colby College

AREAS OF SPECIAL INTEREST:

Pyrogeography
Biogeography
Forest ecology
Human-environment interactions

PROFESSIONAL EXPERIENCE:

Graduate Employee, Department of Geography, Winter 2017, Winter 2018

Graduate Student Cartographer, Infographics Lab, Department of Geography, University of Oregon, 2016–2017

Graduate Employee Project Manager, Environmental Studies Program, University of Oregon, 2015–2016

Graduate Teaching Fellow, Environmental Studies Program, Fall 2014–Winter 2015

Analyst, Marstel-Day, LLC, 2012-2014

GRANTS, AWARDS, AND HONORS:

Dissertation Research Fellowship, University of Oregon College of Arts and Science, 2019-2020

Paleoenvironmental Change Specialty Group Student Poster Award (PhD Level Poster), American Association of Geographers Annual Meeting, 2019

Global Oregon Graduate Research Award, University of Oregon, 2018

Sandra Pritchard Mather Graduate Fellowship, University of Oregon Department of Geography, 2017

Best Panel, University of Oregon Graduate Research Forum, 2017

Magna cum Laude, Colby College, 2011

Phi Beta Kappa, member, 2011

PUBLICATIONS:

Peterson, M., **L. Hendricks**, G. Bailes, L. Pfeifer-Meister, P. Reed, S. Bridgham, B. Johnson, S. Robert, E. Waddle, H. Wroton, D. Doak, B. Roy, W. Morris. In press. Latitudinal gradients in population growth do not reflect demographic responses to climate. Ecological Applications.

Silva, L.C.R., R.S. Corrêa, J. L. Wright, B. Bomfim, **L. Hendricks**, D.G. Gavin, R.V. Santos, A.W. Muniz, G.C. Martins, A.C.V. Motta, J.Z. Barbosa, V.F. Melo, S.D. Young, M.R. Broadley, W.G. Teixeira. In press. A new hypothesis for the origin of Amazonian Dark Earths. Nature Communications.

ACKNOWLEDGMENTS

I would like to express my sincerest gratitude to everyone who has supported me and helped me through my graduate school journey. To my advisor, Dr. Dan Gavin, for the amazing opportunity to travel to and work in Borneo. To my Department of Geography committee members, Dr. Patrick Bartlein and Dr. Lucas Silva, for providing invaluable feedback and research support along the way. And to my fourth committee member, Dr. Alison Carter, for sharing an outside perspective on my findings.

Thanks to Professor Gusti Anshari and Universitas Tanjungpura for acting as my Indonesian counterpart for this research, and to both him and Monika Ruwaimana for their work on sample export. I would also like to thank Kergis Hiebert and Rose Nittler for their tireless work on sample analysis in the lab—I was fortunate to have two assistants who genuinely enjoy counting charcoal!—as well as Ardiansyah, Wawan Setiawan, Yon, and Monika Ruwaimana for their assistance with sample collection in the field. Thanks to Jamie Wright and Toby Maxwell for their assistance with troubleshooting temperamental instruments and running samples. And to my fellow graduate students, both within the Long-Term Environmental Change Research Group and without, for excellent comradery (and at times commiseration), and overall great community.

Finally, to my family and friends outside of academia: I couldn't have done it without your encouragement and support. Thank you for everything you do for me every day. Hikes, skiing, ultimate tournaments, dog sitting, and much more—it all means a lot!

This work was supported by National Science Foundation award number 1561099, the University of Oregon College of Arts and Sciences Dissertation Research Fellowship, the University of Oregon Department of Geography Sandra Pritchard Mather Graduate

Fellowship, the Global Oregon Graduate Research Award, and the University of Oregon Department of Geography Rippey Award. Additional thanks to the Gunung Palung National Park office (BTNGP)and the Cabang Panti Research Station, as well as the staff and researchers with Yayasan Palung and One Forest Project (especially Brodie Philp, Beth Barrow, and Terri Breeden), for facilitating this research. Finally, thank you to the Directorate of Natural Resource Conservation and Ecosystems (KSDAE) – Ministry of Environment and Forestry, the Indonesian Institute of Sciences (LIPI), and the Ministry of Research and Technology / National Research and Innovation Agency (RISTEK / BRIN) for their sponsorship and for granting permission to conduct research in Gunung Palung National Park.

TABLE OF CONTENTS

Chapter Page

LIST OF FIGURES

Figure Page

Figure Page

LIST OF TABLES

Table Page

CHAPTER I

INTRODUCTION

Tropical forests are globally recognized as critically important ecosystems. In addition to being home to incredible biodiversity—over half of all terrestrial plant and animal species—they are also important in regional and global climate patterns and biogeochemical cycling (Gaston 2000, Malhi et al. 2008, 2014, Lewis et al. 2015). Tropical forests are also a disproportionately important global store of carbon; though they make up approximately 51% of global forests by area, they store approximately 55% of global forest carbon (Pan et al. 2013). Humans have been interacting with and modifying tropical forest for millennia, through hunting—sometimes resulting in major extinction events—and extraction of other food resources, as well as more direct landscape management (Roberts et al. 2018). Although the scale of human impact on tropical forest has varied with space and time throughout history and is still the subject of much debate, it is indisputable that the rate of directly human-caused conversion of tropical forest to other habitat types has peaked in recent centuries (Malhi et al. 2014). Less than 50% of the world's tropical forests remain today (Brancalion et al. 2019). Despite considerable efforts at conservation at local and global scales (e.g., REDD+), tropical forests remain highly threatened ecosystems.

Humans directly and indirectly threaten tropical rainforests. Direct threats include large- and small-scale resource extraction such as logging and mining, as well as continued conversion of forest to agricultural and other land uses. Indirect threats are mostly consequences of anthropogenic climate change, such as rising global temperatures and changes in precipitation patterns. One of the most visible threats is increased fire, which is caused by humans both directly (e.g., increased ignitions) and indirectly (e.g., increased

forest fragmentation and edge area, which is more likely to burn; Cochrane and Laurance 2002, Langner et al. 2007, Hébert-Dufresne Laurent et al. 2018).

Massive fires across the three major tropical rainforest basins—the Amazon Basin, the Congo Basin, and Southeast Asia—have received considerable international attention in recent years. Headlines such as "The Amazon, Siberia, Indonesia: A World of Fire" and permutations of "Borneo is burning" have become common (Aldhous 2004, Pierre-Louis 2019). Because fire is typically rare in tropical rainforest on the scale of a human life, these large recent fires are often thought of as highly unusual events with major consequences. Fires in tropical forests have implications for (1) human health (e.g., poor air quality due to smoke); (2) wildlife, including critically endangered species (e.g., orangutans); and (3) the release of carbon stored in forest and peat into the atmosphere as carbon dioxide, a greenhouse gas (Harrison et al. 2009). On longer time scales, fire—and particularly, repeated fire—could have implications for forest resiliency; it may change forest structure beyond a point from which it can recover, as observed both on Borneo (Siegert et al. 2001) and in the Amazon (Cochrane et al. 1999). Modern fires are typically linked to the escape of intentionally set fire used to clear land in conjunction with strong droughts related to global climate patterns such as the El Niño-Southern Oscillation (Cochrane 2003, Hendon 2003, Chen et al. 2011, 2016, Wooster et al. 2012).

Despite common misconceptions among the public that fire in tropical rainforest is entirely unprecedented due to high moisture, multiple studies have found evidence of past fire throughout the Holocene in tropical rainforests of the Amazon Basin, Africa, and Southeast Asia (Goldammer and Seibert 1989, Kershaw et al. 1997, Carcaillet 2001, Cochrane 2003, Bowman et al. 2011, Hubau et al. 2012). However, our understanding of

fire in tropical forest is still limited; the frequency and intensity of these fires is not fully understood, and distinguishing between natural and human-caused fires can be challenging. Bowman et al. (2011) note that "[t]ropical rain forests rarely burn naturally because of the very low coincidence of lightning with climate conditions suitable to carry fire. Even if a fire is initiated, the high moisture content in fuels generally prevents propagation." Consequently, if evidence of fire in paleorecords—often charcoal in soil or sediment cores—is coincident in time and space with archaeological evidence of human presence, the fire is typically attributed to human ignition sources (Bowman et al. 2011). It is more difficult to determine if a fire was likely due to human or natural causes where archaeological evidence is sparse or lacking; one common strategy is to consider evidence and timing of fire events at the landscape scale, under the assumption that human caused fires are more localized than those due to climate events, and would thus be asynchronous across the landscape (Marlon et al. 2013, da Silva Carvalho et al. 2018).

Within the major tropical forest basins, Southeast Asia is particularly understudied. In this dissertation, I seek to improve our understanding of the historical patterns of fire in the tropical rainforest of Borneo and how it affects modern carbon storage in these forests. Borneo is within the "heart of the ever-wet rain forest" (Meister et al. 2012), with over 2,000 mm of precipitation annually. Yet, fire has been a frequent occurrence in recent decades, most often during strong El Niño events which manifest as drought in much of Southeast Asia. A better understanding of the role that fire played in tropical forest ecosystems will improve our understanding of the resilience of these forests to large-scale disturbances.

In Chapter II, this research reconstructs the history of fire events in the primary

rainforest at Cabang Panti Research Station (CPRS), located in Gunung Palung National Park (West Kalimantan, Indonesia; Figure 1.1). Determining if a fire detected in the historical record was human caused or due to natural phenomenon is particularly challenging in Borneo, where archaeological data is rare (Anshari et al. 2001, Vleminckx et al. 2014). I make use of a gradient of fire susceptibility across forest types at CPRS, wherein the forest types that are most likely to experience a fire caused by humans (e.g., swidden agriculture) are least likely to experience a naturally occurring fire and vice versa. Using 50 accelerator mass spectrometry ^{14}C dates ("radiocarbon dates") of charcoal collected from across the research area in conjunction charcoal abundance data, I examine how both events in human history and climate phenomena interact to create a history of fire over the last 3,200 years in this tropical rainforest.

Figure 1.1. Location of Cabang Panti Research Station.

This chapter includes unpublished material co-authored by Gusti Anshari and Dan Gavin.

Whether natural or anthropogenic in origin, fire results in the conversion of some above-ground, living carbon to pyrogenic carbon (PyC) products, such as charcoal, which enter the soil carbon pool. Relative to non-pyrogenic forms of soil carbon, PyC is resistant to decomposition and turnover times can be orders of magnitude higher (Schmidt and Noack 2000a, González-Pérez et al. 2004, Singh et al. 2012, Bird et al. 2015). PyC is also ubiquitous in soil profiles across the globe, and is estimated to make up, on average,

approximately 14% of total soil organic carbon (Reisser et al. 2016). However, our knowledge of the contribution of PyC to carbon pools across the globe is still limited, particularly in tropical soils. A number of different methods are used to quantify PyC; while some methods are straightforward and involve little specialized equipment or supplies, others are very expensive and not accessible to many researchers. While each method has its strengths and weaknesses, they often target slightly different portions of the PyC pool and thus are not interchangeable (Zimmerman and Mitra 2017).

Chapter III assesses a newer, simple and inexpensive chemical oxidation method for quantifying pyrogenic carbon—the Kurth, McKenzie, and DeLuca (KMD) method (Kurth et al. 2006)—with a particular focus on the role of formation temperature for PyC. I also compare the results of the KMD method with visual identification and isolation of charcoal sieved from soil, a traditional method for quantifying PyC. In Chapter IV, I return to CPRS and use the method evaluated in Chapter III to quantify carbon pools, with a particular focus on PyC, between seven tropical forest types as well as by depth in the soil profile.

As a body of work, this dissertation explores the role that fire has played in tropical rainforests in the late Holocene, and how this history of fire is still expressed in the soil. Understanding the history of fire better enables us to contextualize modern fire events and what their long-term consequences could be.

CHAPTER II

FIRE IN THE RAINFOREST: A 3,200 YEAR HISTORY OF FIRE IN TROPICAL RAINFORESTS OF GUNUNG PALUNG NATIONAL PARK, WEST KALIMANTAN, INDONESIA

This chapter is co-authored by myself, Gusti Anshari, and Dan Gavin. I was the primary contributor to the sample collection and analysis and did all the writing. Dan Gavin contributed substantially by designing the original sample collection plan, obtaining funding, and providing extensive feedback on analysis and data interpretation. Gusti Anshari acted as my Indonesian counterpart for my visa and provided invaluable assistance for sample export, as well as providing feedback on my final results.

1. **Introduction**

The beginning of the 21st century has seen multiple very large fire events in tropical rainforest across the world. These fires can be devastating to local and national economies, and cause health issues—particularly smoke inhalation—for local residents as well as those that live thousands of kilometers downwind of fires (Cochrane 2009, Koplitz et al. 2016). Large fires in tropical rainforest also can have major ecosystem impacts, ranging from direct effects such as wildlife and vegetation mortality to indirect effects such as disruption of evapotranspiration-rainfall feedback loops that help maintain regional climate (Cochrane 2009). While it remains to be seen how tropical rainforest communities will reassemble following these recent fire events, initial evidence suggests that, in the wake of an initial fire, rainforests become more susceptible to additional fire and can eventually transition to non-forest landcover types (Haberle et al. 2001, Cochrane 2003, Murphy and Bowman 2012). Tropical rainforests are also a major global carbon sink, and fire can release vast

amounts of carbon into the atmosphere (Van Der Werf et al. 2003, Brando et al. 2019). On the scale of a human life, these fires seem entirely unprecedented and have garnered substantial international attention while also spurring significant advances in the study of modern fire in tropical rainforest. Although it is now understood that the typically humid air and high-moisture soil and litter of tropical rainforest understories do not preclude the possibility of fire, the long-term history of fire in tropical rainforest remains poorly understood (Haberle et al. 2001, Cochrane 2009). The connection between humans and fire over past centuries and millennia is of particular interest, given that human are responsible for the vast majority of modern fires in tropical rainforest (Brando et al. 2019).

In intact everwet rainforest under non-drought (and in the case of seasonally wet rainforest, non-dry season) conditions, the many-layered canopy maintains fuel moisture levels high enough that even frequent lightning strikes rarely result in fire (Cochrane 2009). Even when a lightning strike does ignite a fire, it rarely leads to a major disturbance under normal conditions because of the high moisture under tropical rainforest canopy maintained via canopy-atmosphere decoupling and, ultimately, evapotranspiration "recycling" (Jarvis and McNaughton 1986, Eltahir and Bras 1996, Kumagai et al. 2004, Chapin et al. 2011, Dommain et al. 2015). Fires are most likely to occur near forest edges—where fuels exposed to direct solar radiation can become dry—but rarely penetrate into the core of intact forest (Cochrane and Laurance 2002, Langner et al. 2007). However, during extended periods of moisture stress, fuels can reach a critical threshold of dryness even away from edges and any ignition, whether natural[1] or anthropogenic, could result in a major fire (Brando et al. 2019). Drought alone does not lead to fire, but where ignitions are

[1] We define 'natural' fire as fire ignited by non-anthropogenic sources such as lightning, volcanic activity, and, in certain regions, persistently burning coal seams

present, fire is a very real possibility in rainforest.

Many tropical tree species—particularly those found in the wettest tropical rainforest—are poorly adapted to fire, lacking adaptions such as thick bark, resprouting, or serotiny common in fire-prone forests (Cochrane 2011, Keeley et al. 2011) and exhibit high mortality, leading to concern about the ability of tropical forests to recover following large fire events (Slik et al. 2010). In fact, the presence or absence of fire in a system can be a primary driver of savanna-forest thresholds in high precipitation tropical regions, as savanna and rainforest are alternative stable states driven by tree cover-fire feedbacks (Hoffmann et al. 2012, Murphy and Bowman 2012). However, this does not preclude the possibility that fire has had a role in tropical rainforests around the world throughout recent history. Paleorecords across the tropical rainforest basins of the world show that fire occurs in tropical rainforest with return intervals ranging from hundreds to thousands of years (Cochrane 2003).

Paleorecords rely on a multitude of proxies such as pollen, stable isotopes, and charcoal and are used to extend records of earth systems well beyond the range of written records. Charcoal, the most unambiguous evidence of paleo-fire compared to other biomarker methods, is produced by the incomplete combustion of wood and other organic matter during a fire and in soil can persist for thousands of years (Bird et al. 2015, Reisser et al. 2016). Charcoal can be radiocarbon dated using accelerator mass spectrometry (AMS) to obtain a relatively precise estimate of when a fire occurred, with the caveat that this date reflects when the wood stopped assimilating atmospheric carbon and this precedes the fire event by up to centuries in some forest types (Gavin 2001). However, in tropical rainforest where wood litter decays at a fast rate, this inbuilt-age unlikely to exceed

decades. While charcoal presence—particularly when paired with AMS or other dating methods—can be used to evaluate fire frequency, with abundance as a proxy for past fire activity, it is important to note that charcoal abundance may also be related to fire size, intensity, and severity (Whitlock and Larsen 2001, Conedera et al. 2009, Vleminckx et al. 2014, Iglesias et al. 2015). Subsequent fires can also consume existing charcoal, effectively erasing evidence of earlier fires and making abundance at best a rough indicator of relative fire activity across a study area (Conedera et al. 2009).

In tropical forest, presence of charcoal is often interpreted as evidence of human presence and activity (Kershaw et al. 1997, Bush et al. 2008), but without additional evidence it is not possible to determine from charcoal whether a fire was the result of human or natural ignition. In some cases it is possible to infer human influence on fire regimes when fires represented in the charcoal record correspond spatially and temporally to archaeological evidence, though climate-fire relationships must still be considered even in these cases (Haberle et al. 2001, Bowman et al. 2011). Where direct archaeological evidence is lacking, many studies rely on the relative timing of fire events at the landscape scale as an indicator of human influence, reasoning that natural fires related to climate events and other landscape scale factors would be somewhat synchronous, whereas human caused fires would exhibit greater temporal variation across the same landscape (Marlon et al. 2013). However, disentangling the effects of climate and humans on fire and fire regimes remains challenging.

The influence of humans on fire regimes in tropical rainforests is an area of active research and some controversy. In the everwet portions of the western Amazon Basin, humans were likely the primary source of ignitions through the late Holocene and natural

fires were rare (Bush et al. 2015). The seasonally wet forests of the central and eastern Amazon Basin also experienced fire in the middle and late Holocene, and periods of increased fire were associated with regional climate changes as well as human occupation (Bush et al. 2008, Goulart et al. 2017). Similarly, the middle and late Holocene history of fire in Central Africa's Congo Basin rainforest is associated with both increased human activity and drought, though Hubau et al. (2015) note that fires in the heart of this rainforest were more likely of natural origin. Others posit that humans have been the primary source of fire in tropical rainforest in much of central Africa, particularly in the late Holocene, and especially in areas with distinct seasonality (Tovar et al. 2014, Morin-Rivat et al. 2016). The third major area of everwet tropical rainforest, Southeast Asia, has also experienced fire throughout the Holocene (e.g., Goldammer and Seibert 1989, Kershaw et al. 1997, Haberle et al. 2001). As in the Amazon and Congo basins, fire in Southeast Asia has been tied to human activity (*sensu* Haberle et al. 2001, Carcaillet et al. 2002, Hunt and Premathilake 2012, Hunt et al. 2012, Cole et al. 2019), though it has been particularly difficult to disentangle human and natural fires due to both the very long history of human occupation and significant changes in vegetation since the Last Glacial Maximum (for discussion on vegetation change, see Heaney 1991, Hope et al. 2004, Bird et al. 2005, Wang et al. 2009, Cannon et al. 2009, Reeves et al. 2013). Paleofire on Borneo in particular is understudied, despite the great extent of rainforest (over 75% until the 1970s) and it being the location of multiple very large fire events in the last 40 years (Gaveau et al. 2014). While several other studies have found and dated charcoal in Borneo—for example, Goldammer and Seibert (1989) described evidence for repeated fires in lowland Dipterocarp rainforest in East Kalimantan (Indonesian Borneo) from the late Pleistocene to

the beginning of European colonial presence in Southeast Asia, and Hope et al. (2005) found that charcoal in East Kalimantan is more abundant in sites that are accessible from waterways—there have been no landscape-scale studies of spatial and temporal patterns of fire on Borneo.

To better understand the setting in which modern fires are occurring, we set out to study the long-term history of fire in a primary Dipterocarp rainforest (Gunung Palung National Park;), located in southwestern Borneo. We have two primary research questions. First, we ask: **what is the history and spatial patterning of fire in Gunung Palung National Park's tropical rainforests?** How long has it been since fire has occurred in primary rainforest, and did it occur more frequently in some forest types than others? Second, we ask: **what role did humans play in fire occurrence in Gunung Palung National Park's tropical rainforest?** This study takes advantage of a natural gradient of fire susceptibility and is one of the first efforts to disentangle the history of human vs. natural fire in island Southeast Asia, as well as one of only a few to explicitly aim to understand the history of fire in Southeast Asia's tropical rainforest.

2. Materials & Methods

2.1 Study Site

Cabang Panti Research Station (CPRS; 1.216°S 110.106°E) is located within Gunung Palung National Park, West Kalimantan, and has a total area of approximately 1500 hectares. Two steep parallel ridges running west to east rise from an elevation of approximately 40 m a.s.l. to broad peaks just short of 1000 m a.s.l. Two perennial streams flow through the study area; one of these flows through the valley between the two ridges. Seven forest types, which vary in their soil properties and elevation as well as forest

structure, phenology, and species composition, are located around CPRS (Table 1; Cannon and Leighton 2004, Paoli et al. 2006, 2007). All seven forest types contain large emergent trees in the Dipterocarp family, and figs (*Ficus* spp.) and woody climbers (i.e., lianas) are also common throughout (Cannon et al. 2007). Mean annual rainfall is approximately 4000 mm with the least rain in August and September (200 mm each); precipitation can be as little as 15 mm per month during strong El Niño events (e.g., 1997, 2015). Mean daily minimum and maximum temperature in lowland areas are 23.6°C and 27.6°C respectively, varying little through the year, with relative humidity typically >90%. Higher elevation areas experience cooler temperatures; during one year of data logging (2017) at approximately 1000 m a.s.l., temperatures ranged from 19.2°C (mean daily minimum) to 23.6°C (mean daily maximum). Relative humidity values as low as 70% were recorded in August and September of that year, though relative humidity was normally >90% throughout the remainder of the year.

No above-ground evidence of fire exists with the study site. However, we expect that the forest types differ in their susceptibility to fire from different ignition sources. We expected that fire from anthropogenic sources would be most common in alluvial bench and lowland sandstone forest types (locations easily accessible to humans via river) and least common in peat, upland granite, and montane forest types (more difficult to access). We also expected that fire from natural ignition sources would be most common in lowland granite and upland granite forest types (lower canopy height and thin well-drained soils), and least common in alluvial bench and freshwater swamp forest types (Figure 2.1).

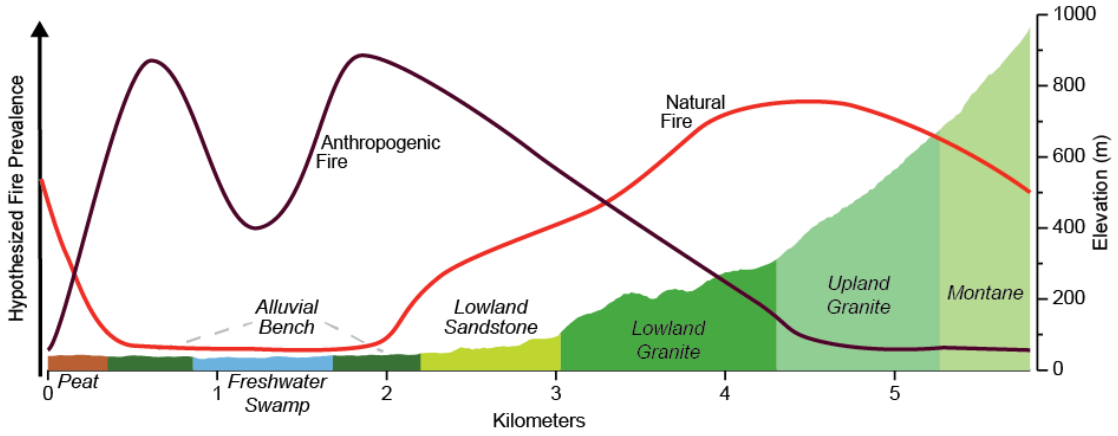

Figure 2.1. Forest types of Cabang Panti Research Station (West Kalimantan, Indonesia) with hypothesized fire prevalence.

2.2 Sample Collection and Analysis

We collected a total of 108 samples at 34 sites. Each sample consisted of two parallel soil cores from the surface of the A horizon to a depth of 20 centimeters, divided into 5-centimeter segments. Although this shallow sampling depth does limit the time period represented in the soil core, it also allowed us to sample a greater number of sites. Furthermore, initial fieldwork suggested that charcoal abundance sharply declines below 20 cm. We collected cores with an AMS® bulk density sampler (5-cm diameter). Due to the density of clay-rich soils, in many locations the sampler required forceful hitting with a mallet to reach 20-cm depths.

We used a spatially nested sampling scheme, with samples clustered in groups of three per site; each sample was approximately 20 meters from the others within the group and sites were spaced approximately 200 meters from each other (Table 2.1). We aimed for six sites per forest type. In the freshwater swamp, consisting of frequently-flooded hollows and soils on hummocks above flood level, we paired sampling of inundated areas and hummocks, with three sites within each (six samples per group). In the other six forest types, we located the sampling sites within small hollows or locally level areas as much as

possible to increase the likelihood that organic matter and charcoal in each core was produced and retained locally (*sensu* Ohlson and Tryterud 2000), in light of the tendency of organic matter and charcoal to be eroded downhill (Abney and Berhe 2018).

The two cores per sample were processed using different methods. One core was wet-sieved (2 mm) after soaking each segment in a solution of 10% sodium pyrophosphate ($Na_4P_2O_7$) to disperse colloids. We identified, isolated, counted, and weighed all charcoal fragments greater than 2 mm. We used the other core to calculate oven-dry bulk density for each segment following Kellogg Soil Survey Laboratory Method 3B6a, with soils dried at approximately 90°C in a liquid propane gas drying oven for 36 hours in the field (Soil Survey Staff 2014). After drying, we removed all other material (roots, rocks, etc.) >2 mm and soil mass and volume were adjusted to account for this material when calculating bulk density. While removing material >2 mm to calculate bulk density, we also identified and collected charcoal fragments >2 mm to increase the amount of charcoal available for radiocarbon dating. We expressed charcoal mass as a fraction of soil mass (mg/g) in each 5-cm core segment and as the mean charcoal mass per soil mass for each 20-cm core sample. To assess the mass of charcoal >2 mm on a per-site basis, we also calculated the mean amount of charcoal in each set of samples within a site.

We used three spatial groupings to compare charcoal abundance over the study area: seven forest types (described in Table 2.1; Figure 2.2), two forest type groups (Table 2.1), and three spatial zones within the study area (Figure 2.2). Due to the differences in soil type and the possibility for charcoal fragments to be translocated by water movement, we excluded all inundated forest sites (freshwater swamp and peat forest) from direct comparison with other groupings (including within spatial zones). The forest type groups

Table 2.1. Description of forest types and soils, number of sites and samples within each forest type, correspondence between forest type and forest type group, as well as distribution of radiocarbon dates between habitat types both before and after duplicate removal was performed. Note that modern dates are excluded from these counts of radiocarbon dates. For detailed information on forest composition and structure, see Cannon and Leighton 2004, Paoli et al. 2006, Cannon et al. 2007. Tree density data from Cannon et al. 2007.

Forest Type	**Basic Soil Description[1]**	**Forest Type Description**	**Trees >60 cm DBH (number per ha^2)**	**Elevation**	**Number of Sites**	**Number of Samples (Total)**	**Number of 14C Dates**	**Number of 14C Dates after Duplicate Removal**	**Forest Type Group**
Peat	Varying depths of organic matter overlying coarse sand; nutrient poor	. Lianas/woody climbers very common.	9.6	5-10 m	3	9	1	1	Inundated
Freshwater Swamp	Poorly drained; seasonally flooded; gleyic soils; nutrient rich	Lianas/woody climbers very common.	14.2	5-10 m	3	15	3	3	
Alluvial Bench	Recently deposited from upstream sources; well-drained; frequently flooded; mixed sandstone and granite parent material; nutrient rich	Very large lianas/woody climbers common. Low species richness and diversity.	16.2	5-50 m	6	18	16	12	Lowland
Lowland Sandstone	Well drained; sandstone parent material with high clay content	Intermediate species richness and diversity.	22.8	20-200 m	6	18	8	7	
Lowland Granite	Well-drained; granite parent material	Low density of woody climbers. Highest species richness and diversity.	22	200-400 m	6	18	9	9	Upland
Upland Granite	Well-drained; granite parent material	Low density of woody climbers. Highest species richness and diversity.	12.4	350-800 m	5	15	3	3	
Montane	Granite parent material	Few to no figs or woody climbers.	3.4	750-1100 m	5	15	2	2	
	TOTAL				34	108	42	37	

were based upon soil type and drainage: upland forest vs. lowland forest (Table 2.1). The grouping by zone was designed to capture differences in fire history between the major ridge systems ("north" and "south") which extend from lowland sandstone through montane forest types (Figure 2.2) and non-ridge (alluvial bench) sites. All sets of spatial groups were assessed for significant differences at both the site (sample means) and the sample level. For all tests of significant difference, we used site and sample means rather than individual segment values. For the purposes of comparing between spatial groupings we assumed that all charcoal was formed where we found it.

To compare the amount of charcoal between forest types, we used a cube root transformation to better meet the assumptions of normality and equal variance for analysis of variance. However, there were still substantial violations of these assumptions, so we used the *boot* package (Canty and Ripley 2020) in R (v 3.6.1; R Core Team 2019) to perform a randomization procedure with 5000 simulations to compare the F-ratio of the data to a distribution of F-ratios created by resampling the data. Where the null hypothesis that group means of charcoal mass were the same was rejected, we then performed post-hoc multiple comparisons via randomization (5000 simulations) and the Holm correction on the resulting p-values to control for the family-wise error rate (Holm 1979). We also used the same randomization procedure to compare the amount of charcoal between peat and freshwater swamp sites, as well as between frequently-flooded hollows and hummocks within freshwater swamp sites.

We selected 50 single-piece charcoal fragments to submit for radiocarbon dating at the National Ocean Sciences Accelerator Mass Spectrometry (NOSAMS) facility at Woods Hole Oceanographic Institution, which were submitted in four batches. One of the

fragments was found just beyond the bottom of the core, approximately 22 cm below the surface of the A horizon (Appendix Table 2.1). The remaining 49 fragments were found within a core.

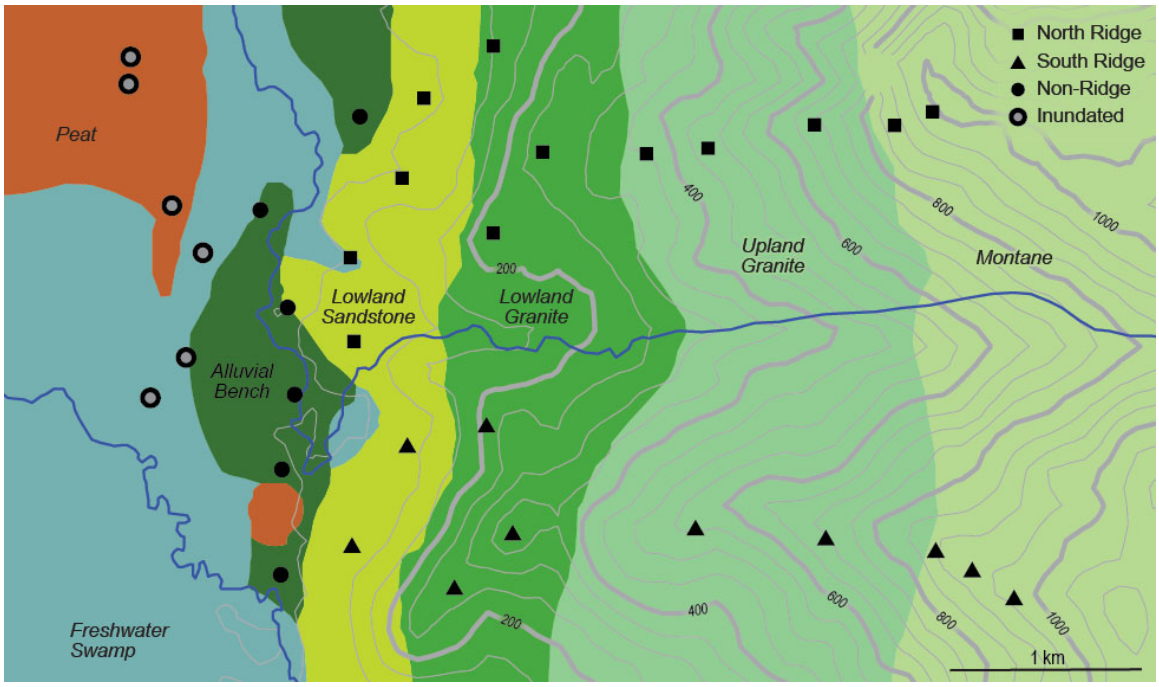

Figure 2.2. Location of sites, with both forest type and zone definitions shown. Inundated sites are not directly compared with any other groupings within these analyses.

We used a warm acid-base-acid rinse procedure to prepare the samples for radiocarbon dating. We selected fragments that had characteristics typical of wood charcoal (black, cubic, reflective), though our criteria for selection became more stringent (discernible wood structure) in later submissions as we received results from earlier batches and determined that some morphologies were likely not wood. For example, we encountered several very black pieces with larger transverse holes that dated modern (post-1950); we hypothesize that they may be formed by insects (Appendix Figure 2.1). The presence of hornblende, a group of minerals found in igneous rock that can appear similar to charcoal, also made manual identification difficult. These 50 fragments were divided between 26 sites, as we were unable to identify a suitable piece for submission at eight sites

(three montane, one upland granite, one lowland sandstone, one alluvial bench, and two peat sites). Of the eight sites with no material submitted for dating, seven had very little charcoal >2 mm (median charcoal mass of 0 mg per g soil and mean charcoal masses ranging from 0 to 0.169 mg per g soil). The remaining site had a moderate amount of charcoal, but initial cleaning with warm KOH caused the fragments to break apart (suggesting herbaceous material); after cleaning, no single fragment was suitable for submission. One date was removed from the analysis due to a very large error estimate, likely due to low carbon concentration. Nine fragments at eight sites dated as modern from the first two batches; upon re-examination of photos of all dated fragments, we determined that seven of the fragments that dated modern had questionable morphology (wood-cell structure not apparent) and were actually not charcoal (see Appendix Figure 2.1) so were excluded from further analysis. This resulted in 42 acceptable dates among 24 of 34 sites sampled. Four of these dates were from inundated sites, so were not included in the analyses described below.

We calibrated pre-modern (i.e., pre-1950) radiocarbon dates in R (version 3.6.1; R Core Team 2019) with the package *rcarbon* (version 1.2.0) using IntCal13 (Hogg et al. 2013, Reimer et al. 2013, Bevan and Crema 2018), and all post-modern dates with OxCal online (version 4.3) using the SH Zone 3 bomb radiocarbon calibration curve (Hua et al. 2013). Five sites had multiple dates within 100 uncalibrated radiocarbon years of each other; given the possibility that dates of similar age within a site could represent the same fire event due to the "inherited" or inbuilt age of wood at the time of fire, we only retained the youngest of the dates where multiple dates were within 50 years of each other. We chose to use a cutoff age of 50 radiocarbon years (rather than 100, as used in Gavin et al.

2020 based on the distribution of age-differences of dates and the observation that dead wood decays quickly in rainforest settings. Using this criterion, we removed five dates from our analyses (resulting n = 33; Table 2.1). We also analyzed time-since-fire (TSF) by considering only the most recent date from each dated site, excluding the two sites where dated charcoal was determined to be modern (n = 20).

In addition to analyses of all sites within our study area, we repeated all radiocarbon data analyses with two types of spatial groupings, with the same definitions as in the charcoal abundance data analysis: forest type group (Table 2.1) and zone (Figure 2.2). Again, we excluded all peat and freshwater swamp forest type sites from this analysis. We did not perform any quantitative analyses by forest type due to small sample size for some types.

We created summed probability distributions (SPDs) to model fire activity over time using the spd function of *rcarbon* (Bevan and Crema 2018). While SPDs are also common in paleoecological research (see Gavin et al. 2020 for a recent example), here we specifically draw upon the literature and framework of archaeology, where the use of SPDs has been applied since the late 1980s when Rick (1987) pioneered the use of "dates as data," with the assumption that abundance of dateable artifacts is correlated with human occupation and population growth. In our interpretation of SPDs, we substitute fire activity for human occupation. As the shape of the radiocarbon calibration curve affects SPDs, we used a 200-year rolling mean to decrease the possibility of over-interpreting small-scale fluctuations resulting from idiosyncrasies in the calibration curve (Bamforth and Grund 2012, Timpson et al. 2014). Based on the recommendation of Weninger et al. (2015) we assessed both normalized (ensuring the calibrated probability distribution sums to 1) and

unnormalized calibrations; ultimately we used unnormalized calibrations in the creation of our SPDs to avoid artificial spikes created by steep portions of the calibration curve (also see Bevan et al. (2017) for greater discussion of calibration normalization). While some authors have suggested that a minimum of 500 radiocarbon dates is needed for reliably accurate SPDs, these assessments are based on relatively large laboratory error (e.g., 100+ years), and this method has been found to be robust to small sample sizes (Williams 2012, Broughton and Weitzel 2018). We created SPDs for both the full set of radiocarbon dates (after potential duplicate removal) and for site-level TSF.

To quantitatively evaluate our SPDs of TSF, we compared each observed SPD with a theoretical null model based on the methods described in Shennan et al. (2013) and modified to model fire history as a TSF distribution. Their method to rigorously assess whether an observed SPD trend is significantly different than a null model of no change has been used to assess population growth by Timpson et al. (2014), Crema et al. (2016), Broughton and Weitzel (2018) and others using logistic and exponential null models. For TSF, we used a negative exponential null model. Our approach models fire as a Poisson random process, assuming that the probability of burning in any given year is constant over both time and space. We compared the distribution of the observed time-since-fire distribution against a null model of spatially and temporally homogeneous fire. Deviations from the null model were then identified as periods of higher or lower fire activity than expected by chance.

To create our negative exponential null model, we first calculated the hazard of burning (the probability of a given point burning in any given year), λ, using a maximum likelihood method following Reed et al. (1998), assuming our stratified random sample

represents the entire CPRS landscape. Using the youngest median calibrated age for each site (as calculated by *rcarbon*'s calibrate function using IntCal13) as the time since fire, we modeled the empirical age distribution as a negative exponential of the form $A(t) = e^{-\lambda t}$ and calculated the maximum likelihood value of the parameter λ using the fitdist function from the R package *fitdistrplus* (version 1.1-1; Delignette-Muller and Dutang 2015). However, this method suffers from the "missing tail" problem (Finney 1995) in that we don't have information on time-since-fire for ten sites where we do not have a radiocarbon date. Sites with no charcoal sufficient for radiocarbon may have a TSF longer than the oldest dates at our site (>2500 years). Therefore, we also calculated the hazard of burning with a right-censored dataset, where sites without a radiocarbon date are included in the model by defining the upper known bound of the dataset—a maximum age for which dates are included—as 2500 years before present (BP; 1950), which is approximately 1.5 times older than the oldest time-since-fire. Sites without a radiocarbon date are included as being older than the defined upper bound. We then calculated the maximum-likelihood value of the parameter λ for the censored distribution using the fitdistcens function of *fitdistrplus*. We refer to this method as "censored" and the previous method as "non-censored." We report the inverse of the hazard of burning, often termed the fire cycle, which can be interpreted as the mean expected fire return interval under spatiotemporal homogeneity, calculated with both censored and non-censored datasets. The choice of upper bound is not arbitrary; older upper bounds result in monotonically increasingly smaller λ values (and thus longer fire cycle values). We chose to use an upper bound of 2500 years BP, as very few of our dated charcoal pieces were older than 2500 calibrated years BP; this indicates that macrocharcoal may become highly degraded within the soil beyond that age at most sites (Appendix

Figure 2.2).

We used the fitted value for λ to simulate a set of TSF ages for the number of sites in the subset of interest. We then uncalibrated the ages using *rcarbon's* uncalibrate function (which generates a single randomized uncalibrated age), assigned a randomly generated error between 5 and 70 years for each uncalibrated date, and recalibrated the dates using the error and IntCal13 to make a SPD using *rcarbon*'s spd function. We repeated this simulation 1000 times and for each year calculated the envelope containing 95% of the simulations. Finally, we compared the observed SPD with the 95% critical envelope of the simulations; time periods where the observed SPD is outside of this envelope represent locally significant deviations from the null model. We only report deviations of 50 years or longer to avoid erroneously assigning significance to deviations that are artifacts of the calibration curve or the randomization procedure. To assess the overall significance of deviations from the null model, we calculated a global p-value by comparing the area of the observed SPD that is outside of the 95% critical envelope with the area of every simulated SPD that is outside of the 95% critical envelope; the p-value is the proportion of simulated SPDs with more area outside of the critical envelope when compared to the area of the observed SPD outside of the critical envelope. We compared the TSF distribution for all sites against the null model, and also repeated the process for each grouping by forest type and by spatial zone (as described for the charcoal abundance tests) using the fitted value of λ calculated for each grouping, using both the censored and non-censored methods.

We also quantitatively compared fire activity between spatial groupings by comparing the area of overlap of two SPDs with a randomization method. We randomly shuffled the radiocarbon dates between the spatial groups (without replacement and

keeping the same number of dates per group), generated new SPDs for each pseudo-group, and calculated the area of overlap; this was repeated 3000 times and the observed area of overlap was compared to the distribution of areas of overlap from the simulations. To avoid introducing biases due to uneven distribution of radiocarbon dates between groups, these SPDs were normalized.

3. Results

3.1 Charcoal Abundance

Charcoal >2 mm is nearly ubiquitous at CPRS, with only one of 34 sites having no charcoal (Figure 2.3). However, we acknowledge that our mass estimates for charcoal >2 mm may overestimate the amount of charcoal in this size class, as we could not obtain a date at seven sites where charcoal samples did not meet identification criteria.

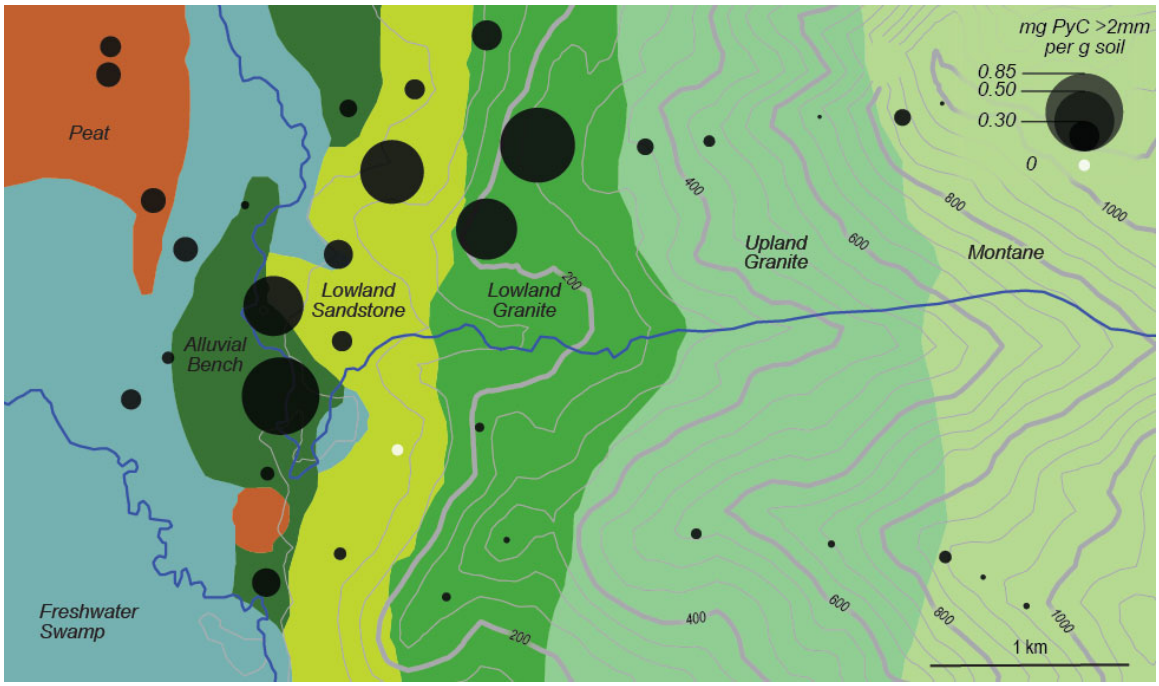

Figure 2.3. Mean mass of charcoal >2 mm per site at Cabang Panti Research Station. Differences between forest types are not significant.

At the site level, differences in mean charcoal abundance are not significant for any of the spatial groupings. Of 108 samples, 23 have no charcoal >2 mm. On a per sample

basis, there are significant differences between the mass of charcoal >2 mm per gram of soil in alluvial bench and montane forest types and alluvial bench and upland granite (Figure 2.4a; p = 0.007 and p = 0.031, respectively). However, no other pairs of forest types are significantly different. When forest types are pooled into lowland and upland forest groups, the lowland forest group has significantly more charcoal than the upland group (p = 0.003; Figure 2.4b). Differences are also significant by zone, with the south ridge having significantly less charcoal compared to both the north ridge sites (p = 0.005) and non-ridge sites (p = 0.001), though the north ridge sites are not significantly different than non-ridge sites (Figure 2.4c).

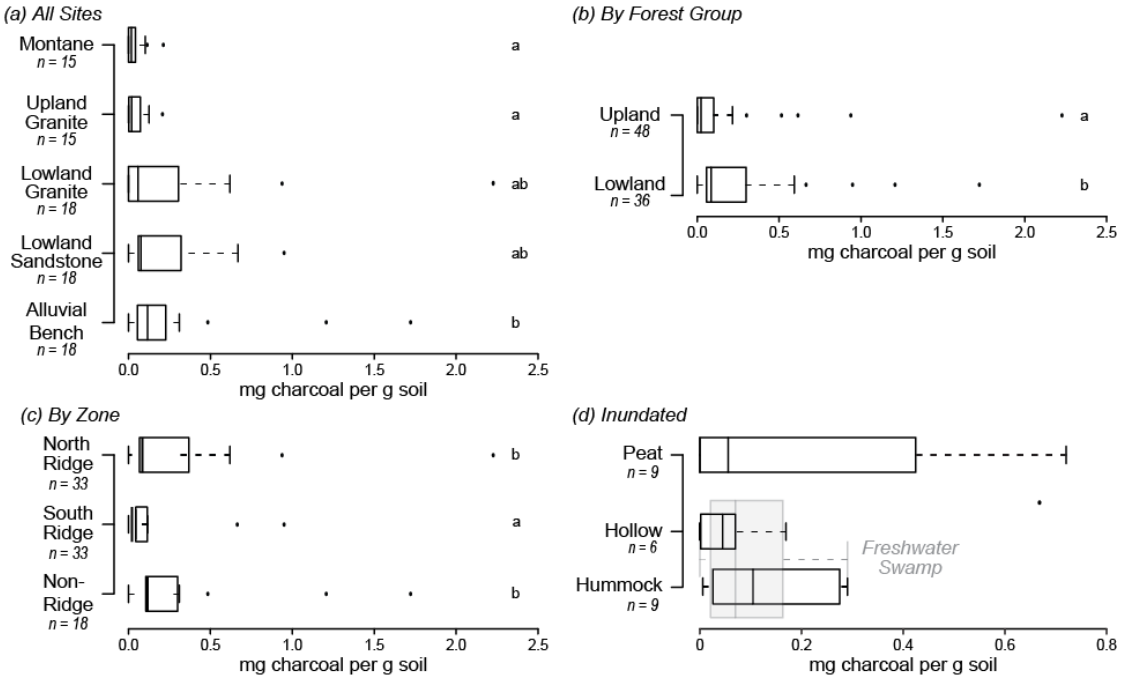

Figure 2.4. Amount of charcoal >2 mm per sample at Cabang Panti Research Station by (a) forest type; (b) forest group (see Table 2.1 for definitions); (c) spatial zone; and (d) inundated site type. Letters indicate significant differences from post-hoc multiple comparisons via randomization (Holm correction).

There are no significant differences between the two inundated forest types (freshwater swamp and peat forests) on either a per site or a per sample basis. Furthermore, there are no significant differences in charcoal abundance between hummocks and

frequently flooded hollow sites within freshwater swamp sites, or between hummocks, frequently flooded hollows, and peat forest sites.

3.2 Fire History

In total, 40 pieces of charcoal dated before 1950 and two dated after 1950. Both post-1950 fragments were from inundated sites; one fragment from a peat site calibrated to 1976 CE, and a fragment from a freshwater swamp site calibrated to 2004 CE. Four sites exhibited age reversals, where a charcoal fragment from deeper in the soil profile was younger than a charcoal fragment from closer to the surface; at three of these sites the age reversals were within the same core. However, we were only able to date multiple pieces for 13 sites, so we cannot assess charcoal mixing dynamics across the site. One date from a lowland granite site was substantially older than any other piece found at CPRS, with a 95% calibrated age range of 12,535–12,720 calibrated years BP (Appendix Figure 2.3). Due to its age, we have excluded it from the remaining analyses to better assess variability at a finer scale. Five additional dates were excluded because they were within 50 radiocarbon years of another younger date at the same site.

There is a broad peak in fire activity around 1450 CE spanning 1400-1550 CE, as well as a few smaller peaks around 700 CE, 50 CE, and 1050 BCE (Figure 2.5a). The peak around 1450 CE is also present when lowland or upland sites are considered separately, though its exact location and extent varies somewhat (Figure 2.5b). Although the oldest piece of charcoal found in the study area was in an upland forest type, the majority of the older pieces were located in lowland forest types, and this is reflected in fire activity continuing from around 450 CE to around 1650 CE as well as 550 BCE to 350 CE in lowland forest types (Figure 2.5b). In upland sites, there is one older date around 70 CE but

all other fire activity is within the last 750 years.

Similarly, when individual SPDs are created based on zone, the peak around 1450 CE is present on both the north and south ridge as well as in non-ridge sites, though its relative magnitude is similar to other peaks in non-ridge sites (Figure 2.5c). The south ridge sites also exhibit an additional peak in activity around 1850 CE which is not present or as prominent in other groupings. Excepting the oldest piece, the record of fire activity is much shorter on the south ridge with the oldest fire period being no older than 950 CE. Non-ridge sites were the only sites to see fire activity between 1550 BCE and 50 BCE.

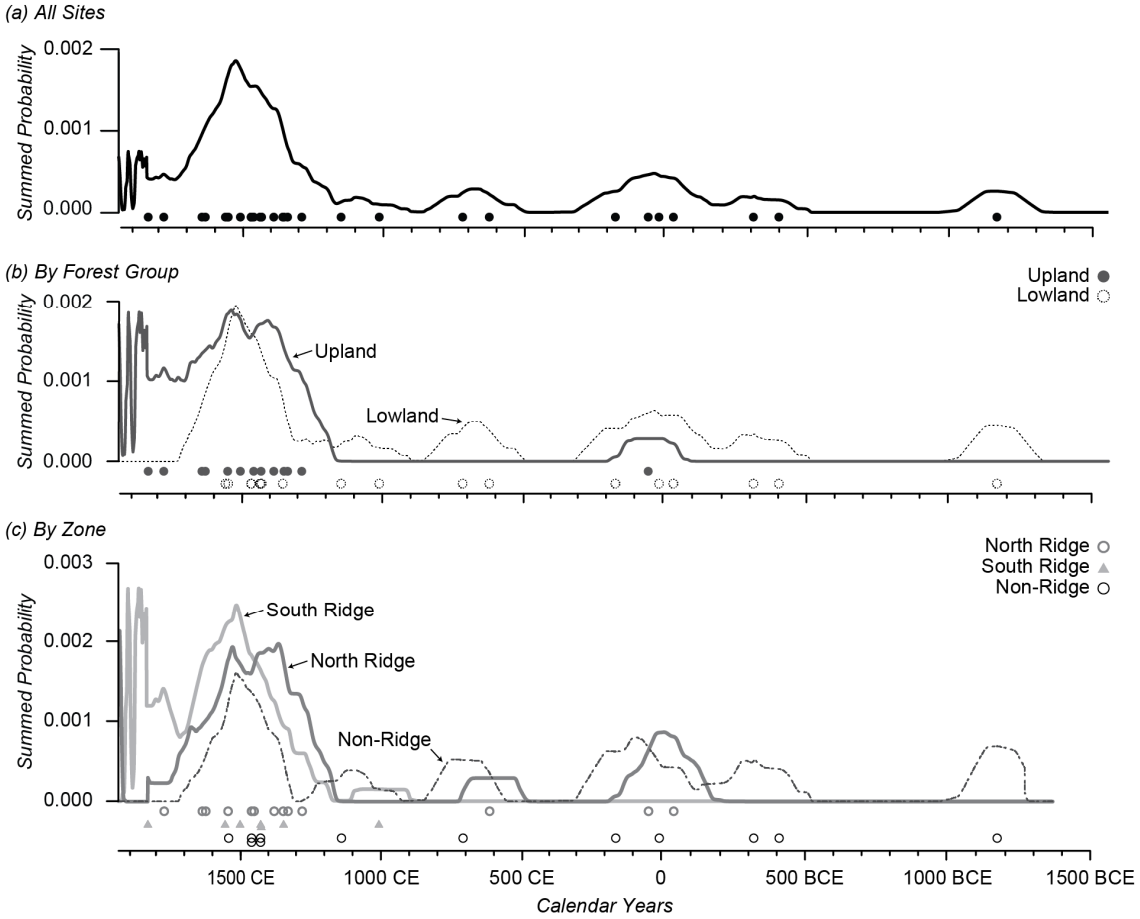

Figure 2.5. Summed probability distribution of (a) 32 radiocarbon dates from 5 forest types at CPRS (excluding inundated sites and a single upland date over 12,000 years old); (b) 19 radiocarbon dates from 10 lowland sites and 14 radiocarbon dates from 10 upland sites; and (c) 13 radiocarbon dates from 10 north ridge sites, 8 radiocarbon dates from 5 south ridge sites, and 12 radiocarbon dates from 5 non-ridge sites at CPRS. Solid lines represent each SPD smoothed with a 200-year rolling average and dots/triangles at the bottom of the figure represent the median calibrated radiocarbon age for each date used to create the SPD. With all SPDs, unevenness is due to the shape of the underlying calibration curve.

The fire cycle (1/λ) for the entire research area—excluding inundated portions—is 1590 years when sites without dated charcoal fragments are modeled as censored data (older than 550 BCE; Table 2.2). When those sites are excluded (non-censored method), the fire cycle is 590 years. As expected, fire cycles calculated with the censored method are longer than fire cycles calculated with the non-censored method, though there is substantial overlap in the confidence intervals from the two methods for lowland, non-ridge, and north ridge sites (Figure 2.6). Fire cycle estimates calculated with the censored method are also sensitive to the number of sites without charcoal; when more than two sites are modeled as censored data, there is no overlap in confidence intervals from the two methods for that group. It is important to note that all fire cycle estimates reported here were used primarily for development of a null model of fire activity and not for comparison of fire regimes, as we do not expect the assumptions of the fire cycle method to apply to our study site (e.g., ignitions are not distributed randomly through the study area).

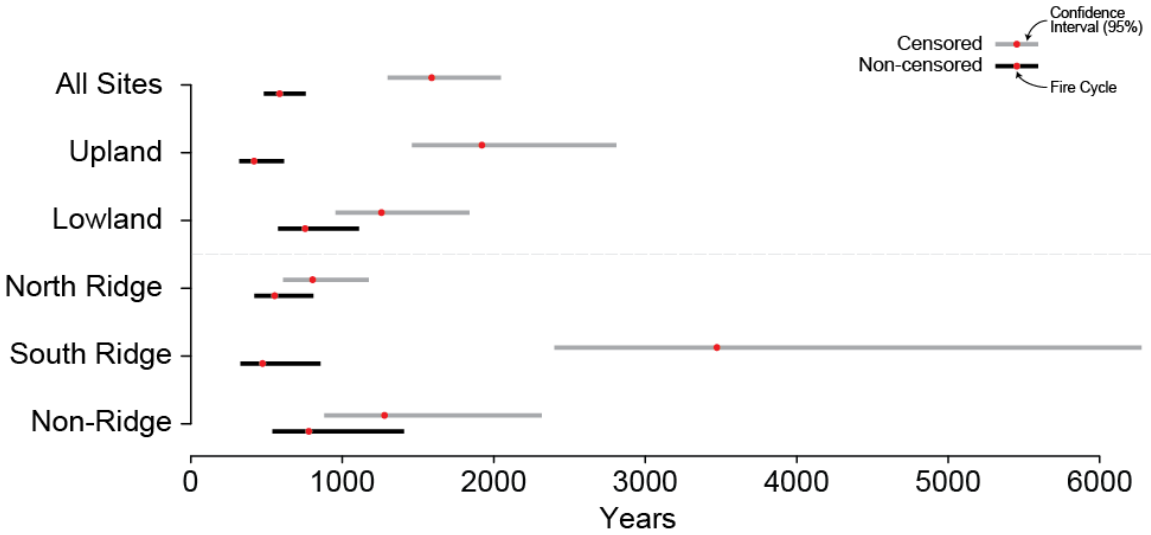

Figure 2.6. Fire cycle (inverse of hazard of burning) and confidence intervals for all spatial groupings. The fire cycle is shown in red, with the confidence interval shown in grey (censored method) and black (non-censored method). For confidence interval boundaries, see Appendix Table 2.2.

Table 2.2. Fire cycle (inverse of hazard of burning) and global p-value for comparison of the observed SPD to simulations of the negative exponential null model for different spatial groupings of sites. We excluded inundated sites (freshwater swamp and peat) in the analysis. In the censored version, the number of sites includes sites that had no radiocarbon dates. * indicates a significant result at a significance level of 0.05.

	Non-censored			Censored		
	Number of Sites	Fire Cycle Length (years)	Global p-value	Number of Sites	Fire Cycle Length (years)	Global p-value
All Sites	20	590	<< 0.001*	28	1590	<< 0.001*
Upland	10	421	0.108	16	1922	0.002*
Lowland	10	759	0.038*	12	1258	<< 0.001*
North Ridge	10	553	0.009*	11	803	0.008*
South Ridge	5	474	0.999	11	3473	<< 0.001*
Non-Ridge	5	779	0.343	6	1279	0.258

Despite the differences in fire cycle length, overall fire activity at CPRS is strongly significantly different than a negative exponential null model for time-since-fire regardless of the method used to calculate hazard of burning to generate the null model ($p << 0.001$; Table 2.2). The peak in activity around 1450 CE present in SPDs created using the full complement of radiocarbon dates (Figure 2.5a) is also present when only the most recent dates at each site (TSF) are considered, and it is a positive significant local deviation from the null model (Figure 2.7).

For all other spatial groupings, results are consistent between fire cycle method where there is overlap between confidence intervals for censored and non-censored estimates of fire cycle. Where there is no overlap in the confidence intervals (upland forest group and south ridge zone), the observed fire history is significantly different from a null model created with fire cycle estimates from the censored method but not significantly different from a null model created with fire cycle estimates from the non-censored method. In the case of south ridge sites—where the censored fire cycle estimate is over seven times longer than the non-censored estimate—the censored model is strongly

significant ($p << 0.001$) and the non-censored method is not significant ($p = 0.99$), though this is likely an artifact of the different sample size. With the censored method, the observed SPDs for all spatial groupings except non-ridge sites are significantly different than a null model. With null models based on uncensored fire cycle estimates, only one of each spatial grouping has an observed SPD that is significantly different from the null model: lowland sites (forest type groups) and north ridge sites (zones).

All groupings of sites exhibit around 1450 CE a locally significant positive deviation from a null model created with a censored fire cycle estimate, though the time period of positive deviation extends much later in time (to 1899 CE) for sites on the south ridge when compared to other spatial groupings (Figure 2.8). In general, the non-censored method produces similar results, with shorter locally significant positive deviations around 1450 CE for all spatial groupings except for south ridge sites, which have no locally significant deviations with the non-censored method (though the small number of south ridge sites with TSF estimates decreases the power of this analysis). With the non-censored method, a few spatial groupings (all sites, lowland forest group, and north ridge zone) also exhibit locally significant negative deviations from the null model within the last 200 years. Also of note is that non-ridge sites have a locally significant positive deviation around 150 CE. However, despite the differences in locally significant deviations from the null model, pairwise comparison of the overall difference in SPDs for TSF did not result in significant differences for any spatial groupings.

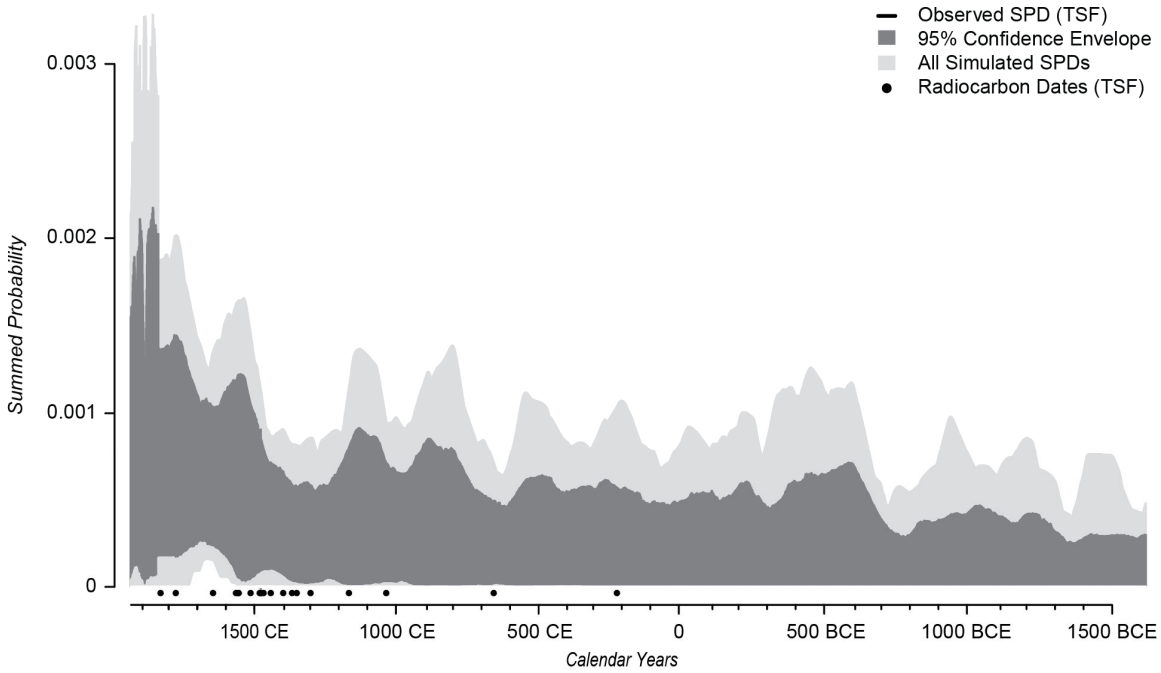

Figure 2.7. Summed probability distribution for observed time-since-fire from radiocarbon dates from 20 CPRS sites (black line) and 1000 SPDs for simulated data generated using the hazard of burning calculated for the observed data (censored method), with all SPDs reported in calendar years. The dark grey band indicates the 95% confidence envelope of the simulated SPDs, and the light grey bands indicate the maximum and minimum probability of all simulated SPDs for each year. Periods where the observed SPD is outside of the 95% confidence interval are locally significant deviations (also see Figure 2.8). Black dots at the bottom of the figure represent the median calibrated radiocarbon age for each date used to create the observed SPD, reported in calendar years.

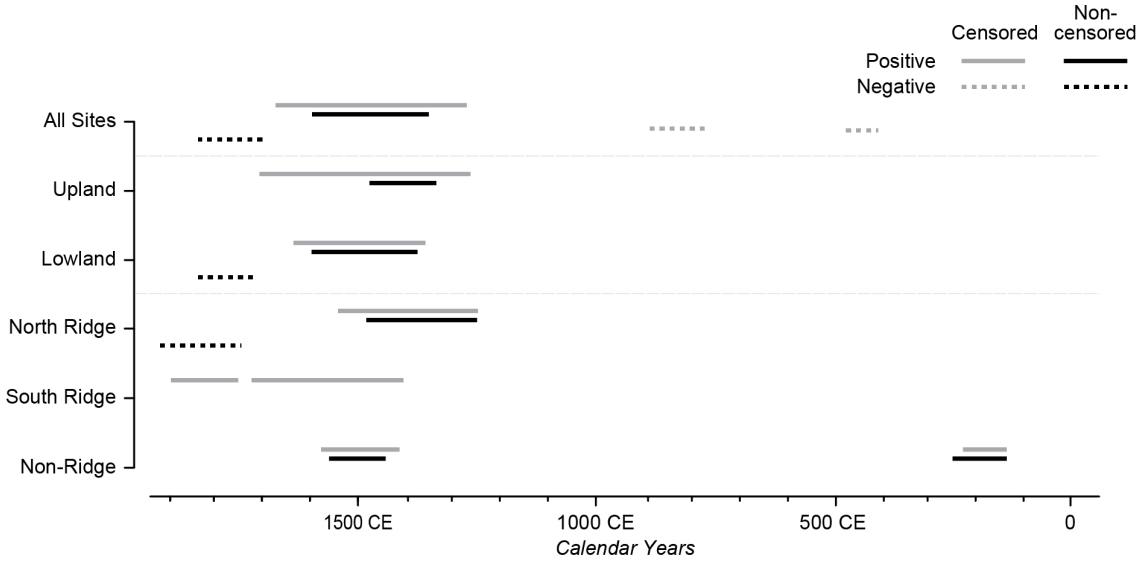

Figure 2.8. Time periods of locally significant positive deviation for different spatial groupings (forest type and spatial zone) of observed and simulated SPDs of TSF. Results from the censored method are shown in grey and results from the non-censored method shown in black; solid lines indicate positive deviations and dashed lines indicate negative deviations. See Appendix Table 2.2 for time periods of locally significant deviation.

4. Discussion

We found charcoal at 33 of 34 sites—including 24 sites with dateable single fragments—indicating that fire was prevalent in the past in this primary rainforest dominated by large Dipterocarp trees. The prevalence of charcoal agrees with evidence that fire occurred in other Dipterocarp dominated rainforest throughout the Holocene at sites across Borneo (Goldammer and Seibert 1989, Anshari et al. 2001, Hope et al. 2005, Hunt and Prematilake 2012).

The amount of charcoal in lowland sites is significantly higher than upland sites due to large quantities of charcoal in alluvial bench sites and low quantities of charcoal in montane and upland granite sites (Figure 2.4). While it is possible that the larger amount of charcoal in lowland areas is at least partially due to transportation and subsequent deposition of charcoal from upland to lowland areas by erosion (e.g., overland flow; Wondzell and King 2003, Rumpel et al. 2006, 2009, Abney and Berhe 2018), this mechanism does not explain the significant differences in charcoal quantities between the two prominent ridges in the study area, or the lack of difference between the north ridge and non-ridge areas. If fire activity were the same across the study region and erosion was the dominant mechanism driving the distribution of charcoal, we would expect there to be less charcoal in steeper areas—where there is more erosion and charcoal is transported from—and more charcoal in lowland depositional areas, where charcoal is transported to by erosional processes (Cotrufo et al. 2016). Similarly, as the two ridges in the study area are geomorphically similar, with similar slope angles, we would expect them to both have less charcoal than lowland depositional areas but not be different from each other. Furthermore, although there is more charcoal in lowland areas—particularly alluvial bench

sites—there is little to no geomorphic evidence of recent depositional events at most sites and weathered B horizon soils are within the top 20 cm of the soil profile. The differences between the two ridges paired with the lack of difference between the north ridge and non-ridge sites implies that fire activity has not been uniform throughout the study area.

Differences in charcoal abundance must be interpreted with care, as they could be due to variations in fire frequency, intensity, or severity across the study area. When paired with estimates of time of fire occurrence, we can expand our interpretation of fire records. There is significantly less charcoal in upland forest types when compared to lowland forest types at CPRS, and the timing and frequency of fire events reflected in our record also varies substantially. Fire was a semi-regularly occurring phenomenon in lowland forest types from ca. 550 BCE to 1750 CE, with only two short periods without fire activity (350–480 CE and 870–920 CE). The relative abundance of charcoal in these sites also reflects this frequency. In contrast, fire was exceedingly rare in upland forest sites prior to approximately 1150 CE, with only two sites recording fires prior to this time. This the opposite of the pattern that we would expect in a system dominated by natural fire, as lowland forest types support larger trees and more dense and shaded understories which maintain high humidity levels. In comparison, upland forest types have smaller, shorter trees and fewer canopy layers and dry out faster in periods of moisture deficit. During periods of drought we would expect to see fires in upland forest types first, and only in lowland forest types during extreme or prolonged drought. The general pattern at CPRS from ca. 550 BCE to 1150 CE is the opposite, with fire present only in lowland forest types.

Few paleorecords exist near the study area with sufficient resolution to address

hydroclimate of the last 2000 years, and more distant paleoclimate studies show somewhat variable patterns. Records from the western and central Pacific show multiple periods of dry conditions for much of the last millennium (Cobb et al. 2007, Sachs et al. 2009). In cave speleothems from northern Borneo, Partin et al. (2007) found evidence for decreasing rainfall from its peak ca. 5000 years ago. In contrast, Konecky et al. (2013) report a general increase in precipitation over eastern Java through the last millennium based on terrestrial plant wax compounds preserved in lake sediments; Fukumoto et al. (2015) also found generally wetter climate recorded in a highland caldera lake in central Bali (~900 km southeast of CPRS) for the last 3100 years, though they note that this is in opposition to trends throughout the region and invoke orographic effects as a possible explanation for the different results. In an 8000-year peat record from Central Sumatra, Biagioni et al. (2015) found greatly increased charcoal concentration from 500 BCE to 900 CE, possibly resulting from stronger ENSO events known to have increased at the time. Multiple records, including several from east Java (~750 km southeast), also show several periods of major drought and increased fire activity in the last 1000 years (Rodysill et al. 2012, 2013, Konecky et al. 2013, Wündsch et al. 2014). A period of strong drought from ca. 1450-1650 CE is reflected in several records from east Java as well as a record from Sulawesi, indicating regional drought (Crausbay et al. 2006, Rodysill et al. 2012, Wündsch et al. 2014). Records from the central Pacific show dry conditions through much of this time period (Sachs et al. 2009). Taken together, these drought records indicate a long period of droughts from approximately 950-1150 CE, 1310-1330 CE, and 1450-1650 CE. Although it is not possible to place precise boundaries on fire periods from our data, there consistently high fire activity during the latter two of these three drought periods (Figure

2.9), suggesting that, like Java and Sulawesi, southwestern Borneo was experiencing more frequent drought.

The majority of droughts in Southeast Asia are attributed to warm phases of the El Niño-Southern Oscillation (ENSO), which has been a dominant climate phenomenon in the tropics for thousands of years (Quinn et al. 1978, Hendon 2003, Crausbay et al. 2006). High resolution records from Java as well as records from the tropical Pacific Ocean indicate a regime shift in ENSO activity around 1650 CE, with ENSO event duration shifting from multi-decadal to annual scales (Cobb et al. 2003, Crausbay et al. 2006, Rodysill et al. 2013). While this shift is not strongly indicated in our record, it is worth noting that the only negative deviations from our null model—indicating unusually low fire activity—occur well after 1650 CE and are driven by the absence of fire in the lowland forest types, suggesting that they are less vulnerable to fire caused by shorter drought periods compared to multiyear droughts and less vulnerable than upland forest types.

Although the period of highest fire activity in the study area does coincide with a regionally strong drought, both earlier and later periods of strong drought are not well represented at CPRS. For example, Wündsch et al. (2014) found an increase in fire activity, which they attribute to drought conditions, around Lake Kalimpaa (Sulawesi) ca. 1090–1190 CE; similarly, evidence from Lake Logung (Rodysill et al. 2012) in East Java indicates a period of strong drought from 930–1130 CE. Although it is possible that this drought was present but not as severe in the region of CPRS, it is also possible that ignition events were simply less frequent. In fact, there is a negative deviation in fire across CPRS for much of the ninth century, though this occurs only for the null model calculated with the censored method. Another period of strong drought from the late 1700s through the

mid-1800s, peaking ca. 1790-1810, is similarly indicated in several lake records from eastern Java (Rodysill et al. 2012, 2013). This drought is also absent from CPRS, with only two fires—both in upland areas—recorded after 1700 CE, and locally significant negative deviations in fire activity for both lowland forest types and the entire research area.

Despite high variability in our observed SPD post-1800 CE, there is little evidence for fire during the last 200 years. This high variability is an artifact of the calibration curve, causing age distributions to span up to 1950 CE, rather than true variability in fire activity at CPRS. In addition, two charcoal fragments in inundated sites that aged to within the last 70 years—after the establishment of GPNP and well within the range of modern records—may have been transported to the site by overland flow of water, as the charcoal was found in a frequently-flooded hummock (e.g., Abney and Berhe 2018, or by aerial transport from areas of human habitation near the coast.

Given the spatial and temporal pattern of fire, it is likely that humans played an important role in applying fire to the landscape of CPRS as elsewhere in Borneo and in other areas of tropical rainforest around the world (Barker et al. 2017). Both the abundance of charcoal and evidence of repeated fire in lowland forest types over the last 2500 years indicates that humans were an important source of ignitions at CPRS. Evidence from other tropical rainforest regions suggests that, in general, human presence—and accompanying landscape modification—was most likely near rivers and lakes, and the lowland forest types of CPRS are easily accessed from the two rivers that run through the study area (Sheil et al. 2012, Bush et al. 2016, Roberts et al. 2017). Swidden agriculture, also known as shifting cultivation, in which humans use a combination of manually felling trees and fire to clear small plots of forest for short-term agricultural use and then let the forest

regenerate, has been in use for at least 10,000 years in Southeast Asia (Kershaw et al. 2007). On Borneo, indigenous groups have been using swidden techniques for centuries, and its use persists to this day (King 1993, Lawrence et al. 1998, Lawrence 2004). Although theoretically swidden agriculture plots could be located anywhere in the forest, in reality they are not distributed randomly. The interior rainforest of CPRS has rugged topography bordered by level basins or coastal plains; lowland areas are accessible by river and have deep, high-nutrient soils, whereas upland forest types are typically too steep, with thin, rocky soils, for agriculture to be successful (Paoli et al. 2006). The deep soils of the alluvial bench areas at CPRS are particularly well suited to agricultural uses, and colonial Dutch records indicated the presence of several villages in the vicinity of CPRS (Topographisch Bureau, Batavia 1989). Fire could also have been used to aid in fishing and hunting, as posited by Hope et al. (2005) in East Kalimantan (Indonesian Borneo), where charcoal was found to be much more abundant in sites that are accessible from waterways.

Despite the differences in charcoal abundance and fire frequency prior to 1150 CE, upland and lowland forest types share a locally significant positive deviation—indicating high fire activity—from ca. 1370–1650 CE (censored method; ca. 1390-1490 CE with uncensored method; Figure 2.8). The positive deviation around 1450 CE is also present in all groupings by spatial zone, and there is a prominent peak around the same time in all SPDs created using all radiocarbon dates from CPRS. This indicates that during this time period some combination of a sufficiently dry climate to carry a fire and a source of ignitions was present across in our study area. It is unlikely that swidden agriculture expanded into upland forest types; instead, we believe that dry conditions allowed fires started in lowland forest types to creep upslope into upland forest types.

Although archaeological evidence in West Kalimantan is sparse (Smith 2016), the increase in fire activity at CPRS coincides with several important events in the human history of Borneo, which would have provided more possible ignition sources (Figure 2.9). The Kingdom of Majapahit, based on Java but with influence throughout Southeast Asia and presence on Borneo's coasts, reached its zenith in the 14th century CE (Noorduyn 1978, Sellato 1999). As Majapahit declined in the late 14th and 15th century CE, Malacca—based on the Malay Peninsula—came to prominence and facilitated the spread of Islam throughout Southeast Asia. Although Islam was not universally adopted by the indigenous groups of Borneo, the presence of a shared religion served to reinforce ties between Borneo and the surrounding islands (Tsing 1993). The kingdom of Tanjungpura, an important center of trade in the 15th and early 16th centuries CE, is reported to have ruled much of southern Borneo in the 1400s CE, though much of its history, including the location of its capital and its total extent, is unknown (Smith and Smith 2011). The arrival of European colonial powers in island Southeast Asia in the early 1500s CE ultimately destabilized the region, with multiple smaller kingdoms competing to control trade (Wilson 1994). Tanjungpura likely controlled the region around CPRS, and Dutch trading posts were also established in the vicinity of CPRS by the early 1600s CE (Smith and Smith 2011, Smith 2016). In particular, the Dutch and later English trading post at the coastal town of Sukadana, about 35 km from CPRS, was important in the diamond trade (Smith and Smith 2011). All these events increased resource extraction as well as the movement of people between Java and Borneo, increasing land use in interior regions of Borneo and providing more opportunities for land-use (and escaped fires) to occur further inland from the coast.

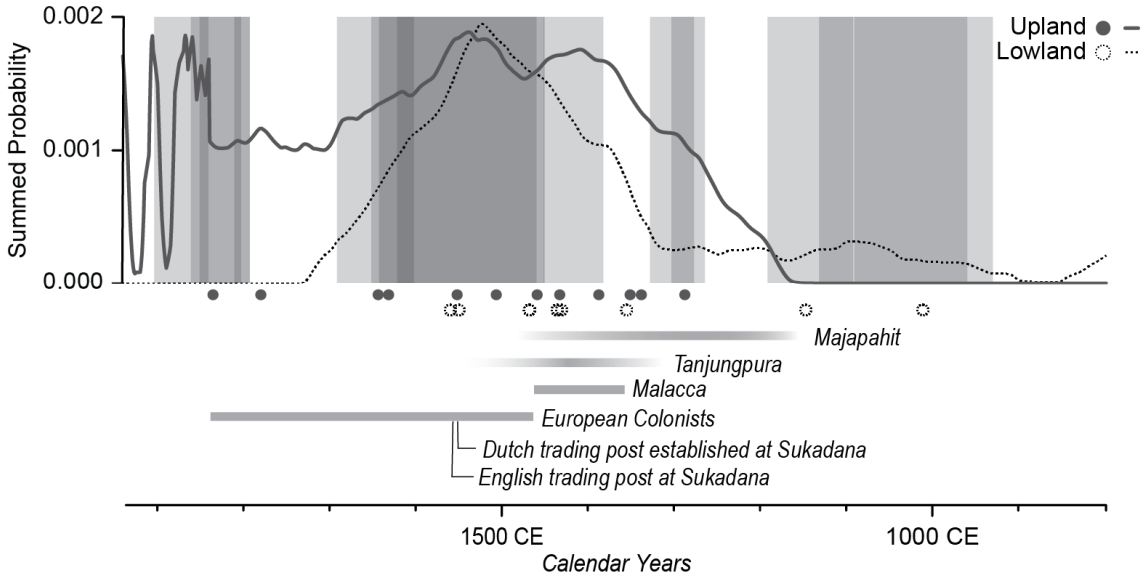

Figure 2.9. Fire activity in upland and lowland areas at CPRS in relation to regional drought and human events. Horizontal grey bars represent approximate time periods of major human history events. Vertical grey bars represent approximate time of major regional droughts (Java, Bali, Sulawesi); darker grey color indicates that the drought appeared in multiple records (Crausbay et al. 2006, Rodysill et al. 2012, 2013, Konecky et al. 2013, Wündsch et al. 2014, Fukumoto et al. 2015).

There is no above-ground evidence of fire in the forests of CPRS, but the charcoal within the soil profile tells a story of a forest that has experienced multiple fire events in the last 3000 years. While some fires were likely of natural origin, the relative prevalence of fire in lowland forest types compared to upland forest types, and the coincidence of increased fire with changes in the local governance and economy, points to human use of fire as a landscape modification tool at CPRS. Major peaks in fire activity are coincident with both increased resource extraction and a period of regional drought in the 15th and 16th centuries CE, highlighting the vulnerability of tropical rainforest to fire during times of water stress. Yet, the forests of CPRS are populated by very large, emergent trees with dense understories, indicating that these forests have largely recovered from the period of high fire activity of 300-500 years ago. However, there may be some imprints of past fire remaining on the landscape. In particular, the lower tree diversity of alluvial bench forests compared to other non-inundated forest types reported in Cannon and Leighton (2004),

Paoli et al. (2006), and Cannon et al. (2007) could be a reflection of past fire disturbances from swidden agriculture, as swidden agriculture has been documented to lead to a decrease in species diversity nearby areas of West Kalimantan (Lawrence 2004). Although we cannot verify that the forest community composition remains the same as it was before this fire period, we can conclude that the Dipterocarp dominated forests of CPRS were resilient to prolonged periods of fire within the last millennium.

5. Bridge to Chapter III

In Chapter II of this dissertation, I found that charcoal >2 mm is found across the forest types of CPRS, but it is significantly more abundant in lowland forest types. However, the amount of charcoal contained in smaller size fractions could be substantial. Furthermore, other combustion products (e.g., soot) produced by fire are difficult to detect with the manual identification and methods implemented in Chapter II. Thus, the results reported in this chapter are not representative of all pyrogenic carbon—carbon that has been altered by fire—contained in the soil. In Chapter III, I explore a newer method which theoretically measures pyrogenic carbon more comprehensively in soil. With this method, manual counting is replaced by a chemical oxidation to remove non-pyrogenic carbon (e.g., decomposing organic matter in the soil) followed by measurement with an elemental analyzer. In recognition of the fact that pyrogenic carbon in the soil encompasses a range of combustion products produced at different temperatures and exhibiting different recalcitrance to oxidation, I begin with a laboratory-based evaluation of the performance of the method on pyrogenic carbon produced at different temperatures. In addition, I compare the oxidation method to a manual method similar to that used in Chapter II as a way to quantify pyrogenic carbon, as well as comparing the radiocarbon ages of pyrogenic

material isolated by the different methods. Finally, I assess the performance of the oxidation method on soils from CPRS.

CHAPTER III

EVALUATING THE PERFORMANCE OF A HYDROGEN PEROXIDE – WEAK NITRIC ACID OXIDATION FOR MEASURING PYROGENIC CARBON IN TROPICAL FOREST SOILS

1. **Introduction**

Soil is indisputably the largest pool of terrestrial carbon (C), and is estimated to be at least three times larger than vegetation, the next largest terrestrial pool (Duarte-Guardia et al. 2019). However, quantifying the size of the soil C pool has proven difficult, with estimates varying from 504 Pg to 3000 Pg (Scharlemann et al. 2014). Global C budgets include total soil organic C (SOC) and total soil inorganic C (SIC) pools, but the production of pyrogenic C (PyC)—which makes up a non-negligible portion of the global SOC pool and can persist for centuries to millennia—is rarely explicitly included (Santín et al. 2015, 2016, Reisser et al. 2016, Jones et al. 2019). PyC is globally ubiquitous, but few estimates of global soil PyC storage exist, and generally rely on extrapolating from relatively few point estimates of the proportion of SOC that is made of PyC and in some cases a few other variables such as land use and soil properties (Bird et al. 2015, Reisser et al. 2016). These estimates suggest PyC comprises around 14% of total SOC on average, though it can be as much as 60% of individual SOC pools, making it an important and potentially large component of the soil C pool that is governed by different, slower decomposition kinetics compared to nonpyrogenic SOC[2] (Bird et al. 2015, Santín et al. 2016, Reisser et al. 2016). As there remains considerable uncertainty to the size of soil PyC stocks at regional and

[2] Henceforth when we refer to SOC we are referring to the non-pyrogenic portions of the total SOC pool, though we do consider PyC to be a part of the overall pool

global scales, there is need for more local studies that explicitly quantify PyC (Reisser et al. 2016). Furthermore, numerous and diverse techniques are used to isolate and quantify PyC in soil, which can make quantitative comparison less straightforward (Hammes et al. 2007, Zimmerman and Mitra 2017). In this study, we compare two very different methods of quantifying PyC in soil: (1) manual counts of macrocharcoal fragments, and (2) an acid-peroxide digestion to remove SOC and directly measuring the residual C with an elemental analyzer.

PyC is formed by the incomplete combustion of biomass and includes a range of components from partially charred biomass to charcoal to soot with different sizes, physical structures, and stability (Preston and Schmidt 2006, Shrestha et al. 2010). Residence times in soil typically range from 250 to 660 years but can be on the order of thousands of years, making it a particular valuable portion of the soil carbon pool from a carbon cycling perspective (Hammes et al. 2008, Knicker 2011, Abney and Berhe 2018). These long residence times are due to chemical structures dominated by condensed aromatic carbon rings which are formed during combustion, making PyC highly recalcitrant (particularly in comparison to other forms of SOC) to thermal, chemical, and microbial breakdown (Bird et al. 2015, Lavallee et al. 2019). In general, higher combustion temperatures correspond to greater aromaticity; the majority of PyC formed at higher temperatures (e.g., 600°C) is considered "stable" or "semi-labile" (residence times of centuries and decades, respectively), whereas PyC formed at lower temperatures (e.g., below 250°C) is mostly composed of labile C (residence times of years; McBeath et al. 2011, 2015, Bird et al. 2015). (Note that while some natural fires can reach temperatures of over 1200°C, they rarely remain at high temperatures for long, and much lower temperatures are more typical;

see González-Pérez et al. 2004, Scott et al. 2013)

Given its role in carbon cycling, quantifying PyC remains an important and very active area of research in several fields. A variety of methods have been proposed to isolate PyC from other forms of C in soil, ranging from nondestructive physical and spectroscopic techniques to destructive chemical, thermal, and molecular marker techniques (see Bird et al. 2015 and Zimmerman and Mitra 2017 for recent review of methods). Commonly used methods involve either visual identification of charcoal from sieved soil or an oxidation step to remove labile forms of SOC, with any remaining C assumed to be PyC due to its resistance to oxidation. Manual counting of charcoal particles from sieved soil and sediment is common in archaeology and paleoecology and has the benefit of requiring no specialized equipment beyond a standard dissecting microscope (Zimmerman and Mitra 2017). Manual counting can also be used on samples with no pretreatment, but a simple oxidation step such as application of hydrogen peroxide (H_2O_2) or nitric acid (HNO_3) is common and can greatly aid in visual identification of larger fragments of PyC (macrocharcoal; Schmidt and Noack 2000). However, manual counting is subjective with potential for misidentification, and can be time consuming even for experienced technicians. Furthermore, there is a lower limit on the size of macrocharcoal fragments that can be detected, so it is biased towards larger particles (Preston and Schmidt 2006, Zimmerman and Mitra 2017). In contrast, measurement of total C using an elemental analyzer potentially measures all PyC, but requires the oxidation of SOC (chemical digestions) prior to measurement and may not be perfectly selective for PyC. This highlights an important issue that complicates comparison of the plethora of methods used to measure PyC: different techniques target different classes of PyC, each with different

size ranges and/or chemical structures (Schmidt and Noack 2000a, Preston and Schmidt 2006).

Several commonly used chemical digestion methods have unique benefits, but all suffer from errors of commission (incomplete oxidation of SOC) and/or omission (overly vigorous oxidation which also removes some PyC). For example, oxidation by potassium dichromate ($K_2Cr_2O_7$) and strong sulfuric acid (H_2SO_4; Walkley-Black Method and derivations) has historically been a common technique to measure both SOC and PyC (by difference between measured total C and SOC), with SOC quantification by back titration of the residual dichromate with ferrous sulfate ($FeSO_4$) with the endpoint determined visually, spectrophotometrically, or potentiometrically (Soil Survey Staff 2014, Bahadori and Tofighi 2016, Hardy and Dufey 2017). Oxidation of SOC by this method is highly variable for different soils and there is much variation in particular steps of the protocol (e.g., whether external heat is applied during the digestion), so application of a correction factor alone is not enough to overcome these issues and allow for comparison between methods and studies (Skjemstad and Taylor 1999, Kurth et al. 2006, Conyers et al. 2011, Bahadori and Tofighi 2017). Other studies have found that some forms of PyC are vulnerable to dichromate oxidation and as a result non-negligible amounts of PyC are oxidized; this is particularly true for soils with less than 0.5% PyC by weight (Kurth et al. 2006, Hardy and Dufey 2017). Regardless, because PyC is measured indirectly, errors in other measurements are easily propagated through the calculations.

Even methods where PyC is measured directly from the residue after oxidation have been found to suffer from both omission and commission errors. For example, Kurth et al. (2006) compared digestion by strong nitric acid and heat to hydrogen peroxide alone

on samples amended with a known quantity of PyC. While digestion by hydrogen peroxide had nearly total recovery of PyC, it is very slow and does not completely remove SOC. In contrast, nitric acid alone is fast but also overly aggressive, as over 50% of PyC was lost. They propose an alternative digestion procedure using both hydrogen peroxide and weak nitric acid, known as KMD (Kurth-MacKenzie-DeLuca, after the authors), to oxidize SOC as an alternative to other chemical techniques (Kurth et al. 2006). In the KMD protocol, PyC is directly measured with an elemental analyzer, most SOC is removed, and recovery rates are more accurate and precise than other methods regardless of PyC content or the size of the PyC particles (Kurth et al. 2006, Pingree 2011). KMD has been widely used on mineral soils from forest environments (e.g., Bélanger and Pinno 2008, MacKenzie et al. 2008, Ball et al. 2010, Licata and Sanford 2012), and modifications have also been proposed for matrices with higher organic content, such as forest floor material (Maestrini and Miesel 2017).

While KMD is a promising alternative to other oxidation techniques, there is evidence that it does not perform equally well for PyC formed under different conditions (Soucémarianadin et al. 2014). PyC formed at higher temperatures tends to have higher aromaticity (more double bonds, so a lower hydrogen to C ratio) and be more recalcitrant to oxidation (Hammes et al. 2006, Ascough et al. 2011, Soucémarianadin et al. 2013). Similarly, older PyC may be more recalcitrant to oxidation than younger PyC, assuming that older PyC is likely comprised primarily of more stable components as less stable components would have already degraded from normal soil respiration processes (Ascough et al. 2011, Eckmeier et al. 2011). Additionally, PyC is not homogeneous, and even different portions of a single charred wood fragment may exhibit a range of

recalcitrance.

In this study we assess the recovery efficiency and replicability of KMD using three approaches. First, we assess how it performs on lab-created soils using charcoal formed at three temperatures. Second, we use tropical forest mineral soils to assess how charcoal age (determined by ^{14}C dating) affects its recalcitrance to oxidation by the KMD method. Third, we use the same tropical forest mineral soils to compare PyC concentration inferred through counting macrocharcoal fragments with PyC stocks estimated with the KMD method to assess PyC stocks.

2. Materials & Methods

2.1 Laboratory Soil Standards

To assess the PyC *recovery efficiency* (proportion of PyC surviving the digestion), *oxidation efficiency* (proportion of SOC removed), and replicability of the KMD digestion in general and with varying charcoal formation temperature, we created 24 standards with a known amount of charcoal created at three temperatures and organic material in a matrix of ground coarse sand. We used charcoal created from silver maple (*Acer saccharinum*) wood at 300°C, 400°C, and >500°C. Wood fragments were wrapped tightly in aluminum foil and heated for 1.5 hours at 300°C or 400°C. The >500°C charcoal was created by heating the 400°C charcoal in a muffle furnace at 500°C for 1.5 hours; oxygen in the pore space of the 400°C charcoal likely combusted a portion of the 400°C charcoal, thus raising the temperature above 500°C for these samples. This two-step combustion is relatively unique in the literature but approximates the fact that in landscape fires, charcoal is formed in the presence of some oxygen, and/or that charcoal from previous fires may be re-combusted by subsequent fires. The organic matter (OM) used was fresh deciduous leaves and small

branches of *A. saccharinum*. After drying for 24 hours at 60°C, all components were ground in a planetary ball mill for approximately two hours at speeds no lower than 600 revolutions per minute until they were visually homogeneous before combining. We measured the C content of each component using an ECS 4010 CHNSO elemental analyzer at the University of Oregon to enable us to accurately calculate the expected C content of our standards (Table 3.1).

Table 3.1. Measured C content of components of standards.

Component	Measured %C
sand	0
leaf and wood litter	48.55
300°C silver maple charcoal	80.87
400°C silver maple charcoal	82.26
>500°C silver maple charcoal (combusted two times)	45.30

Within our standards, expected total C ranged from 10.49–58.95 mg C per g soil. 21 standards contained PyC created at 300°C, 400°C, or >500°C, and were used to assess recovery efficiency and how it varies with charcoal formation temperature. Of these 21 standards, seven contained only PyC and sand (no soil organic matter), with expected PyC content ranging from 10.49 to 58.95 mg PyC per g soil. The remaining 14 standards contained both PyC and soil organic matter; the expected proportion of total C composed of PyC ranged from 28.0 to 67.9%, corresponding to 8.24–34.97 mg PyC per g soil. We also created three standards to assess oxidation efficiency of non-PyC organic matter; these standards did not contain any PyC, and had total C content—comprised entirely of fresh leaf litter and woody material—ranging from 12.40 to 25.26 mg C per g soil.

We assessed replicability of both recovery and oxidation efficiency by randomly selecting nine samples with PyC and one sample with only soil organic matter to be run in duplicate within a single batch of the KMD method. We also assessed between-batch replicability by designating six of our standards as “between-batch” standards to be

included within each of 14 batches of the KMD method on field soils. In total, each between-batch standard had five or six replicates across the entire experiment. We also used these between-batch replicates in our assessment of recovery efficiency.

2.2 KMD Digestion Method

In general, we followed the method described in Kurth et al. (2006) with some modifications. We dried soil samples at 60°C for 24 hours before grinding to a fine powder with a planetary ball mill using a corundum cup and balls. We placed approximately 0.85 g of sample in 125 mL Erlenmeyer flasks, and then added 20 mL of 30% hydrogen peroxide and 10 mL of 1 M nitric acid. Flasks remained at room temperature and were occasionally agitated by hand swirling for 30 minutes before being placed in a water bath at 90°C for 16 hours. In all cases we considered the oxidation complete after 16 hours as no more effervescing was observed, and flasks were then cooled to room temperature. We then filtered through pre-weighed Whatman #1 filter papers (particle retention:11 μm at 98% efficiency) in a plastic funnel. We dried the filter papers and residual material at 60°C for 24 hours before weighing each filter paper and residual material. Each filter paper was sealed in a plastic bag for storage. A sample of the residue was gently removed from the filter paper and C content was measured with an ECS 4010 CHNSO elemental analyzer (Costech Analytical Technologies Inc., Valencia, CA, USA) at the University of Oregon. Although it is possible that some of the C remaining after digestion is not pyrogenic, we refer to post-digestion C values as PyC. We calculated the amount of PyC remaining after oxidation on a per mass basis (g PyC per g of soil) using the following equation:

$\frac{g\ PyC}{g\ soil} = P * \frac{R}{S}$, where P is the percent C measured by an elemental analyzer after digestion, R is the mass of sample after digestion, and S is the mass of sample before

digestion. The large number of samples required multiple days of analysis; to account for day-to-day variation in instrument accuracy, we included multiple replicates of San Joaquin soil (NIST Standard Reference material 2709a). We used the observed and expected value for the San Joaquin soil to calculate an individual correction factor for every day of analysis and applied the appropriate correction factor to the samples analyzed that day. All data used in analysis here reflect the corrected values.

2.3 Field Soils: PyC and Macrocharcoal Identification

To assess KMD performance in relation to other methods, we used soils collected from primary tropical rainforest at Gunung Palung National Park in West Kalimantan, Indonesia. Although there is no record of fire at this site within the last 100 years, charcoal is present in soil across the site. We collected soils from 51 sites at depths from the surface to 20 cm below the surface, divided into 5 cm increments; in total we analyzed 189 samples. Each sample consisted of two segments from parallel cores, located within a few cm of each other, which were processed using two methods: (1) passing dried soil through a 2 mm sieve to remove any material >2 mm, including PyC fragments, and (2) wet-sieving at 2 mm and 0.5 mm.

We measured SOC and PyC content following the same methods as for the laboratory soil standards (total C measured in unmodified soils; PyC measured in KMD-digested soils) in the dried soils. While we did not explicitly remove carbonates, we expect the contribution of SIC to be negligible, as their formation is rare outside of arid to sub-humid conditions; we therefore consider these total C results to represent only SOC (including PyC; Cerling 1984). We also used a dissecting microscope to isolate and count charcoal fragments in soil from the wet-sieved segments ("manual method"). We refer to

PyC isolated using this method as macrocharcoal. We then massed all macrocharcoal 0.5–2 mm and used the bulk density of each sample to convert to a per mass of soil basis.

2.4 Field Soils: Radiocarbon Dating

To assess the role of charcoal age on KMD performance, we submitted five paired macrocharcoal fragments and KMD-digested soils from the same sample to the National Ocean Sciences Accelerator Mass Spectrometry (NOSAMS) facility at Woods Hole, MA for ^{14}C dating using an accelerator mass spectrometer (10 samples total). All radiocarbon dates were calibrated using IntCal13 (Reimer et al. 2013) and the calibrate function in the package *rcarbon* (version 1.2.0; Bevan and Crema 2018) in R (version 3.6.1; R Core Team 2019). A single modern date was calibrated using OxCal 4.4 online with the SH Zone 3 calibration curve (Bronk Ramsey 2009).

2.5 Statistical Analysis

We used ordinary least squares linear regression of the expected vs. observed values of PyC to assess overall recovery and oxidation efficiency of the KMD digestion. Where significant, we interpret the slope of the line as the *recovery efficiency*. *Oxidation efficiency* is the proportion of non-PyC organic matter oxidized by the KMD digestion. Oxidation efficiency is assessed from soil standards that contained only leaf and wood litter.

For our field soils from Cabang Panti Research Station, we compared observed values of total C (pre-digestion) with observed values of PyC using ordinary least squares linear regression. We expect a positive relationship to arise in these measurements if: 1) PyC is a large proportion of total C; 2) oxidation efficiency of the soils was less than 100%, such that a portion of SOC was recalcitrant and survived KMD digestion; or 3) indirect

ecological relationships exist between PyC production and non-PyC input and residence time. To account for the possibility of oxidation efficiency <100%, we also used percentile regression using the rq function in the *quantreg* package (version 5.6.1; Koenker 2020) in R (version 3.6.1; R Core Team 2019) to compare observed values of total C and PyC. Percentile regression allows us to determine the relationship between total C and PyC at the percentile (τ) of interest, and then use the positive residuals to represent a "corrected" PyC value that does not include recalcitrant SOC that was not removed by the digestion. We performed percentile regression for multiple percentiles (τ values), and here report the results of three: the tenth percentile ($\tau = 0.1$), the 25th percentile ($\tau = 0.25$), and the 50th percentile ($\tau = 0.5$, i.e., median regression). We then assessed each percentile regression by comparing the correlation coefficient of total C and the "corrected" PyC values. Finally, we also compared the amount of macrocharcoal isolated with a microscope with PyC measured by the KMD method using ordinary least squares regression, using both the uncorrected and the corrected PyC values.

3. Results

3.1 KMD Digestion Oxidation Efficiency and Recovery Efficiency – Laboratory Soil Standards

We removed one sample from the analysis because the observed PyC was higher than the observed total C, indicating measurement error or that the sample may have been contaminated. This left us with 60 samples of our laboratory-created standards.

We assessed oxidation efficiency of SOC (i.e., non-PyC organic matter), composed of fresh leaf and woody organic matter, using laboratory soil standards containing only organic matter and ground sand matrix (no PyC). Digestion in four replicates of these

samples was complete or nearly complete; three replicates contained no C post digestion, and the fourth contained less than 0.5% of the observed pre-digestion total C.

Of 60 samples containing both PyC and SOC, 48 had less C remaining after digestion than expected. On average, recovery efficiency of PyC is 46% of the expected value. The correlation between expected and observed PyC is moderate ($R^2 = 0.34$). When considering PyC formation temperature, patterns in recovery and oxidation efficiency emerge: there is a clear relationship between temperature of formation of PyC and recovery. The 300°C charcoal standards had less C than expected after digestion, with an average recovery efficiency of 32% ($p << 0.001$; Figure 3.1). In contrast, the 400°C charcoal standards had a 79% recovery efficiency ($p << 0.001$; Figure 3.1) and the > 500°C charcoal standards had 89% recovery efficiency ($p = 0.018$; Figure 3.1). The strength of the correlations between expected and observed PyC by formation temperature exhibits the opposite pattern: standards made with 300°C charcoal have the highest correlation ($R^2 = 0.832$), while standards made with 400°C charcoal have a moderately strong correlation ($R^2 = 0.632$), and standards made with 500°C charcoal have the weakest correlation ($R^2 = 0.479$).

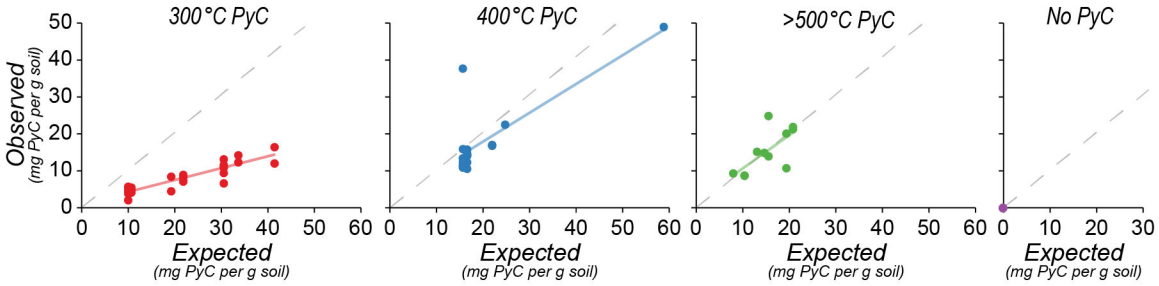

Figure 3.1. Expected vs. observed PyC, divided by formation temperature of PyC used (red = 300°C.; blue = 400°C; green = 500°C; and purple = no added PyC). The colored lines are lines of best fit for the data; the dotted grey lines represent perfect correspondence between expected vs. observed PyC.

3.2 KMD Digestion Replicability – Laboratory Soil Standards

Between-batch replicability was relatively consistent, with interquartile ranges from 0.92 mg C per g soil (300°C charcoal + SOC) to 1.85 mg C per g soil (400°C charcoal + SOC; Figure 3.2), or ca. 5% to 12% of the expected value.

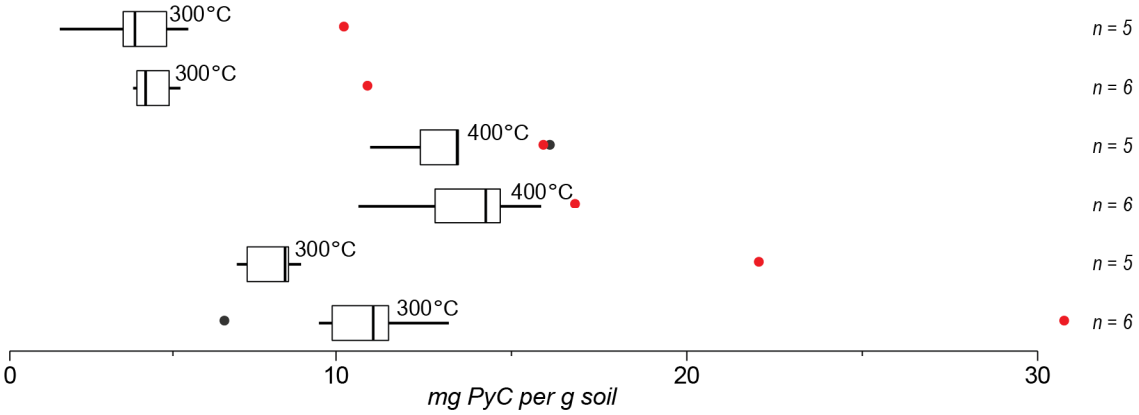

Figure 3.2. Between-batch replicability of measured PyC for KMD digestions of laboratory soil standards. Red dots indicate the expected value for each standard.

When we also include the standards that were used to assess recovery efficiency and oxidation efficiency within a single batch, we see that the range of observed values among replicates is generally higher for standards that include SOC (ca. 2–81% of the expected values) than for samples with only PyC (ca. 0.2–10% of the expected value) (Figure 3.3).

3.3 Field Soils

For field soils from Cabang Panti Research Station, we removed two samples from the analysis that had more PyC (as measured by the KMD method) than total C, indicating either measurement error or sample contamination (final n = 187). Total C ranged from 1.85 to 420.32 mg C per g soil, with a mean value of 53.75 mg C per g soil. PyC (measured by the KMD method) ranges from 0 to 47.80 mg PyC per g soil. The proportion of total C comprised of PyC ranges from 0 to 89% PyC in individual samples. Macrocharcoal (0.5–2

mm, isolated with the dissecting microscope) ranges from 0 to 1.44 mg macrocharcoal per g soil. The proportion of total C comprised of macrocharcoal ranges from 0 to 11% macrocharcoal, with a mean value of 0.3% macrocharcoal.

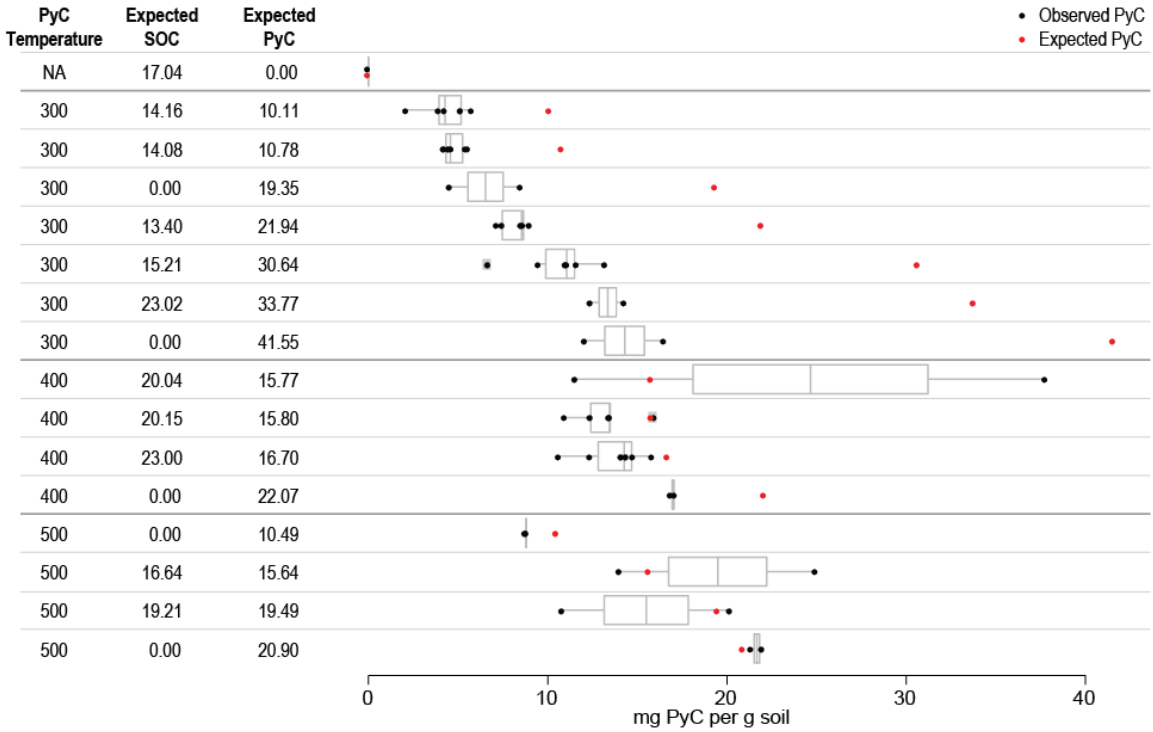

Figure 3.3. Range of observed PyC values for all standards. Black dots indicate the observed value for each replicate, and red dots indicate the expected value for each standard.

PyC comprises 9% of the total C pool ($p << 0.001$). However, there is a moderate positive relationship between total C and observed PyC ($R^2 = 0.544$; Figure 3.4), which is especially evident at low levels of PyC and total C. When percentile regression is used to decouple total C and observed PyC under the assumptions that PyC and total C should be unrelated in the environment when PyC is a small component of total C and some recalcitrant SOC remains following digestion, the strength of the relationship between total C and corrected observed PyC is much reduced for all percentile regressions, with the correlation weakening for higher percentile regressions (Table 3.2). When the corrected values are used, PyC also comprises a smaller portion of the total C pool (Table 3.2).

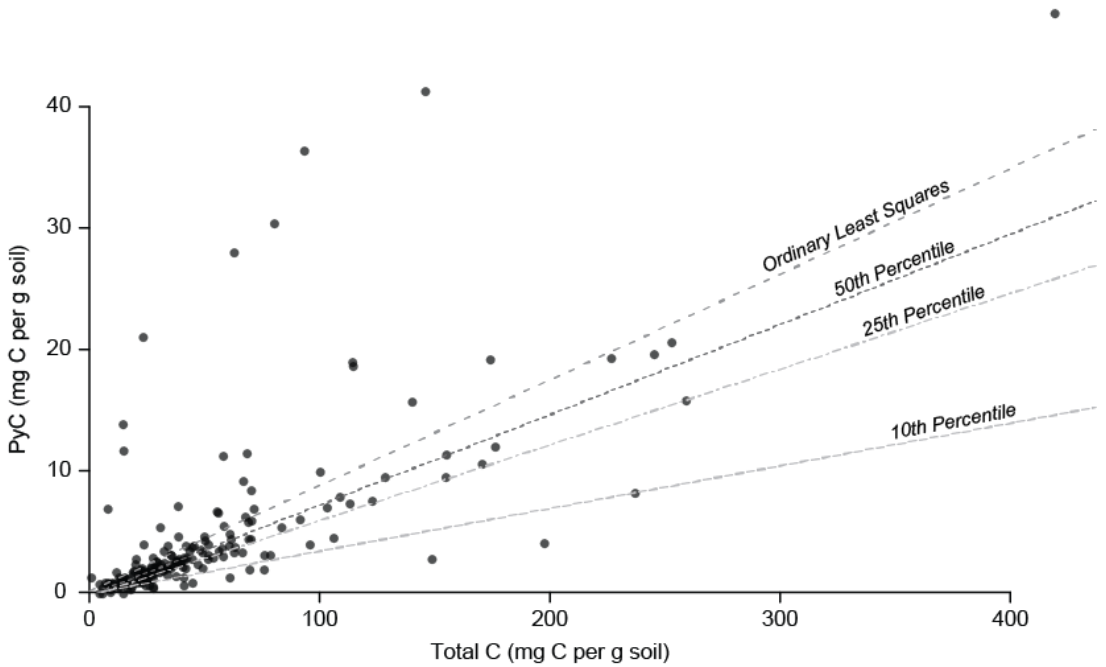

Figure 3.4. Relationship between total C and PyC measured by KMD digestion for soils from primary tropical forest (n = 187; Gunung Palung National Park, West Kalimantan, Indonesia). Data points are raw data; different regression lines are shown with different dotted lines.

Table 3.2. Relationship between total C and PyC for CPRS when percentile regression is used to correct the observed PyC values for three different percentiles. PyC contribution to the total C pool is the slope of the regression line relating total C and PyC (where applicable, corrected PyC); ** indicates $p << 0.001$. Note that 50th percentile regression is equivalent to median regression.

Correction Type	R^2 (total C vs. observed PyC)	Estimated SOC Contribution to PyC Pool	Mean PyC Percentage of Total C Pool	Mean PyC, Individual Segments (mg C per g soil)	Median PyC, Individual Segments (mg C per g soil)	PyC Range, Individual Segments (mg C per g soil)	PyC Percentage of Total C Pool Range, Individual Segments
None	0.544	--	9%**	4.76	2.5	0–47.80	0–89%
10^{th}	0.268	3%	5% **	3.05	1.2	0–36.3	0–87%
25^{th}	0.113	6%	3% **	2	0.46	0–32.5	0–85%
50^{th}	0.068	7%	2% **	1.55	0	0–30.7	0–84%

Overall, the amount of PyC measured by the KMD method is much higher than that measured by manually picking charcoal pieces with a microscope. Median and mean amounts of PyC measured by the KMD method are 2.50 and 4.76 mg PyC per g soil,

respectively; after accounting for recalcitrant SOC using quantile regression the amount of PyC is substantially reduced (Table 3.2). In contrast, median and mean amounts of macrocharcoal as measured by the manual method are 0.04 and 0.11 mg macrocharcoal per g soil, respectively. Of 187 samples, only three had no PyC as measured by the KMD method, whereas 75 had no charcoal according to the manual method. There is no correlation between the PyC and macrocharcoal values, regardless of whether un-oxidized SOC is corrected using percentile regression ($R^2 = 0.014$ for uncorrected PyC; $R^2 = 0.010$ for 10th percentile corrected PyC; $R^2 = 0.008$ for 25th percentile corrected PyC; $R^2 = 0.008$ for 50th percentile corrected PyC; Figure 3.5, Appendix Figure 3.1).

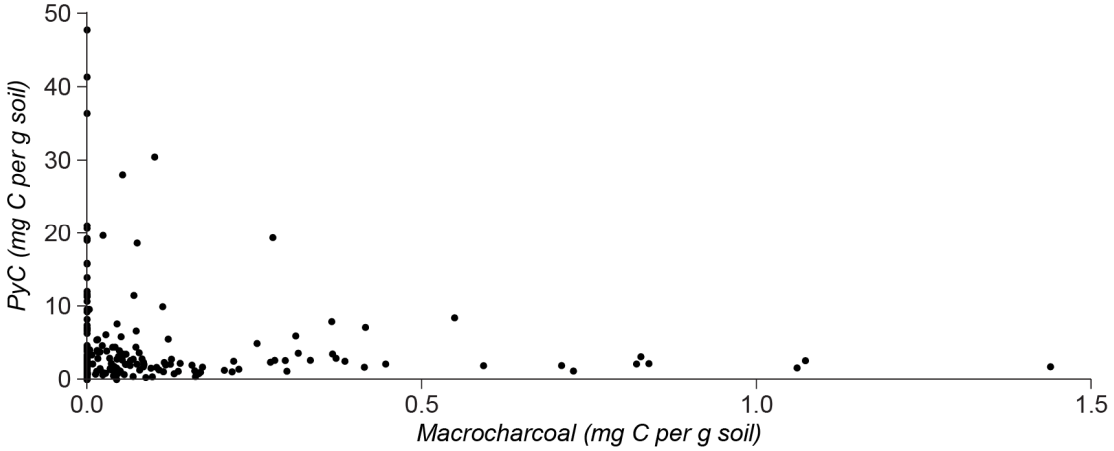

Figure 3.5. Relationship between macrocharcoal (0.5–2 mm) from the manual method from parallel soil cores from primary tropical forest (Gunung Palung National Park, Indonesia) compared to PyC as measured by the KMD method, using unadjusted PyC values. Each point represents a 5-cm core segment (90.6 cm^3). Soil cores were limited to the upper 20-cm of soil.

There is no correlation between age of PyC post-digestion and age of macrocharcoal from the same sample. For three of the five samples, the PyC obtained from the KMD method is younger than the PyC isolated from the >2mm fraction (Table 3.3).

Table 3.3. Comparison of accelerator mass spectrometry radiocarbon ages on single macrocharcoal pieces and PyC fraction obtained by KMD digestion from an adjacent soil sample. Soils were from tropical forest in West Kalimantan, Indonesia. A negative age difference indicates that the PyC is younger than the macrocharcoal fragment.

	Macrocharcoal Fragments			PyC (KMD Digestion Residue)			
Sample ID	Laboratory Code (NOSAMS)	Radiocarbon Age ± 1 SD	Calibrated Age Range (95%, Calendar Years)	Laboratory code (NOSAMS)	Radiocarbon age ± 1 SD	Calibrated age range (95%, CE/BC)	Age difference (PyC – Macrocharcoal Median Ages)*
MT01 D 0-5	OS-153007	445 ± 15	1430-1450 CE	OS-142577	1410 ± 15	550-650 CE	800
MT01 F 10-15	OS-153008	2170 ± 20	280-350 BCE; 250-260 BCE	OS-135949	880 ± 15	1150-1210 CE	-1470
MT04 B 15-20	OS-152867	1420 ± 15	610-650 CE	OS-142450	5670 ± 25	4450-4550 BCE	5130
HB16 F 10-15	OS-152866	10650 ± 55	10770-10580 BCE	OS-135860	1450 ± 15	580-640 CE	-11290
GP90 B 0-5	OS-153006	350 ± 25	1460-1530 CE; 1540-1630 CE	OS-142582	> Modern	1956 CE	-398

*Median age as reported by rcarbon's *calibrate* function.

4. Discussion

4.1 Laboratory Soil Standards

This study represents the one of first efforts to explicitly assess the effect of charcoal formation temperature on recovery efficiency of PyC for the KMD acid-peroxide digestion method. While focusing on microcharcoal for both age and quantification of PyC has been posited as a better way to account for cooler fires (e.g., grass fires) which rarely result in large pieces of PyC, our results show the acid-peroxide digestion is greatly affected by temperature of charcoal formation (Eckmeier et al. 2011, Gosling et al. 2019).

While the KMD digestion method resulted in a PyC recovery, on average, of 46%, recovery varies substantially by formation temperature of the PyC. Our finding that PyC recovery is lowest for charcoal formed at lower temperatures is consistent with the literature (Kurth 2004, Maestrini and Miesel 2017), indicating that low-temperature charcoal material is more vulnerable to oxidation. This is particularly true for charcoal formed at 300°C; in our study, well over half of the expected PyC was removed by the KMD digestion, suggesting that it was composed primarily of labile and semi-labile carbon. In contrast, approximately 10% of the expected PyC was oxidized in standards created with charcoal formed >500°C, providing additional evidence that charcoal formed at higher temperatures is more recalcitrant, as much less PyC is oxidized than in standards created with charcoal formed at lower temperatures. Ascough et al. (2011), using ^{13}C CPMAS NMR, found that that 400°C is an important transition point in the chemical structure of PyC—in particular, the formation of aromatic structures, which are more resistant to oxidation. Consistent with Ascough et al. (2011), our standards created with charcoal formed at 400°C have a much higher recovery efficiency than standards created

with charcoal formed at 300°C (78% vs. 32%), suggesting that much of the charcoal has already undergone the transition to stable carbon structures. However, even a single piece of charcoal is not homogenous and will contain a range of structures with different recalcitrance to oxidation (Bird et al. 2015). Standards created with charcoal formed at 300°C, which had a high correlation between observed and expected PyC, likely had a higher proportion of consistently easily oxidized PyC. Charcoal pyrolyzed at the transition point of 400°C may have more mixed structures with variable recalcitrance to oxidation, which is reflected in the lower correlation with expected PyC.

The weaker correlation of expected and observed PyC for standards created with charcoal formed >500°C could be a result of impurities in the digestion reagents being sorbed by the charcoal, as postulated by (Kurth 2004) with a nitric acid only digestion. (Glaser et al. 2002) note that charcoal formed at higher temperatures—and thus having more aromatic structures—have higher adsorption capacity, making this phenomenon more likely in our >500°C charcoal. In fact, seven of 11 samples with >500°C charcoal contained slightly more PyC than expected, indicating that some sorption did occur. The amount of sorbed impurity would likely vary by sample, and different impurities would also exhibit different resistance to oxidation, resulting in a lower correlation between expected and observed PyC. While the presence of impurities could also artificially raise our recovery efficiency, our approach of using the slope of the line of best fit for all of our samples should limit this effect.

4.2 Field Soil

We expected that PyC isolated by the KMD digestion would be older than manually isolated microcharcoal under the assumption that soils are enriched in older and

more recalcitrant PyC, as shown by Abiven et al. (2011). Furthermore, we expect that older and more recalcitrant PyC would survive oxidation. However, this pattern was only true for two of our five comparisons. Though surprising, our results are not entirely inconsistent with the literature; in particular, our finding of no relationship between PyC and manually isolated macrocharcoal age is consistent with Eckmeier et al. (2011), who found that there was little systematic difference in age of hand-picked macrocharcoal and microcharcoal samples separated via UV oxidation, though microcharcoal fractions tend to be older.

Younger PyC relative to macrocharcoal ages could indicate that the KMD method did not remove all SOC (non-pyrogenic C) from the samples, and that the PyC dated is in reality a mixture of SOC C and PyC material. Non-pyrogenic organic matter is highly heterogeneous and may also be protected by its mineral matrix, with many types of organic matter with different turnover times (Krull et al. 2006, Pessenda et al. 2006, Trumbore and Zheng 2006). Trumbore (1993) found that the majority of soil carbon in upper horizons of a tropical soil in the Amazon Basin has a residence time of less than ten years. If soil carbon dynamics in Borneo are similar, the presence of un-digested, non-pyrogenic organic carbon in our dated soil would bias our results substantially younger.

The positive correlation between observed total C and observed PyC in field soils—which *a priori* we expect to be uncorrelated—indicates that some SOC C in tropical soils is recalcitrant enough to survive oxidation during the KMD digestion procedure. We estimate that between 3% and 7% of measured PyC is actually SOC that survived the KMD digestion, as indicated by our percentile regressions. Chen et al. (2020) that charcoal-like structures with condensed aromatic rings—which would presumably have a similar resistance to oxidation as PyC—can form during aerobic decomposition in wheat straw,

and it is possible that organic matter inputs to our field soils could also contain non-pyrogenic aromatic structures formed during decomposition. Our laboratory standards, in contrast, were created by undecomposed leaf and wood litter. Recalcitrant SOC remaining after the KMD digestion procedure could be either younger or older than PyC, contributing to the lack of pattern in the relationship of the ages of PyC and macrocharcoal.

Regardless of whether or not the KMD digestion removed all non-PyC, PyC dates will likely not reflect the age of the oldest charcoal particle in the soil because soils are bioturbated and integrate fire events with the resulting age reflecting the mean age of the particles likely arising from a range of fire dates. PyC could have originally been part of a larger piece of PyC that has broken down over time, or it could have entered the soil profile in its current form. In contrast, macrocharcoal dates are from a single (relatively large) piece and will reflect the age of that single piece—which may have been transported by bioturbation, erosion, or other soil mixing processes, and may result from the same fire event as the PyC particles found in its proximity (Carcaillet 2001, Hubau et al. 2012, Abney and Berhe 2018). PyC particles are also affected by soil mixing processes, but could respond differently due to their smaller size (Abney and Berhe 2018).

Similarly, the amounts of PyC and macrocharcoal found in the same soil sample were not correlated. We expected that there would be more PyC than macrocharcoal in our samples because some size classes of PyC are too small to be identified and isolated with a conventional stereoscope at 50x magnification. We found this to be true for 184 of 189 samples—including 63 of 65 samples with no manually identified macrocharcoal—but did not expect the differences to be as large or the relationship to be as variable. While the KMD method is not infallible (see above) and some of the differences could be due to

incomplete removal of non-PyC material, it is more likely that this instead reflects the inability of manual methods to quantify all size classes of PyC. Furthermore, it highlights the difficulties of manually counting PyC particles due to inconsistencies with identification and other human errors.

5. Conclusion

In conclusion, we have four major findings. (1) The KMD digestion method is effective for removing non-PyC from samples and in general exhibits consistently moderate recovery rates, though recalcitrant C remaining in tropical soils could result in an overestimate of PyC. (2) Charcoal created at higher temperatures is more resistant to oxidation via the KMD digestion than charcoal created at lower temperatures. There is a critical threshold in recalcitrance between 300°C and 500°C. This limits the ability of the KMD digestion to capture information concerning charcoal (and other forms of PyC) sourced from cooler fire events, such as grass fires. (3) While macrocharcoal and PyC data can be used to investigate similar questions, they are not interchangeable. This is true for quantifying carbon pools as well as dating PyC, as there are not reliable or consistent relationships between macrocharcoal and PyC for either quantity or age. (4) Estimates of pyrogenic soil carbon pools should not rely on macrocharcoal alone, as it greatly underestimates the amount of PyC. Measuring PyC via chemical digestion includes smaller size classes of PyC and is less susceptible to errors in charcoal identification.

6. Bridge to Chapter IV

Chapter III focused on assessing the performance of a chemical oxidation method, the KMD method, that requires only readily available laboratory equipment and equipment. In that chapter I showed that the KMD method reliably has very high recovery efficiency

for pyrogenic material produced above 400°C, making it a suitable alternative to other, more expensive or complicated methods for quantifying pyrogenic carbon for environments where fires typically exceed 400°C (i.e., not grass fires). While it has a tendency to slightly underestimate pyrogenic carbon in samples made with "fresh" charcoal, soils collected from CPRS contain highly recalcitrant, non-pyrogenic carbon that leads to overestimation of pyrogenic carbon. The KMD method is suitable for use in tropical mineral soils, but should be paired with total carbon measurements to adjust for this recalcitrant non-pyrogenic fraction. After showing the utility of the KMD method for quantifying pyrogenic carbon in tropical mineral soils in Chapter III, in Chapter IV I make use of this method to quantify pyrogenic carbon pools across forest types and by depth at CPRS. I also quantify the total carbon pool, which includes both pyrogenic and non-pyrogenic carbon.

CHAPTER IV

THE CONTRIBUTION OF PYROGENIC CARBON TO SOIL CARBON POOLS IN AN EQUATORIAL TROPICAL RAINFOREST

1. Introduction

The tropical forest biome is one of the most carbon dense in the world, with carbon stored both above ground (living biomass) and below ground (soil organic carbon) (Jobbágy and Jackson 2000, Saatchi et al. 2011, Pan et al. 2011). Within the tropics, Indonesia is among the countries with the largest areas of forest and the highest carbon stocks (Saatchi et al. 2011). However, Indonesia has also experienced significant forest loss in recent decades, particularly in Kalimantan (Indonesian Borneo) and Sumatra (Stibig et al. 2013, Hansen et al. 2013). Borneo is a "deforestation hotspot," with approximately 30% of its forest cover lost from 1973 to 2010 (Gaveau et al. 2014, McAlpine et al. 2018). As the third largest island in the world—over 746,000 km^2—which as recently as 1973 was over 75% covered by old-growth, mainly intact rainforest, this is a substantial loss of forest cover and change in global carbon budgets (Gaveau et al. 2014, McAlpine et al. 2018). Logging, conversion to plantation agriculture (e.g., oil palm and *Acacia mangium*), and fires have been identified as the major causes of forest cover loss on Borneo (Langner et al. 2007, Stibig et al. 2013, Gaveau et al. 2014, 2018). Because of their area and carbon density, understanding the carbon storage capacity of Borneo's intact evergreen tropical forest is important for carbon budgets and projecting how carbon storage could change under different deforestation (and reforestation) trajectories.

On a global scale, the soil carbon pool is the largest component of the terrestrial carbon pool, with most recent estimates in the range of 1400–1600 Pg C (range: 504–3000

Pg C; Lal 2005, Scharlemann et al. 2014, Silva 2017, Delgado-Baquerizo et al. 2017, Duarte-Guardia et al. 2019, Borchard et al. 2019). Most global and regional estimates of the soil carbon pool are based on point measurements of soil carbon, and there are relatively few estimates from tropical forests in Oceania (Scharlemann et al. 2014). Attempts at down-scaling soil organic carbon estimates are often unable to adequately predict soil organic carbon stocks at landscape levels due to substantial spatial heterogeneity, and perform particularly poorly in undisturbed ecosystems (Wieder et al. 2013, Duarte-Guardia et al. 2019). More point and landscape scale estimates, particularly in understudied high carbon biomes such as tropical forest, will ultimately allow for more accurate estimates of global carbon pools.

The soil carbon pool includes both organic and inorganic carbon. The inorganic component is estimated to make up about one third of the global total soil carbon pool, though its contribution is typically negligible outside of arid and semi-arid regions and (Batjes 1996, Lal 2008). Organic soil carbon is comprised of plant residues, living plant parts (e.g., roots) and soil biota (e.g., bacteria, nematodes, and fungi), decaying biomass and decomposition byproducts, relatively stable decomposition remnants that are physically protected (i.e., humus), as well as charcoal and other forms of pyrogenic carbon (González-Pérez et al. 2004, Wieder et al. 2017). Pyrogenic carbon (PyC)—formed from incomplete combustion of biomass during a fire—includes a continuum of combustion products, ranging from partially charred material to charcoal to soot (Bird et al. 2015). Most forms of PyC are relatively resistant to decomposition due to condensed aromatic ring structures and can persist in soil for thousands of years, though residence times are typically in the range of several hundred years (Schmidt and Noack 2000a, González-Pérez

et al. 2004, Singh et al. 2012). PyC is ubiquitous in soil profiles around the world and comprises approximately 14% of total soil organic carbon on average, though values as high as 60% have been reported (Reisser et al. 2016). Consequently, PyC is an important component of soil carbon pools due to its quantity and its longevity. However, outside of the *terra preta* soils of the Amazon Basin, few estimates of PyC in tropical soils exist. Furthermore, many methods do not explicitly account for pyrogenic carbon, and the amount of carbon that is stored in this form is not well quantified (Batjes 1996, Santín et al. 2015, Reisser et al. 2016, Jones et al. 2019). Particularly in warm, high rainfall biomes, where non-pyrogenic carbon residence times are among the shortest of all forest types (Carvalhais et al. 2014), there is need for better quantification of PyC in soils, which can then be incorporated into global carbon budget models.

There is particular urgency to quantify PyC in equatorial rainforest. Fire is a major cause of deforestation in these forests, and has substantial potential to alter regional and global carbon budgets through the release of carbon into the atmosphere through combustion as well as the transfer of carbon from aboveground biomass (e.g., trees) to charcoal and other forms of PyC within the soil carbon pool (Langner et al. 2007, Cochrane and Ryan 2009, Sedjo and Sohngen 2012). In this study, we quantify soil organic carbon pools in tropical rainforest on the island of Borneo. Specifically, **our objective was to quantify soil organic carbon stocks at Cabang Panti Research Station (West Kalimantan, Indonesia) and how it varies across an elevation and habitat-gradient, as well as identify what proportion of this carbon is pyrogenic**. We investigated how carbon storage changes with depth within the top portions of the soil profile, as well as how soil characteristics such as texture and pH may be related to carbon stocks. Finally, we

evaluated the effectiveness of soil color as an indicator of total and pyrogenic carbon in tropical soil.

2. Materials & Methods

2.1 Study Area

Cabang Panti Research Station (CPRS; 1.216°S 110.106°E) is a long-term research station located in Gunung Palung National Park (GPNP) in West Kalimantan, Indonesia. GPNP is home to several types of dipterocarp-dominated, evergreen tropical rainforest typical of Borneo. GPNP's history of protection dates to 1929, when it was first designated a protected area by the Dutch; it was upgraded to a national park by the government of Indonesia in 1989 (Curran and Leighton 2000). Consequently, human disturbance has been severely restricted in the last century, with the exception of small small-scale non-mechanized logging and poaching, and there are no records of fire within the study area (Webb and Peart 2000, Cannon and Leighton 2004). A recent study (Hendricks et al., in prep) found a history of fire at the site, especially between ca. 1450 and 1650 CE. While macrocharcoal was found at most sites in that study, it is possible that some sites in the study area have not burned in over 2000 years.

CPRS encompasses a single watershed (approximately 15 km^2) of a coastal mountain complex with two steep east-to-west parallel ridges, with elevations ranging from near 40 m a.s.l to 1000 m a.s.l. Lowland sites include poorly drained and seasonally flooded freshwater swamp and peat forests, as well as alluvial bench forest along the main river, the Air Putih. Upland sites are typically well-drained and support several forest types, including montane forest above 700 m (Curran and Leighton 2000, Cannon et al. 2007). In general, lowland soil types are derived from sedimentary parent materials (e.g., sandstone)

and upland soil types are granite derived (Cannon and Leighton 2004). The climate is aseasonal with over 4000 mm of rain annually, though periods of moderate to strong drought (typically associated with El Niño events) occur on a semi-regular basis (Quinn et al. 1978, Petersen 1991, Curran and Leighton 2000, Paoli et al. 2006). Mean daily minimum and maximum temperature in lowland areas are 23.6°C and 27.6°C respectively, with somewhat cooler temperatures at higher elevations; at approximately 1000 m a.s.l., mean daily minimum and maximum temperatures were 19.2°C and 23.6°C, respectively, in one year of data collection (2017). Relatively humidity is typically >90% throughout the year, though lower values have been observed during dry periods.

2.2 Sample Collection

We collected soil from 43 sites distributed between seven forest types (Figure 4.1; Table 4.1). With one exception, sites were clustered in groups of three (14 total groups), with approximately 20 m between sites within a group and a minimum of 200 m between groups. One group located in seasonally inundated freshwater swamp included four sites, with two sites in low-lying, frequently flooded areas and two sites in rarely flooded adjacent hummocks. Much of CPRS is steeply sloped, so we located sampling sites in small hollows and locally level areas to better capture PyC which is easily eroded away from where it is formed (Abney and Berhe 2018).

For each site, we collected two parallel soil cores from the surface of the A horizon to a depth of 20 cm using an AMS® bulk density sampler (ca. 5 cm diameter, 90.59 cm3 volume) and, where necessary, a mallet to reach the appropriate depths, with each core collected in 5 cm segments. At 9 sites the depth to regolith was less than 20 cm. In total, we collected and analyzed 156 segments.

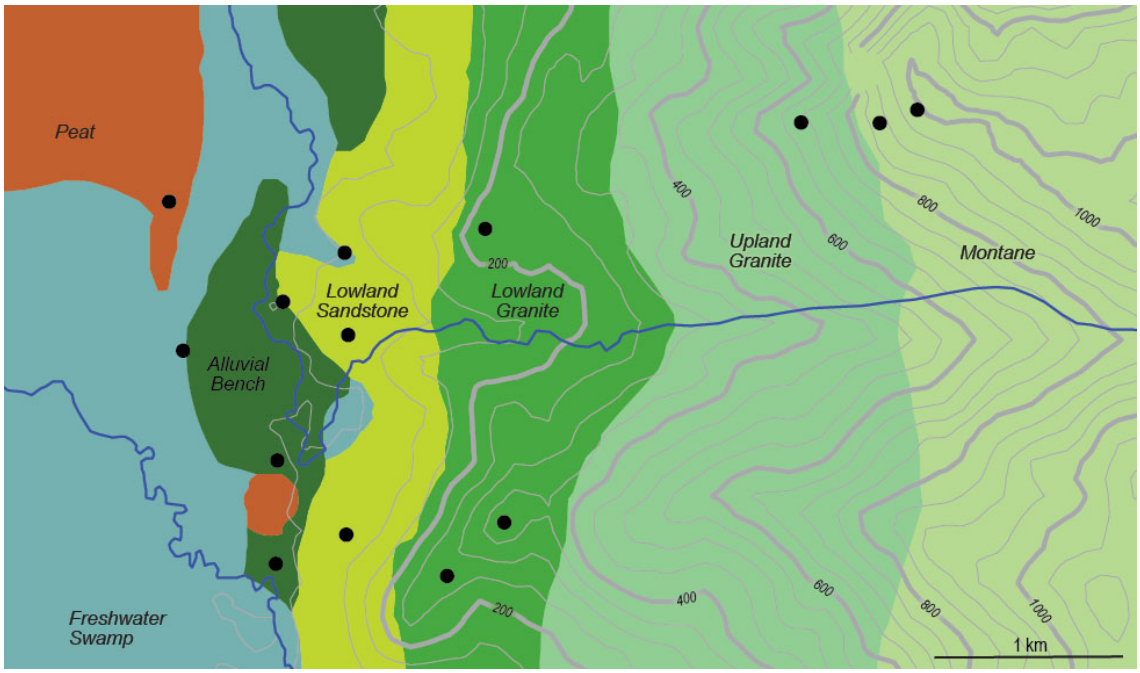

Figure 4.1. Map of habitat types and grouped site locations (black circles) at CPRS. Each grouped site represents three sampling sites (four in the freshwater swamp group).

Table 4.1. Description of soil and elevation of seven different forest types at CPRRS, as well as the number of locations sampled (groups) and the total number of sites sampled.

Forest Type	Basic Soil Description[3]	Elevation (m)	Number of Groups	Number of Sites (Total)
peat	Varying depths of organic matter overlying coarse sand; nutrient poor	5–10	1	3
freshwater swamp	Poorly drained; seasonally flooded; gleyic soils; nutrient rich	5–10	1	4
alluvial bench	Recently deposited from upstream sources; well-drained; frequently flooded; mixed sandstone and granite parent material; nutrient rich	5–50	3	9
lowland sandstone	Well drained; sandstone parent material with high clay content	20–200	3	9
lowland granite	Well-drained; granite parent material	200–400	3	9
upland granite	Well-drained; granite parent material	350–800	1	3
montane	Granite parent material	750–1100	2	6

[3] After Cannon and Leighton 2004, Paoli et al. 2006, 2008 and personal observations.

While restricting our sampling to the top 20 cm limits our ability to measure the full carbon pool, Jobbágy and Jackson (2000) found that the top 20 cm of the soil profile of tropical evergreen forests holds 30% of the carbon contained in the top 3 m. Furthermore, shallower sampling at each site enabled us to sample more sites.

2.3 Sample Analysis

We used one of the two parallel cores at each site for quantifying microcharcoal >0.5 mm. To quantify macrocharcoal, we soaked each segment in 10% sodium pyrophosphate ($Na_4P_2O_7$) to disperse colloids. We then sieved each segment at 2 mm and 0.5 mm and identified, isolated, counted, and weighed all macrocharcoal fragments in each size fraction (>2 mm and 0.5–2 mm) after drying at 60°C. We applied 3% hydrogen peroxide (H_2O_2) to the 0.5–2 mm fraction for approximately 4 hours to make it easier to separate charcoal from other organic matter. We then calculated the amount of macrocharcoal per square meter for each 5 cm segment, and for each size fraction, using the equation $\frac{g\ macrocharcoal}{m^2} = \frac{g\ macrocharcoal}{core\ volume\ cm^3} \times 5 \times 10{,}000$.

We used the second parallel core for measuring several soil properties. We dried each 5-cm segment at approximately 90°C in a liquid propane gas drying oven for 36 hours in the field and then removed all material (roots, rocks, etc.) >2 mm to calculate bulk density according to Kellogg Soil Survey Laboratory Method 3B6a (Soil Survey Staff 2014). We were then able to calculate the amount of macrocharcoal in each segment on a per mass basis, using the equation

$$\frac{mg\ macrocharcoal}{g\ soil} = \frac{g\ macrocharcoal}{core\ volume\ cm^3} \times \frac{1}{segment\ bulk\ density\ (\frac{g}{cm^3})} \times 1{,}000.$$ We measured the color of dried soils using a WR10 tristimulus colorimeter (FRU, Shenzen, China) by placing approximately 4 g of soil in an aluminum tin so the soil was a minimum

of 5 mm deep and placing the sensor above the soil surface. We took seven measurements from each sample, moving the sensor within the tin for each measurement, and used the mean value for each color variable (L, a, and b) for subsequent analyses.

We ground ca. 4 g subsamples of the second core (after removal of material >2 mm) to approximately 1 µm with a planetary ball mill. We used an ECS 4010 CHNSO elemental analyzer (Costech Analytical Technologies Inc., Valencia, CA, USA) at the University of Oregon to measure total carbon in the ground soil from each segment, and used the bulk density and the following equation to calculate the mass of carbon in each segment on a per square meter basis: $\frac{g\ macrocharcoal}{m^2} = \frac{\%\ carbon}{100} \times 5 \times BD \times 10{,}000$. We also calculated the mass of carbon per gram of soil.

To measure PyC in each sample, we followed a slightly modified version of the method presented in Kurth et al. (2006). We digested ca. 1 g of ground soil with 30% hydrogen peroxide and 1 M nitric acid (HNO_3) for 16 hours in a water bath at 90°C and then washed the sample through a pre-weighed Whatman #1 filter paper. We weighed each filter paper and residual material and measured the carbon content of the residual material using the same ECS 4010 CHNSO elemental analyzer. Assuming that the oxidation was complete and the digestion step removed all non-pyrogenic carbon, we then calculated the amount of PyC per gram of soil using the equation $\frac{mg\ PyC}{g\ soil} = \frac{C1 \times M1}{M2} \times 1000$, where M_1 = mass of digested sample, C_1 = % carbon of digested sample, and M_2 = mass of original sample. Hendricks et al. (in prep) found that the total carbon and PyC as measured by this method are strongly correlated, especially at low carbon percentages, despite an expectation of no correlation. This correlation suggests that a fraction of non-PyC survives the acid-peroxide digestion. We used percentile regression of PyC on total carbon to

statistically estimate this fraction, with the positive residuals from the regression line representing "adjusted PyC." A linear regression placed at the 10th percentile effectively reduced the correlation. After adjustment, we converted all values to a g PyC per square meter basis. Note that because we removed all material >2 mm—including macrocharcoal—prior to this analysis, these PyC values represents the amount of charcoal and other pyrogenic carbon products <2 mm in the soil. To obtain a more comprehensive value for soil PyC, we combined the adjusted PyC and macrocharcoal >2 mm values for each segment, giving us a "total PyC" value.

We measured pH and soil texture on un-ground subsamples. To measure pH, we used Kellogg Soil Survey Laboratory Method 4C1a2a1 to measure the 1:2 water pH by making a 1:2 soil to reverse osmosis water slurry, shaking on a shaker table overnight, and then measuring the pH of the supernatant just above the settled soil. We measured soil texture with a modified micro-pipette method based on Miller and Miller (1987). This method relies on Stoke's Law, which relates settling time and particle size, and involves weighing the amount of material that remains in solution at two pre-determined timepoints. After shaking overnight in solution with 0.5% sodium hexametaphosphate ($Na_6[PO_3]_6$) to disperse colloids, a small aliquot (2.5 mL) of sample is dispensed into a pre-weighed tin at approximately 12 seconds (exact times are temperature dependent), and another aliquot is dispensed into a second tin at approximately 122 minutes. The material still in solution and removed at the first timepoint consists of silt and clay, and the % sand (0.05–2 mm) is calculated by subtracting the amount in solution from 100. Material in solution that is removed at the second timepoint contains only clay (<0.002 mm), and the % clay is directly calculated. The % silt (0.002–-0.05 mm) is calculated by subtracting % sand and % clay

from 100. We then assigned each sample to the appropriate USDA texture classification using the % sand, silt, and clay values.

2.4 Statistical Analysis

We assessed soil properties by depth and forest type for six variables: bulk density, soil pH, soil color (L, a, and b), macrocharcoal (with 0.5–2 mm and >2 mm size fractions separated, as well as all material >0.5 mm), adjusted PyC, and total carbon.

To compare between depths, we used traditional analysis of variance. We performed this analysis for the entire data set as well as within each forest type. To compare between forest types, we calculated the mean value of each variable for each site for all variables except soil texture. We then used a parametric randomization procedure with 1000 simulations to compare between forest types due to violations of the assumptions of traditional analysis of variance (i.e., unequal number of samples per forest type). To do this, we used the *boot* package (Canty and Ripley 2020) in R (version 3.6.1; R Core Team 2019) to compare the F-ratio of the data to a distribution of F-ratios created by resampling. We performed post-hoc multiple comparisons via randomization (1000 simulations) where the null hypothesis was rejected, and then controlled for the family-wise error rate by correcting the resulting p-values using the Holm correction.

Finally, we assessed the relationship between our descriptive soil variables (bulk density, soil pH, soil color) and our carbon variables (total carbon, macrocharcoal, and PyC on a per mass basis) using ordinary least squares linear regression and Pearson correlations. Where the relationship between the variables was significant, we interpret the slope of the regression as the relationship between the variables. We the values for individual sample segments, rather than site means, so as to preserve relationships between the variables that

may vary throughout the soil profile. We used a similar approach to determine the relationship between our pyrogenic carbon data (macrocharcoal and PyC) and total carbon, with the slope of the regression line representing the portion of the total carbon pool made up of pyrogenic carbon. These analyses were performed for the entire data set as well as within each depth category and each forest type.

3. Results

3.1. Soil Description

3.1.1 Bulk Density

At the site level, bulk density ranges from 0.59 g/cm3 to 1.26 g/cm^3, with a mean value of 0.90 g/cm^3. In individual segments, bulk density can be as low as 0.05 g/cm^3 (peat site, 0–5 cm) and as high as 1.63 g/cm^3 (alluvial bench site, 15–20 cm). Bulk density varies significantly by forest type ($p << 0.001$); lowland sandstone sites have significantly higher bulk density than lowland granite and montane sites (Figure 4.2a). Across the entire research area, bulk density increases with depth; ANOVA reveals significant differences between depths ($p << 0.001$; Figure 4.2b), This overall trend also holds within each forest type, with differences being significant for all forest types except montane.

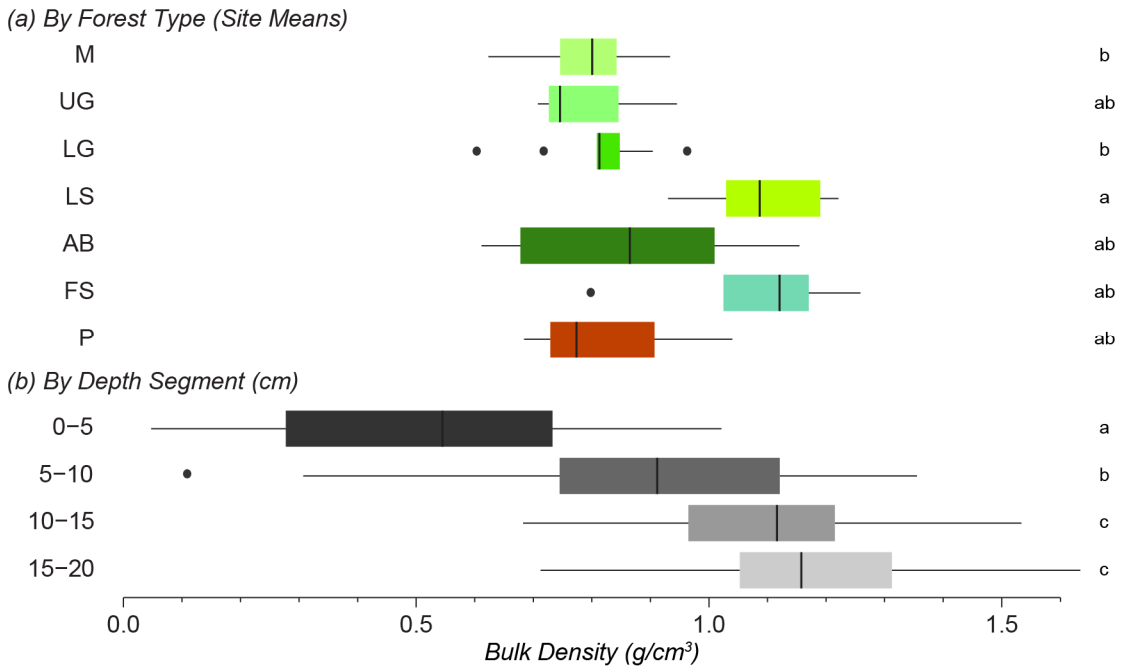

Figure 4.2. Bulk density (a) by forest type (site means) and (b) by sample depth range in centimeters (individual segments) for all sites at CPRS. In (a) small letters indicate significant differences as calculated with post-hoc multiple comparisons via randomization; in (b) small letters indicate significant differences as calculated by Tukey post-hoc tests. For forest type, M = montane (n = 6); UG = upland granite (n = 3); LG = lowland granite (n = 9); LS = lowland sandstone (n = 9); AB = alluvial bench (n = 9); FS = freshwater swamp (n = 4); P = peat (n = 3). All depths are measured in centimeters; 0−5 cm (n = 42); 5-10 cm (n = 41); 10−15 cm (n = 38); 15−20 cm (n = 35).

3.1.2 Soil Texture

Clay and/or sand are dominant features of most samples; with a few exceptions (mostly alluvial bench and lowland sandstone sites), most soil segments contain very little silt (Figure 4.3). The most common USDA soil classifications are clay and sandy clay loam (n = 36, respectively), followed by sandy loam (n = 21) and clay loam (n = 17). Peat sites tend to be the most different, with the most sand and the least clay (loamy sand and sandy loam). In general, sand decreases and clay increases with depth. We were unable to measure soil texture for 14 segments, distributed between 8 sites.

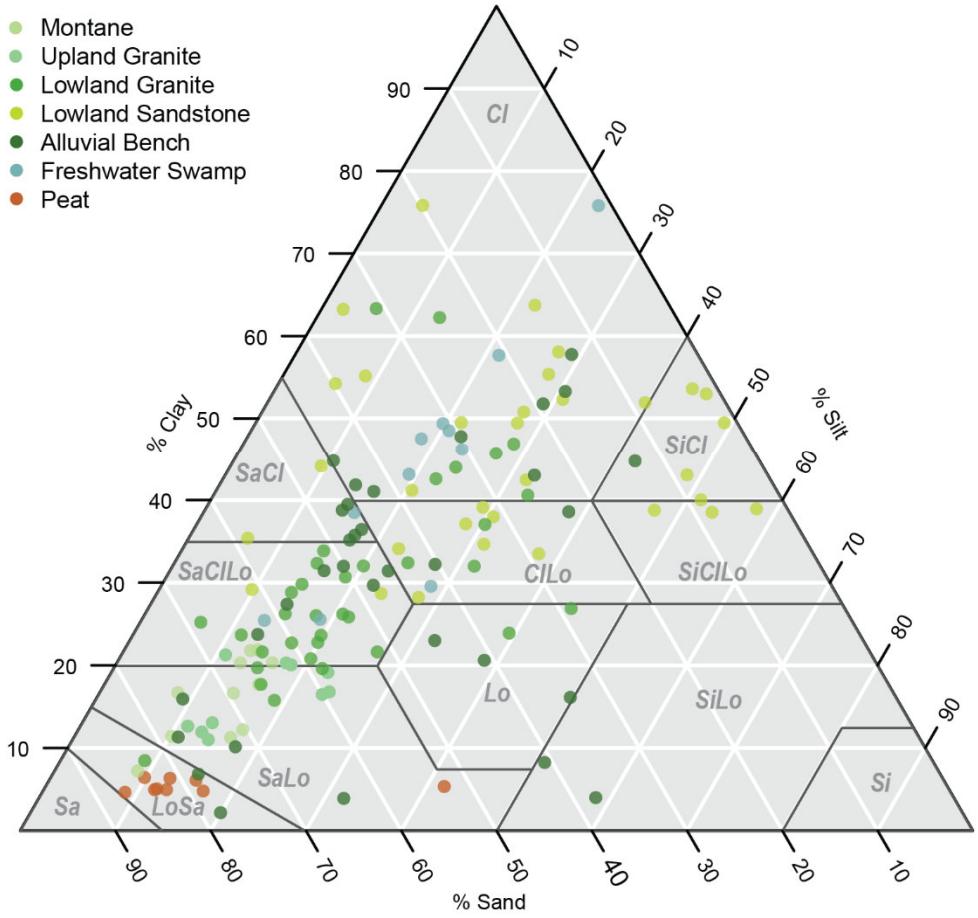

Figure 4.3. Soil texture of all individual segments from CPRS, colored by forest type (n = 372). Cl = clay; SiCl = silty clay; SaCl = sandy clay; ClLo = clay loam; SiClLo = silty clay loam; SaClLo = sandy clay loam; Lo = loam; SiLo = silty loam; SaLo = sandly loam; LoSa = loamy sand; Sa = sand; and Si = silt.

3.1.3 Soil pH

Soils at CPRS are acidic, with site means ranging from 3.77 to 4.74, with a mean value of 4.36. pH varies substantially by forest type, but differences are not significant according our randomization method (Figure 4.4a). In general, pH increases with depth, and differences are significant ($p << 0.001$; Figure 4.4b).

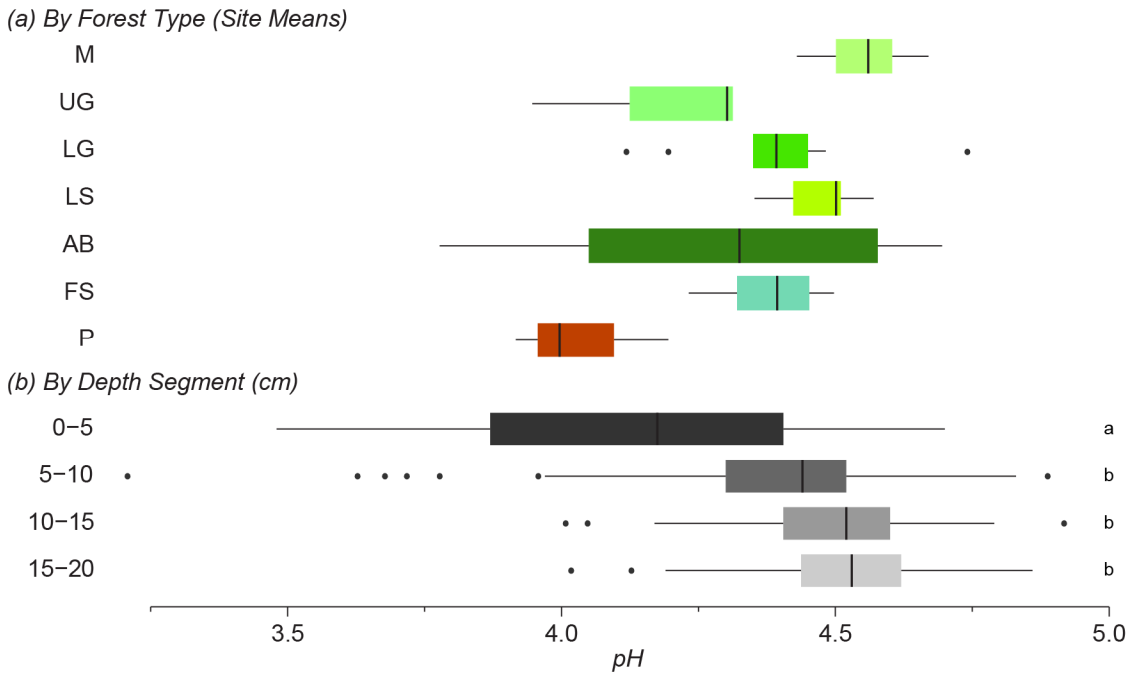

Figure 4.4. pH from a 1:2 soil to water slurry (a) by forest type (site means) and (b) by sample depth (individual segments) for all sites at CPRS. In (b), small letters indicate significant differences as calculated by Tukey post-hoc tests. For forest type, M = montane (n = 6); UG = upland granite (n = 3); LG = lowland granite (n = 9); LS = lowland sandstone (n = 9); AB = alluvial bench (n = 9); FS = freshwater swamp (n = 4); P = peat (n = 3). All depths are measured in centimeters; 0−5 cm (n = 34); 5-10 cm (n = 37); 10−15 cm (n = 35); 15−20 cm (n = 32).

3.1.4 Soil Color

In general, soils tend towards black (L), red (a), and yellow (b) (Figure 4.5). Differences are significant by forest type for L, a, and b values ($p << 0.01$, $p << 0.01$, and $p = 0.01$, respectively; Figure 4.5s). L, a, and b values all increase with depth through the soil profile; this corresponds to soil color getting lighter (more white), redder, and more yellow (Figure 4.5n). Whereas L values do vary significantly with depth ($p << 0.001$), differences are not significant by depth for a or b values.

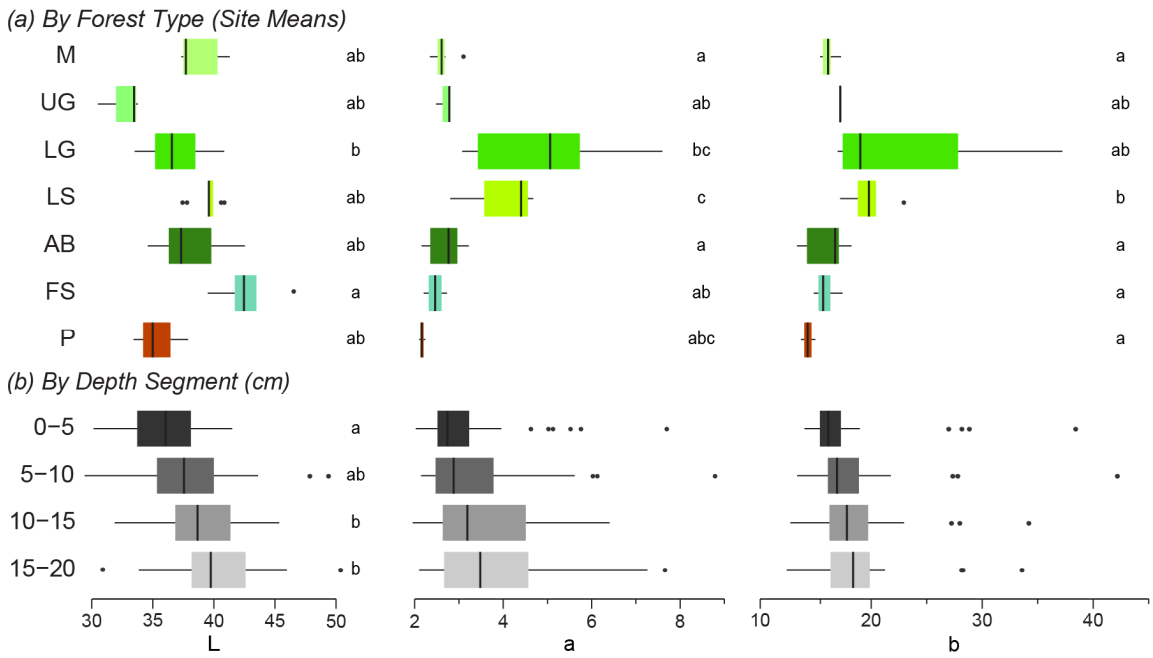

Figure 4.5. Soil color (a) by forest type (site means) and (b) by sample depth (individual segments, cm) and for all sites at CPRS. Small letters in (a) indicate significant differences post-hoc multiple comparisons via randomization; small letters in (b) indicate significant differences as calculated by Tukey post-hoc tests. For forest type, M = montane (n = 6); UG = upland granite (n =v 3); LG = lowland granite (n = 9); LS = lowland sandstone (n = 9); AB = alluvial bench (n = 9); FS = freshwater swamp (n = 4); P = peat (n = 3). All depths are measured in centimeters; 0−5 cm (n = 42); 5-10 cm (n = 41); 10−15 cm (n = 38); 15−20 cm (n = 35).

3.2 Macrocharcoal and PyC

3.2.1 Macrocharcoal >0.5 mm

Macrocharcoal is ubiquitous in the soils of CPRS, with only seven of 43 sites having mean macrocharcoal values of 0. At the site level, total macrocharcoal values range from 0 to 2.09 mg/g soil, with a mean value of 0.25 mg/g soil. The maximum amount of macrocharcoal in an individual segment is 3.35 mg/g soil. There are no significant differences in the amount of macrocharcoal > 0.5 mm by depth or by forest type (Figure 4.6a; Figure 4.7a).

The masses of charcoal in the two size classes of macrocharcoal are poorly correlated ($R^2 = 0.35$). The strength of the correlation between the two size classes increases with depth (Table 4.2).

3.2.1.1 Macrocharcoal >2 mm

The amount of macrocharcoal >2 mm at the site level ranges from 0 to 1.21 mg/g soil, with the maximum amount in a single segment being 2.32 mg/g soil. 11 sites had no macrocharcoal >2 mm. Again, there are no significant differences in the amount of macrocharcoal in this size class by depth or by forest type (Figure 4.6b; Figure 4.7b).

3.2.1.2 Macrocharcoal 0.5–2 mm

Divided by size class, the amount of macrocharcoal 0.5–2 mm at a site ranges from 0 to 0.88 mg/g soil, though the maximum amount of macrocharcoal in the same size class in a single segment is 1.44 mg/g soil. 14 sites had no macrocharcoal 0.5–2 mm, including all peat sites and all upland granite sites. There are no significant differences in the amount of macrocharcoal in this size class by depth or by forest type (Figure 4.6c; Figure 4.7c).

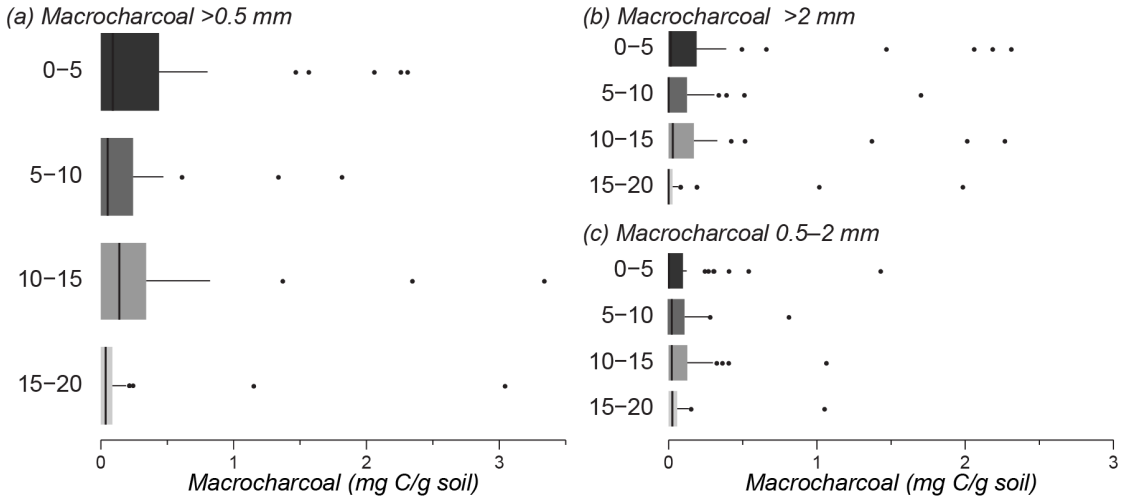

Figure 4.6. Macrocharcoal by depth for (a) all macrocharcoal >0.5 mm, (b) macrocharcoal >2 mm, and (c) macrocharcoal 0.5–2 mm. There are no significant differences between depths for any of the size classes. All depths are measured in centimeters; 0−5 cm (n = 42); 5-10 cm (n = 41); 10−15 cm (n = 38); 15−20 cm (n = 35).

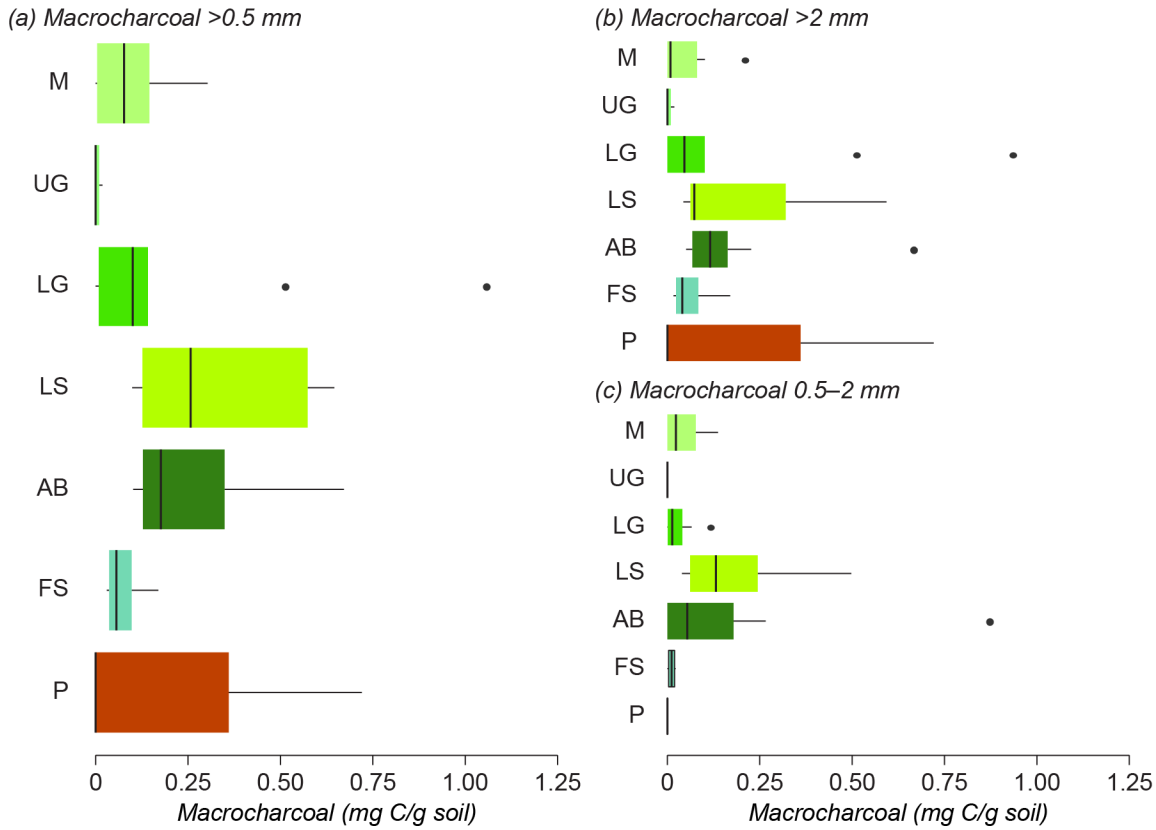

Figure 4.7. Macrocharcoal by forest type for (a) all macrocharcoal >0.5 mm, (b) macrocharcoal >2 mm, and (c) macrocharcoal 0.5–2 mm. There are no significant differences between depths for any of the size classes. For forest type, M = montane (n = 6); UG = upland granite (n =v 3); LG = lowland granite (n = 9); LS = lowland sandstone (n = 9); AB = alluvial bench (n = 9); FS = freshwater swamp (n = 4); P = peat (n = 3).

Table 4.2. Pearson correlation coefficients between macrocharcoal >2 mm and macrocharcoal 0.5-2 mm by depth (all data).

Depth (cm)	R
0–5	-0.072
5–10	0.340
10–15	0.669
15–20	0.906

3.2.2 PyC

3.2.2.1 PyC <2 mm

A 10th percentile regression effectively decreased the strength of the relationship between total carbon and PyC (R^2 = 0.544 before correction; R^2 = 0.268 after correction; Figure 4.8). All following PyC values reported are "adjusted" PyC values, which are the positive residuals from the regression line.

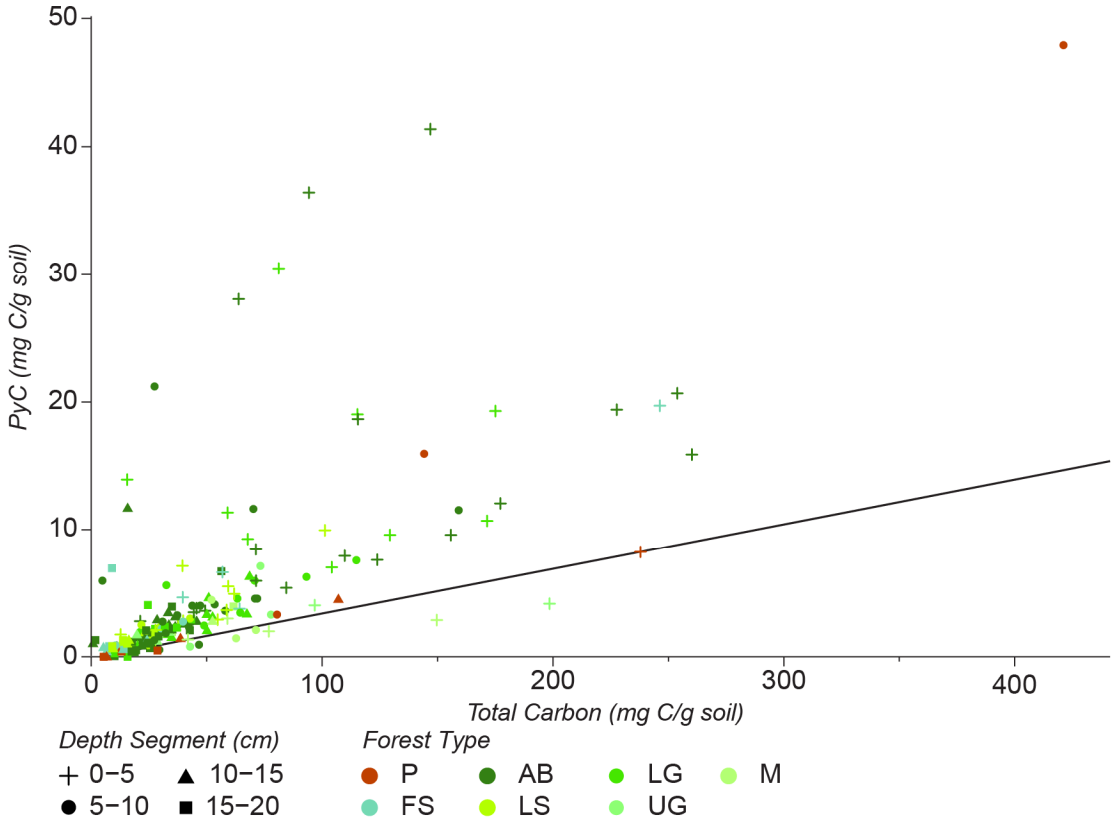

Figure 4.8. Relationship between total carbon and unadjusted PyC for individual segments at CPRS. The black regression line is the 10th percentile regression used to adjust PyC values. For forest type, M = montane; UG = upland granite; LG = lowland granite; LS = lowland sandstone; AB = alluvial bench; FS = freshwater swamp; P = peat. All depths are measured in centimeters.

Mean PyC (adjusted) at each site ranges from 0 to 18.21 mg/g soil. Again, PyC is ubiquitous; only two sites (of 43) have no PyC and the maximum amount of PyC in a single segment is 36.34 mg/g soil. In general, PyC decreases with increasing soil depth; segments from 0–5 cm have significantly more charcoal than other depths ($p << 0.01$). In particular, upland granite sites tend to have more charcoal in deeper segments, though the differences are not significant. Differences between forest types are not significant.

3.2.2.2 Total PyC (Adjusted PyC and Macrocharcoal >2 mm)

When the amount of macrocharcoal >2 mm is combined (by individual segment) with adjusted PyC data to assess total PyC (adjusted PyC and macrocharcoal >2 mm), the differences in the mass of total PyC between forest types are significant ($p = 0.04$; Figure

4.9a). This result is driven by significant differences between lowland granite and montane sites and lowland sandstone sites ($p << 0.01$). Similar to adjusted PyC, total PyC decreases with increasing soil depth; the topmost segments have significantly more charcoal (Figure 4.9b).

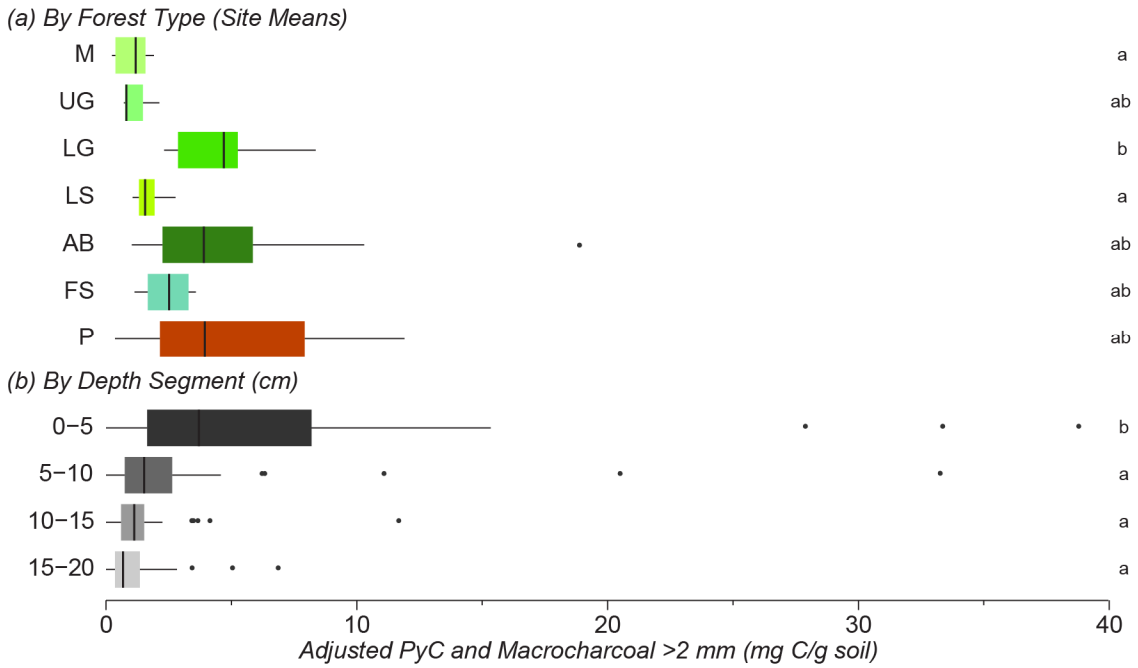

Figure 4.9. Total PyC (adjusted PyC and macrocharcoal >2 mm) (a) by forest type (site means) and (b) by depth for all sites at CPRS. In (a) small letters indicate significant differences as calculated with post-hoc multiple comparisons via randomization; in (b), small letters indicate significant differences as calculated by Tukey post-hoc tests. For forest type, M = montane (n = 6); UG = upland granite (n =v 3); LG = lowland granite (n = 9); LS = lowland sandstone (n = 9); AB = alluvial bench (n = 9); FS = freshwater swamp (n = 4); P = peat (n = 3). All depths are measured in centimeters; 0−5 cm (n = 39); 5-10 cm (n = 41); 10−15 cm (n = 38); 15−20 cm (n = 35).

3.7 Total Carbon

Mean total C ranges from 15.24 to 240.93 mg/g soil. The highest amounts of total C in an individual segment is nearly double the maximum site mean, at 420.31 mg/g soil. The mean amount of total carbon per site is 57.08 mg/g soil. There are significant differences by forest type, though again this largely due to significant differences between lowland granite and lowland sandstone sites, as well as lowland granite and montane sites ($p <<$

0.01; Figure 4.10a). The topmost portions of the soil profile (0–5 cm) have significantly more carbon than other soil segments ($p << 0.01$; Figure 4.10b).

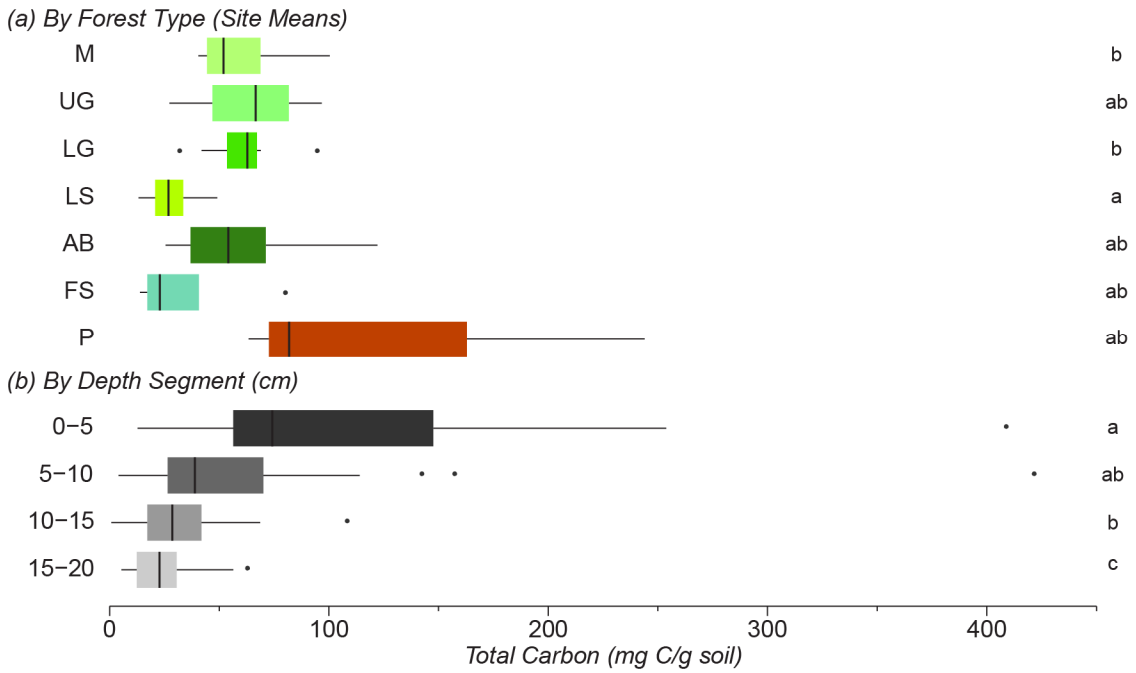

Figure 4.10. Total carbon (a) by forest type (site means) and (b) by depth for all sites at CPRS. In (a) small letters indicate significant differences as calculated with post-hoc multiple comparisons via randomization; in (b), small letters indicate significant differences as calculated by Tukey post-hoc tests. For forest type, M = montane (n = 6); UG = upland granite (n =v 3); LG = lowland granite (n = 9); LS = lowland sandstone (n = 9); AB = alluvial bench (n = 9); FS = freshwater swamp (n = 4); P = peat (n = 3). All depths are measured in centimeters; 0–5 cm (n = 40); 5-10 cm (n = 41); 10–15 cm (n = 38); 15–20 cm (n = 35).

3.8 Relationship Among Parameters

Across the entire research area, the strongest predictors of total carbon content are bulk density, pH, and darkness (L); all three are negatively correlated with total carbon (Table 4.3). The same three variables are also the strongest predictors of total PyC, though the correlations are weaker (Table 4.3). Other predictors, including redness (a) and yellowness (b) are only weakly correlated or effectively uncorrelated with either of our carbon variables. Additionally, while soil redness and yellowness are strongly correlated with each other ($r = 0.89$), but neither is correlated with L. No soil texture variable (% sand, % silt, or % clay) is correlated with either total carbon or total PyC. It is also worth noting

that none of our measures of pyrogenic carbon (macrocharcoal 0.5–2 mm, macrocharcoal >2 mm, macrocharcoal >0.5 mm, PyC, and PyC + macrocharcoal >2 mm) are correlated, with the exception of variables that are the sum of two variables (macrocharcoal >0.5 mm and PyC + macrocharcoal >2 mm) being correlated with one or both of their constituents.

Table 4.3. Pearson correlation coefficients for all CPRS sites with bulk density, pH, and soil darkness.

	Bulk Density	**pH**	**Darkness (L)**
Total Carbon	-0.75	-0.62	-0.46
Total PyC	-0.61	-0.59	-0.32

In general, our predictor variables and total carbon exhibit opposite trends with depth (Table 4.4); bulk density, pH, and soil darkness vary more with increasing depth, whereas total carbon varies less with increasing depth. Consequently, the strength of the correlation between each predictor variable and total carbon tends to be strongest in 0–5 cm and 5–10 cm segments and weaker for deeper segments. The relationship between each predictor variable and total carbon also becomes less extreme for deeper soil segments; for example, total carbon decreases four times faster with increasing bulk density for 0–5 cm segments compared to 15–20 cm. Total PyC has a similar relationship with our predictor variables, though the correlations with each depth segment are generally weaker. Also of note is that the relationship between total PyC and L value is only significant for the 5–10 cm segment.

Table 4.4. Results of linear regression and Pearson correlations for total carbon and total PyC (adjusted PyC + macrocharcoal >2 mm) for bulk density, pH, and soil darkness by forest type and by depth. Significance codes for slopes are as follow: * = 0.05, ** = 0.001, *** = 0.

		Bulk Density			**pH**			**Soil Darkness (L)**		
		slope		correlation	slope		correlation	slope		correlation
Total Carbon	peat	-233.15	**	-0.9	-107.74	**	-0.85	-38.17	**	-0.81
	freshwater swamp	-173.45	***	-0.92	-203.84	***	-0.91	-6.66	*	-0.54
	alluvial bench	-128.62	***	-0.77	-80.46	**	-0.53	-4.69	--	-0.29
	lowland sandstone	-58.94	***	-0.7	-71.44	*	-0.42	-3.7	*	-0.42
	lowland granite	-96.45	***	-0.74	-81.94	***	-0.67	-6.04	**	-0.52
	upland granite	-140	**	-0.91	-150.33	**	-0.94	-11.03	--	-0.38
	montane	-102.38	*	-0.64	-149.92	*	-0.62	-9.47	--	-0.59
	0-5 cm	-212.13	***	-0.72	-128.97	***	-0.7	-11.5	**	-0.46
	5-10 cm	-188.45	***	-0.75	-52.45	**	-0.55	-6.99	**	-0.42
	10-15 cm	-54.39	**	-0.5	-2.43	--	-0.03	-2	*	-0.35
	15-20 cm	-45.14	***	-0.69	-4.78	--	-0.06	-0.89	--	-0.24
Total PyC	peat	-12.65	*	-0.67	-7.92	**	-0.84	-1.96	--	-0.59
	freshwater swamp	-7.71	**	-0.78	-7.79	**	-0.67	-0.15	--	-0.24
	alluvial bench	-16.29	***	-0.66	-7.78	***	-0.68	-1.01	*	-0.42
	lowland sandstone	-4.02	***	-0.63	-1.9	--	-0.14	-0.25	*	-0.37
	lowland granite	-13.98	***	-0.77	-12.64	***	-0.75	-0.67	*	-0.41
	upland granite	-0.06	--	-0.02	-0.79	--	-0.2	0.07	--	0.1
	montane	1.2	--	0.25	3.73	--	0.52	0.1	--	0.21
	0-5 cm	-18.92	**	-0.57	-9.09	**	-0.54	-0.78	--	-0.29
	5-10 cm	-14.62	***	-0.66	-6.39	**	-0.63	-0.49	*	-0.33
	10-15 cm	-3.83	*	-0.38	-2.76	*	-0.34	-0.12	--	-0.23
	15-20 cm	-2.82	*	-0.42	-1.4	--	-0.18	0.05	--	0.13

There are no consistent trends across forest types for our different predictor variables for either total carbon or total PyC (Table 4.4). Although total carbon in peat sites is strongly correlated with each of our predictor variables, lowland sandstone sites consistently exhibit weaker correlations with total carbon. Of particular note is that soil darkness is most strongly correlated with total carbon in peat sites (and the relationship between darkness and total carbon is the most extreme of the forest types), but the relationship between soil darkness and total PyC is not significant (despite having the strongest correlation of all forest types). Overall, total PyC exhibits weaker correlations—and in several cases, a positive correlation where the other forest types are negatively correlated—with bulk density, pH, and soil darkness in upland granite and montane sites.

3.9 Carbon Pools

Using PyC combined with macrocharcoal >2 mm (total PyC) as the most complete representation of all pyrogenic matter, total PyC comprises approximately 5.4% of the total carbon pool across CPRS ($p << 0.01$). Within individual habitats, peat and alluvial bench sites have the highest amount of total PyC at 6.8% and 6.2%, respectively ($p = 0.001$; $p = 0.008$, respectively). The relationship between total PyC and total carbon is not significant for upland granite or montane sites. Total PyC content is greatest in the 5–10 cm segment, at 6.8% ($p << 0.01$).

Across the site, the mean amount of total carbon in the top 20 cm of the soil profile is 6763.9 ± 72.9 g/m^2; the mean amount of total PyC is 386.2 ± 8.4 g/m^2. By forest type, peat has the total carbon pool at over 8,300 g/m^2, but the smallest total PyC pool at only 173 g/m^2. The largest total PyC pool is found in alluvial bench forest, with over 550 g/m^2 (see Table 4.5).

Table 4.5. Mean total carbon and total PyC pools (g/m^2 ± SE) by forest type for the upper 20 cm of the soil profile. Note that we have not included sites where we were unable to sample the full 20 cm in these calculations; consequently, we do not have carbon pool measurements for upland granite or montane forest types.

Forest Type	Total Carbon (g/m^2)	Total PyC (g/m^2)
peat	8342.9 (1121.9)	172.6 (48.5)
freshwater swamp	4682.7 (270.8)	337.4 (53.2)
alluvial bench	7350.6 (323.1)	552.5 (51.6)
lowland sandstone	5785.1 (179.2)	291.3 (12.3)
lowland granite	7908.7 (287.9)	446.7 (14.6)

4. Discussion

In the soils of CPRS, PyC makes up a small but non-negligible portion of the total soil organic carbon pool at approximately 5%. This is much higher than the 1% posited by Bird et al. (2015) for tropical wet forests, though their estimate was based on highly generalized values for the fraction of total carbon made up of PyC. As PyC decomposition is governed by different kinetics than non-pyrogenic carbon, with much longer turnover times for PyC, this highlights the importance of explicitly including PyC in carbon stock calculations. PyC is an important pool of carbon in tropical rainforest soils, particularly given its potential for long-term storage of carbon.

Furthermore, the amount of PyC that can be quantified with a chemical method is orders of magnitude more than what we were able to identify even with a microscope. This underlines the importance of the PyC continuum concept; if our estimate of PyC content relied only on macrocharcoal, its contribution to the total carbon pool would be negligible (less than 0.1%). Our work is also consistent with findings by Zimmerman and Mitra (2017) that different methods of quantifying PyC are not interchangeable, and comparing PyC pools estimated with different methods must be undertaken with extreme caution.

We found the most carbon—total and PyC—in the topmost soil segments and in peat, alluvial bench, and granite-derived soil types. Our finding of more PyC in upper soil

segments is consistent with the findings of da Silva Carvalho et al. (2018) of more soil in shallower soil segments in Amazonian forest. However, that study assessed the first meter of the soil profile and found the most PyC between 30 and 40 cm in ombrophilous forest, which could suggest that our data grossly underestimates the total PyC because of our shallow sampling depth. Koele et al. (2017) found that soil profiles in the Amazon Basin must be sampled to at least 71 cm to capture 50% of the PyC contained in the whole profile. As Koele et al. (2017) used hydrogen pyrolysis (HyPy) to quantify PyC, their data are more easily comparable to our values from the KMD method. Nevertheless, our soil profiles exhibited a significant decrease in PyC from the first 0–5 cm of the soil profile to deeper segments that was not present in the soils sampled by either da Silva Carvalho et al. (2018) or Koele et al. (2017). The findings of Turcios et al. (2016) are more consistent with our data; they found that PyC stocks were highest in upper, rather than intermediate, soil segments and that their results are consistent with some other studies from ecotones to areas of deforestation Amazonia. Clearly, there is no consistent global pattern in the vertical distribution of PyC in soil profiles across tropical regions; the different forest types, fire histories, and land use histories likely play an important role in vertical soil carbon distribution.

The significant differences in PyC pools among forest types could reflect different fire histories within each site; sites with a more recent history of fire, or that experience fire more often, would likely have more PyC in their soils. Although moisture is thought to accelerate degradation of PyC—particularly with alternating wet and dry conditions—we did not find significantly less PyC in freshwater swamp sites where there is often standing water (Foereid et al. 2011). Similarly, there are significant differences in total carbon by

forest type, suggesting that carbon input and/or decomposition dynamics vary across forest types in tropical rainforest.

Compared to other tropical rainforest areas, PyC pools are substantially smaller at CPRS. The aforementioned differences in the vertical distribution of PyC make direct comparison difficult, but if we were to assume that our PyC stock for the top 20 cm of the profile represents only 1/5 of the carbon stock for the top 1 m of the soil profile, carbon stocks at CPRS (1931 g PyC/m^2 for top 1 m of profile) are only 53–86% of the estimates from Amazonia (Table 4.6). Even the forest type with the highest carbon stock—alluvial bench, 2763 g PyC/m^2—still contains less carbon than estimates from da Silva Carvalho et al. (2018) and Koele et al. (2017), and this is likely vastly overestimating the carbon stock for this forest type. Furthermore, da Silva Carvalho et al. (2018) did not include any charcoal material <2 mm, and they note that their estimates of PyC stocks are consequently very conservative.

Table 4.6. PyC stocks for the top 1 m of the soil profile from three studies in the Amazon Basin.

Study Authors	**PyC Stock (g/m^2, 0-100 cm)**
da Silva Carvalho et al. (2018)	3460
Koele et al. (2017)	3620
Turcios et al. (2016)	2240

If we use a similar scaling approach to estimate total carbon pools for the top 1 m of the soil profile at CPRS, we find that the size of carbon stocks at CPRS are consistent with other data from Borneo. Saner et al. (2012) estimated a mean soil organic matter pool size of 3960 g C/m^2 for the top 1 m of the soil profile at 13 previously logged (22 years before sample collection) lowland dipterocarp forest sites in Sabah (Malaysian Borneo), and note that the highest concentrations were found in the top segments of their soil profile. Despite the different land use histories (logged vs. primary forest), our finding of ca. 3380 g C/m^2 across CPRS is consistent with their estimate. Unlogged forest plots elsewhere in

Peninsular Malaysia had much higher carbon stocks (8786 g C/m^2; Abdullahi et al. 2018); it is possible that the high sand content of the soils—and particular, the peat—at CPRS results in less physical protection of soil organic carbon (Razafimbelo et al. 2013).

Although there are significant differences among both forest types and soil depth for most of our soil variables and our measures of pyrogenic and total carbon, the differences are not consistent. Unlike Reisser et al. (2016), we did not find soil properties to be particularly good predictors of PyC. In that study, clay content and soil pH were strong predictors of PyC content. In particular, there was essentially no relationship between clay content and PyC at CPRS. While we did find that pH was moderately correlated with total PyC (soils with a higher pH tended to have less PyC)—the opposite of the relationship found by Reisser et al. (2016). Only montane sites exhibited a positive relationship between PyC and pH, and the correlation was weaker than many other forest types. However, all of our soils had a pH below 5; in that study, they found that soils with a pH below 5 contained much less PyC than soils that were neutral or basic, and it is possible that the relationship between pH and PyC reverses in acidic soils. Furthermore, their study only included four tropical sites—located in the Amazon basin and Central Africa—out of 55 total sites, and the studies drawn from used a variety of approaches to quantify PyC.

We did not find soil color to be a particularly good indicator of either total or PyC content. Unlike in Liles et al. (2013), darkness and redness (L and a, respectively), were not correlated in our soils from CPRS, so it is unlikely that redness is interfering with the relationship. Although that study did examine a broad range of soil orders (Andisols, Alfisols, Inceptisols, Ultisols), our data suggests that carbon contents in tropical soils are more difficult to predict.

5. Conclusions

This study represents one of the first attempts to explicitly quantify PyC in mineral soils from equatorial tropical rainforest of Southeast Asia. We found that PyC is an important component of total carbon pools. Given the long turnover time of PyC relative to non-pyrogenic carbon, explicitly including PyC in carbon pool assessments as well as carbon cycle models is important in tropical rainforest soils. Both pyrogenic and total organic carbon are concentrated in upper portions of the soil profile. However, while there are some differences by forest type, the differences are smaller than expected and mostly restricted to differences between lowland sandstone and lowland granite forest types—two types that are superficially similar and coincident in space, but on soil with different parent materials. However, in general, soil properties are not a good predictor of either PyC or total carbon content, despite relationships observed elsewhere in the tropics. More work is needed to identify the factors most important for predicting carbon pools in the tropical rainforest soils of southwestern Borneo.

CHAPTER V

SUMMARY AND CONCLUSIONS

Despite its perceived historical rarity, fire has been and continues to be an important disturbance in the tropical rainforests of southwestern Borneo. This research set out to improve our understanding of fire in the rainforest in the last 3,200 years, as well as how past fire events are important to modern carbon pools and carbon cycling through the production of PyC. In Chapter II, I explore when and where fires occurred with the goal of elucidating the role humans have played in tropical forest fire. Chapters III and IV focus on a major consequence of fire, the transfer of living biomass such as vegetation to the soil carbon pool by way of combustion and the production of PyC. Though it has been often overlooked in the past, PyC is an important element of soil carbon due to its recalcitrance to decomposition and thus its tendency to persist in soil for hundreds to thousands of years. As a more stable pool compared to non-pyrogenic soil carbon, it is important to explicitly include PyC in future models of carbon pools and turnover time.

In this dissertation, I find that humans have played an important role in the occurrence of fire in the tropical rainforest of CPRS in the late Holocene. Evidence of fire—charcoal >2 mm—is more abundant in forest types where humans would be more likely to live and/or practice swidden agriculture. However, pyrogenic material is ubiquitous across CPRS, showing that all seven forest types have experienced fire in the last millennia. Whereas fire occurred in lowland forest types—where human-caused fire is most likely—throughout the last 3200 years, fire in upland forest types is almost exclusively during periods of major regional drought that have been extensively documented elsewhere in Southeast Asia, when fires could easily creep upslope. Current

fires, which are often ignited by humans but spread into primary rainforest during periods of drought, are mirroring patterns of fire spread that occurred hundreds of years ago, though the scale of burned area is likely different.

Chapters III and IV show that PyC is an important component of total carbon pools (5%) at CPRS. The nitric acid-peroxide digestion (KMD method) I used is straightforward and does not require the use of any particularly dangerous reagents, is easily accomplished in any standard lab with a fume hood, and can be modified for high throughput. Many labs (commercial as well as academic) offer CN analysis for a small fee. Given its precision and accuracy in quantifying PyC in standards, it is an appropriate choice for quantifying PyC in unknown soils from areas where fires typically burn >400°C, including tropical rainforest. Although our finding that there is a small portion of non-pyrogenic carbon that is sufficiently recalcitrant to not be oxidized by the digestion process is an important caveat, it is easily overcome with standard statistical methods. Increased use of the KMD method will enable better quantification of PyC pools in soils from across the globe.

Although the history of fire in tropical rainforest is often not visible on first look, this work shows that fire has had an important role throughout the late Holocene at Gunung Palung National Park. The presence of many very large, emergent trees today shows that these forests have largely recovered from the fire events of approximately 300–500 years, though other imprints of fire on the landscape may remain to be discovered. Future work should pair community diversity data with fire history, to determine if there is an imprint of fire on the plant communities of CPRS. Continued study of PyC production and persistence in soil carbon pools will also be an important contribution to global carbon budgets and carbon cycling models.

This work does not suggest that recent fire events are merely a return to a period of higher fire incidence in rainforest and not a cause for concern. Furthermore, we cannot assume that forests will exhibit the same resiliency that they have shown in the past. It simply shows that fire is not unprecedented in tropical rainforest and that humans have contributed to the occurrence of fire for millennia. As fire continues to be a major disturbance in modern rainforest, it is important to continue to monitor how these forests respond to fire.

APPENDIX

Appendix Table 2.1. Metadata for ^{14}C dated macrocharcoal pieces.

Lab Code	Site ID	Depth (cm)	Forest Type	Forest Group Type	Zone	^{14}C Age (BP)	Year of Fire (95%)	F Modern
OS-142579	RB14 D	0-5	peat	inundated	non-ridge	--	1976*	1.3620 ± 0.0027
OS-151677	FK10 J	15-20	freshwater swamp	inundated	non-ridge	455 ± 15	1440 CE (1428–1450 CE)	--
OS-142631	JM12 B	0-5	freshwater swamp	inundated	non-ridge	220 ± 70	1741 CE (1498–1505 CE)	--
OS-151680	MB21 L	10-15	freshwater swamp	inundated	non-ridge	--	2004*	1.0860 ± 0.0028
OS-142576	BM10 E	0-5	alluvial bench	lowland	non-ridge	310 ± 15	1556 CE (1517–1595 CE)	--
OS-142447	BM10 E	15-20	alluvial bench	lowland	non-ridge	2310 ± 15	391 BCE (401–376 BCE)	--
OS-142448	BM10 E	22	alluvial bench	lowland	non-ridge	1970 ± 20	33 CE (35 BCE–28 CE)	--
OS-144387	CH08 B	15-20	alluvial bench	lowland	non-ridge	1260 ± 20	727 CE (678–773 CE)	--
OS-144390	CH08 E	0-5	alluvial bench	lowland	non-ridge	890 ± 15	1157 CE (1048–1085 CE)	--
OS-144388	ES01 A	0-5	alluvial bench	lowland	non-ridge	385 ± 15	1475 CE (1449–1511 CE)	--
OS-144389	ES01 A	15-20	alluvial bench	lowland	non-ridge	445 ± 15	1443 CE (1431–1454 CE)	--
OS-135952	ES01 B	5-10	alluvial bench	lowland	non-ridge	395 ± 15	1466 CE (1445–1494 CE)	--
OS-142577	MT01 D	0-5	alluvial bench	lowland	non-ridge	445 ± 15	1443 CE (1431–1454 CE)	--
OS-142575	MT01 D	15-20	alluvial bench	lowland	non-ridge	385 ± 15	1475 CE (1449–1511 CE)	--
OS-135947	MT01 F	0-5	alluvial bench	lowland	non-ridge	455 ± 15	1440 CE (1428–1450 CE)	--
OS-135949	MT01 F	10-15	alluvial bench	lowland	non-ridge	2170 ± 20	301 BCE (354–2)	--
OS-135950	MT01 F	15-20	alluvial bench	lowland	non-ridge	2170 ± 20	301 BCE (354–284 BCE)	--
OS-135948	MT01 F	5-10	alluvial bench	lowland	non-ridge	385 ± 20	1480 CE (1446–1519 CE)	--
OS-142578	RB05 C	15-20	alluvial bench	lowland	non-ridge	1820 ± 20	187 CE (132–240 CE)	--
OS-153009	RB05 D	5-10	alluvial bench	lowland	non-ridge	2950 ± 20	1162 BCE (1224–1106 BCE)	--
OS-142573	BK03 D	15-20	lowland sandstone	lowland	south ridge	1000 ± 15	1022 CE (994–1038 CE)	--

Appendix Table 2.1, continued. Metadata for ^{14}C dated macrocharcoal pieces.

Lab Code	Site ID	Depth (cm)	Forest Type	Forest Group Type	Zone	^{14}C Age (BP)	Year of Fire (95%)	F Modern
OS-142450	MT04 B	15-20	lowland sandstone	lowland	north ridge	1420 ± 15	633 CE (607–652 CE)	--
OS-151686	PB07 B	0-5	lowland sandstone	lowland	south ridge	325 ± 15	1566 CE (1494–1509 CE)	--
OS-151684	PB07 B	15-20	lowland sandstone	lowland	south ridge	460 ± 20	1438 CE (1422–1451 CE)	--
OS-142446	SC03 D	0-5	lowland sandstone	lowland	north ridge	645 ± 15	1363 CE (1288–1316 CE)	--
OS-142451	SC03 D	15-20	lowland sandstone	lowland	north ridge	2020 ± 20	18 BCE (86–76 BCE)	--
OS-151683	TL14 C	0-5	lowland sandstone	lowland	north ridge	385 ± 15	1475 CE (1449–1511 CE)	--
OS-151682	TL14 C	15-20	lowland sandstone	lowland	north ridge	430 ± 20	1448 CE (1432–1476 CE)	--
OS-142585	GP33 A	15-20	lowland granite	upland	north ridge	675 ± 20	1296 CE (1277–1308 CE)	--
OS-144391	GP43 B	0-5	lowland granite	upland	north ridge	205 ± 15	1784 CE (1654–1680 CE)	--
OS-151687	GP43 B	15-20	lowland granite	upland	north ridge	280 ± 15	1637 CE (1525–1558 CE)	--
OS-142581	HB16 E	15-20	lowland granite	upland	south ridge	635 ± 15	1359 CE (1292–1320 CE)	--
OS-153011	HB16 F	0-5	lowland granite	upland	south ridge	455 ± 15	1440 CE (1428–1450 CE)	--
OS-135860	HB16 F	10-15	lowland granite	upland	south ridge	10650 ± 55	10676 BCE (10768–10583 BCE)	--
OS-151681	TL23 B	0-5	lowland granite	upland	north ridge	1930 ± 15	71 CE (28–39 CE)	--
OS-151685	TL23 B	15-20	lowland granite	upland	north ridge	560 ± 15	1395 CE (1320–1349 CE)	--
OS-153010	UB17 F	0-5	lowland granite	upland	south ridge	110 ± 15	1839 CE (1689–1729 CE)	--
OS-151678	FS00 B	10-15	upland granite	upland	north ridge	400 ± 20	1466 CE (1442–1499 CE)	--
OS-151676	GP55 F	15-20	upland granite	upland	north ridge	635 ± 55	1346 CE (1277–1409 CE)	--
OS-151679	UB50 F	0-5	upland granite	upland	south ridge	360 ± 15	1513 CE (1459–1522 CE)	--
OS-142580	GP86 B	0-5	montane	upland	north ridge	260 ± 15	1649 CE (1534–1535 CE)	--
OS-142582	GP90 B	0-5	montane	upland	north ridge	350 ± 25	1558 CE (1460–1529 CE)	--

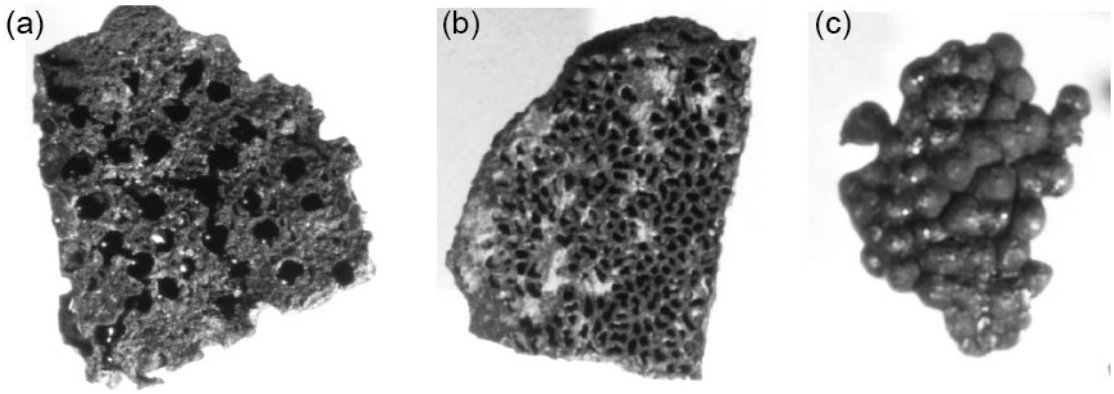

Appendix Figure 2.1. Photographs of material that was determined to not be charcoal. (a) and (b) show pieces with large transverse holes with a radiocarbon date of modern are hypothesized to be formed by insects. (c) shows another common morphology that we determined was not charcoal. Photos not to scale.

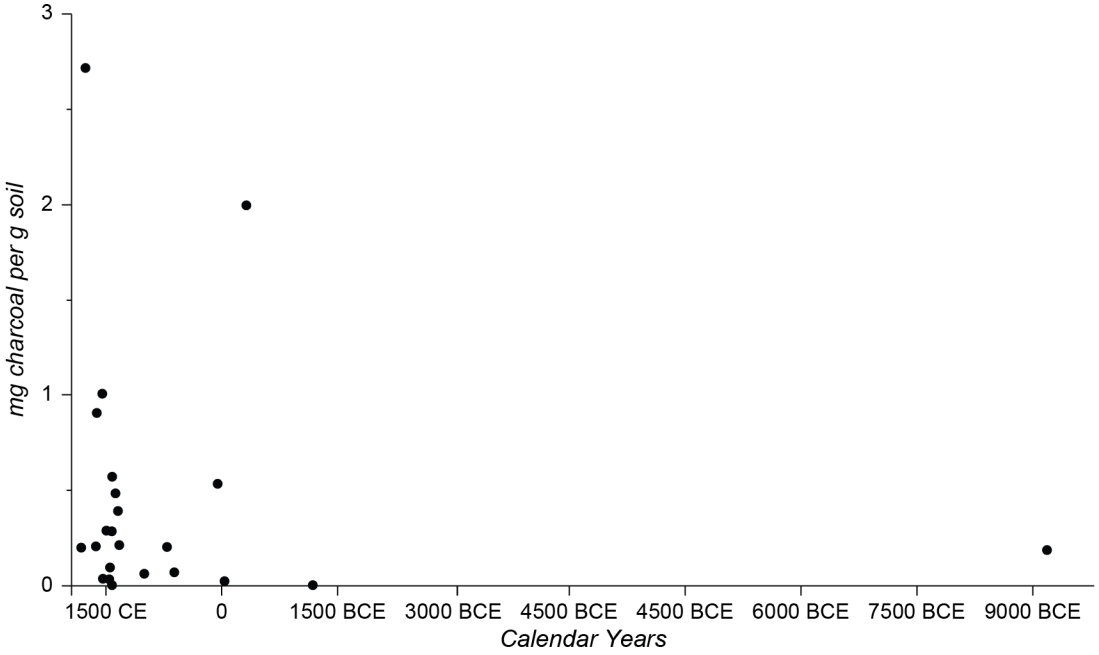

Appendix Figure 2.2. Relationship between median calibrated radiocarbon age and abundance of macrocharcoal >2 mm.

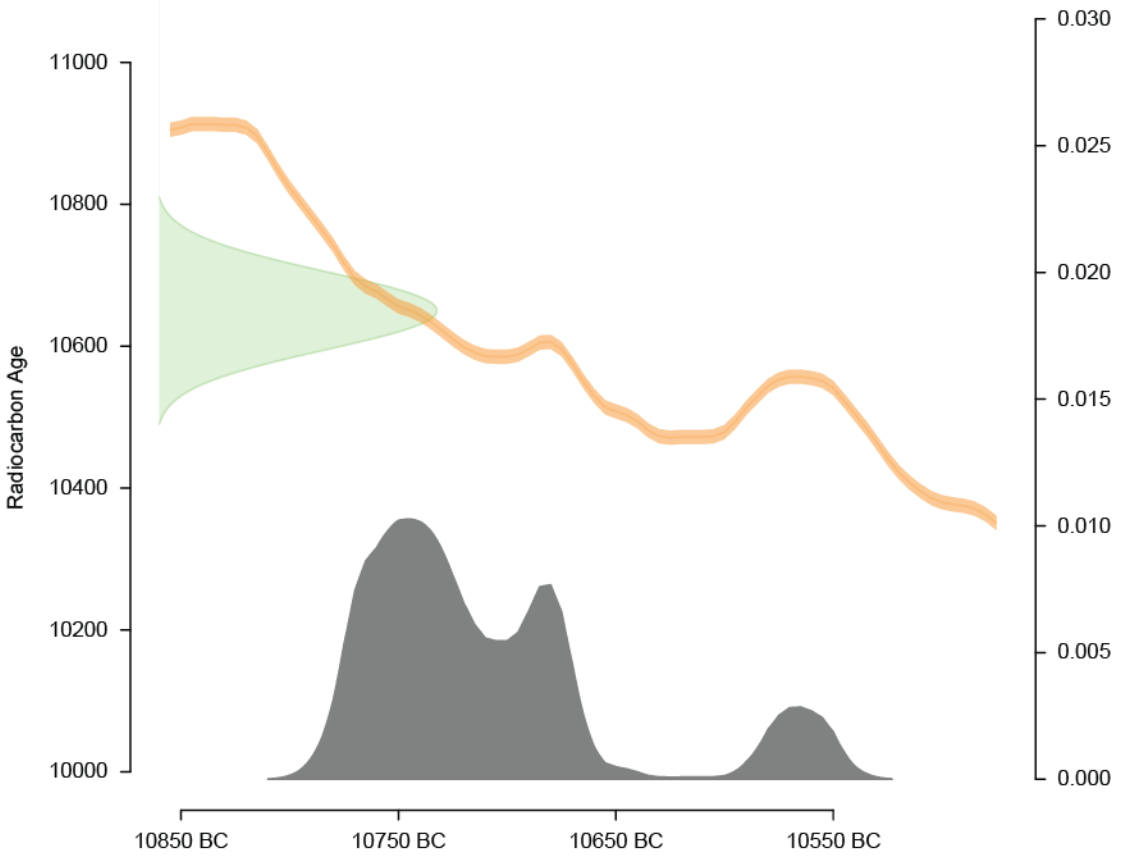

Appendix Figure 2.3. Calibration curve results for charcoal from HB16 F 10-15 cm, the site at CPRS with a date substantially older than all other sites (^{14}C age 10650 ± 55 years BP). The yellow line shows the calibration curve (IntCal13), with thickness representing ±1 standard deviation; the green curve shows the radiocarbon concentration in the sample; and the filled grey curve represents possible ages for the sample.

Appendix Table 2.2. 95% confidence intervals for fire cycle length and time periods of locally significant positive and negative deviation for both censored and non-censored modeling approaches.

	Censored			**Non-Censored**		
	Fire Cycle Length, 95% Confidence Interval (Years)	Positive Deviations (Years CE)	Negative Deviations (Years CE)	Fire Cycle Length, 95% Confidence Interval (Years)	Positive Deviations (Years CE)	Negative Deviations (Years CE)
All Sites	1299-2048	1283–1686	415–484; 761–890	482-760	1363–1609	1714–1894
Upland	1460-2810	1275–1720	None	320-616	1347–1488	None
Lowland	956-1840	1370–1648	None	576-1109	1387–1610	1733–1850
North Ridge	610-1175	1266–1561	None	420-809	1268–1501	1765–1936
South Ridge	2401-6276	1400–1731; 1776–1919	None	327-857	None	None
Non-Ridge	884-2313	127–219; 1406–1572	None	538-1409	128–241; 1436–1555	None

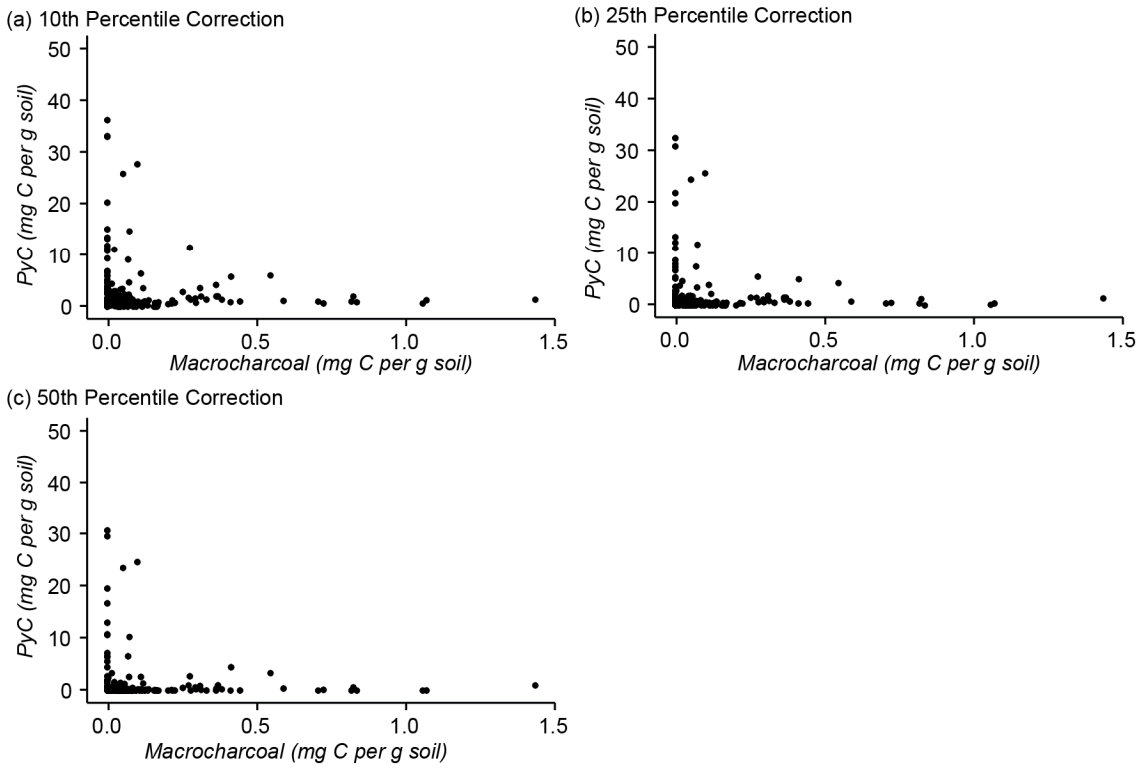

Appendix Figure 3.1. Relationship between mass of macrocharcoal (0.5–2 mm) from the manual method from parallel soil cores from primary tropical forest (Gunung Palung National Park, Indonesia) compared to PyC as measured by the KMD method, using adjusted PyC values. Each point represents a 5-cm core segment (90.6 cm3). Soil cores were limited to the upper 20-cm of soil.(a) uses a 10th percentile regression to adjust PyC values; (b) uses a 25th percentile regression to adjust PyC values; and (c) uses a 50th percentile regression not adjust PyC values.

REFERENCES CITED

Abdullahi, A. C., C. Siwar, M. Isma'il Shaharudin, and I. Anizan. 2018. The effects of forest type and land use on soil carbon stock in Malaysian dipterocarps forests. International Journal of Advanced and Applied Sciences 5:11–17.

Abiven, S., P. Hengartner, M. P. W. Schneider, N. Singh, and M. W. I. Schmidt. 2011. Pyrogenic carbon soluble fraction is larger and more aromatic in aged charcoal than in fresh charcoal. Soil Biology and Biochemistry 43:1615–1617.

Abney, R. B., and A. A. Berhe. 2018. Pyrogenic carbon erosion: Implications for stock and persistence of pyrogenic carbon in soil. Frontiers in Earth Science 6.

Aldhous, P. 2004. Borneo is burning. Nature 432:144.

Anshari, G. Z., A. P. Kershaw, and S. van der Kaars. 2001. A Late Pleistocene and Holocene pollen and charcoal record from peat swamp forest, Lake Sentarum wildlife reserve, West Kalimantan, Indonesia. Palaeogeography, Palaeoclimatology, Palaeoecology 171:213–228.

Ascough, P. L., M. I. Bird, S. M. Francis, B. Thornton, A. J. Midwood, A. C. Scott, and D. Apperley. 2011. Variability in oxidative degradation of charcoal: Influence of production conditions and environmental exposure. Geochimica et Cosmochimica Acta 75:2361–2378.

Bahadori, M., and H. Tofighi. 2016. A modified Walkley-Black method based on spectrophotometric procedure. Communications in Soil Science and Plant Analysis 47:213–220.

Bahadori, M., and H. Tofighi. 2017. Investigation of soil organic carbon recovery by the Walkley-Black method under diverse vegetation systems. Soil Science 182:101–106.

Ball, P. N., M. D. MacKenzie, T. H. DeLuca, and W. E. H. Montana. 2010. Wildfire and charcoal enhance nitrification and ammonium-oxidizing bacterial abundance in dry montane forest soils. Journal of Environmental Quality 39:1243–1253.

Bamforth, D. B., and B. Grund. 2012. Radiocarbon calibration curves, summed probability distributions, and early Paleoindian population trends in North America. Journal of Archaeological Science 39:1768–1774.

Barker, G., C. Hunt, H. Barton, C. Gosden, S. Jones, L. Lloyd-Smith, L. Farr, B. Nyirí, and S. O'Donnell. 2017. The 'cultured rainforests' of Borneo. Quaternary International 448:44–61.

Batjes, N. H. 1996. Total carbon and nitrogen in the soils of the world. European Journal of Soil Science 47:151–163.

Bélanger, N., and B. D. Pinno. 2008. Carbon sequestration, vegetation dynamics and soil development in the Boreal Transition ecoregion of Saskatchewan during the Holocene. CATENA 74:65–72.

Bevan, A., S. Colledge, D. Fuller, R. Fyfe, S. Shennan, and C. Stevens. 2017. Holocene fluctuations in human population demonstrate repeated links to food production and climate. Proceedings of the National Academy of Sciences 114:E10524–E10531.

Bevan, A., and E. R. Crema. 2018. rcarbon: Methods for calibrating and analysing radiocarbon dates.

Biagioni, S., V. Krashevska, Y. Achnopha, A. Saad, S. Sabiham, and H. Behling. 2015. 8000 years of vegetation dynamics and environmental changes of a unique inland peat ecosystem of the Jambi Province in Central Sumatra, Indonesia. Palaeogeography, Palaeoclimatology, Palaeoecology 440:813–829.

Bird, M. I., D. Taylor, and C. Hunt. 2005. Palaeoenvironments of insular Southeast Asia during the Last Glacial Period: a savanna corridor in Sundaland? Quaternary Science Reviews 24:2228–2242.

Bird, M. I., J. G. Wynn, G. Saiz, C. M. Wurster, and A. McBeath. 2015. The pyrogenic carbon cycle. Annual Review of Earth and Planetary Sciences 43:273–298.

Borchard, N., M. Bulusu, N. Meyer, A. Rodionov, H. Herawati, S. Blagodatsky, G. Cadisch, G. Welp, W. Amelung, and C. Martius. 2019. Deep soil carbon storage in tree-dominated land use systems in tropical lowlands of Kalimantan. Geoderma 354:113864.

Bowman, D. M. J. S., J. Balch, P. Artaxo, W. J. Bond, M. A. Cochrane, C. M. D'Antonio, R. Defries, F. H. Johnston, J. E. Keeley, M. A. Krawchuk, C. A. Kull, M. Mack, M. A. Moritz, S. Pyne, C. I. Roos, A. C. Scott, N. S. Sodhi, and T. W. Swetnam. 2011. The human dimension of fire regimes on Earth. Journal of Biogeography 38:2223–2236.

Brancalion, P. H. S., A. Niamir, E. Broadbent, R. Crouzeilles, F. S. M. Barros, A. M. A. Zambrano, A. Baccini, J. Aronson, S. Goetz, J. L. Reid, B. B. N. Strassburg, S. Wilson, and R. L. Chazdon. 2019. Global restoration opportunities in tropical rainforest landscapes. Science Advances 5:eaav3223.

Brando, P. M., L. Paolucci, C. C. Ummenhofer, E. M. Ordway, H. Hartmann, M. E. Cattau, L. Rattis, V. Medjibe, M. T. Coe, and J. Balch. 2019. Droughts, wildfires, and forest carbon cycling: A pantropical synthesis. Annual Review of Earth and Planetary Sciences 47:555–581.

Bronk Ramsey, C. 2009. Bayesian analysis of radiocarbon dates. Radiocarbon 51:337–360.

Broughton, J. M., and E. M. Weitzel. 2018. Population reconstructions for humans and megafauna suggest mixed causes for North American Pleistocene extinctions. Nature Communications 9:5441.

Bush, M. B., A. Correa-Metrio, C. H. McMichael, S. Sully, C. R. Shadik, B. G. Valencia, T. Guilderson, M. Steinitz-Kannan, and J. T. Overpeck. 2016. A 6900-year history of landscape modification by humans in lowland Amazonia. Quaternary Science Reviews 141:52–64.

Bush, M. B., C. H. McMichael, D. R. Piperno, M. R. Silman, J. Barlow, C. A. Peres, M. Power, and M. W. Palace. 2015. Anthropogenic influence on Amazonian forests in pre-history: An ecological perspective. Journal of Biogeography 42:2277–2288.

Bush, M. b, M. r Silman, C. McMichael, and S. Saatchi. 2008. Fire, climate change and biodiversity in Amazonia: A Late-Holocene perspective. Philosophical Transactions of the Royal Society B: Biological Sciences 363:1795–1802.

Cannon, C. H., L. M. Curran, A. J. Marshall, and M. Leighton. 2007. Long-term reproductive behaviour of woody plants across seven Bornean forest types in the Gunung Palung National Park (Indonesia): suprannual synchrony, temporal productivity and fruiting diversity. Ecology Letters 10:956–969.

Cannon, C. H., and M. Leighton. 2004. Tree species distributions across five habitats in a Bornean rain forest. Journal of Vegetation Science 15:257–266.

Cannon, C. H., R. J. Morley, and A. B. G. Bush. 2009. The current refugial rainforests of Sundaland are unrepresentative of their biogeographic past and highly vulnerable to disturbance. Proceedings of the National Academy of Sciences 106:11188–11193.

Canty, A., and B. Ripley. 2020. boot: Bootstrap R (S-Plus) Functions.

Carcaillet, C. 2001. Are Holocene wood-charcoal fragments stratified in alpine and subalpine soils? Evidence from the Alps based on AMS 14C dates. The Holocene 11:231–242.

Carcaillet, C., H. Almquist, H. Asnong, R. H. W. Bradshaw, J. S. Carrión, M.-J. Gaillard, K. Gajewski, J. N. Haas, S. G. Haberle, P. Hadorn, S. D. Müller, P. J. H. Richard, I. Richoz, M. Rösch, M. F. Sánchez Goñi, H. von Stedingk, A. C. Stevenson, B. Talon, C. Tardy, W. Tinner, E. Tryterud, L. Wick, and K. J. Willis. 2002. Holocene biomass burning and global dynamics of the carbon cycle. Chemosphere 49:845–863.

Carvalhais, N., M. Forkel, M. Khomik, J. Bellarby, M. Jung, M. Migliavacca, M. Mu, S. Saatchi, M. Santoro, M. Thurner, U. Weber, B. Ahrens, C. Beer, A. Cescatti, J. T. Randerson, and M. Reichstein. 2014. Global covariation of carbon turnover times with climate in terrestrial ecosystems. Nature 514:213–217.

Cerling, T. E. 1984. The stable isotopic composition of modern soil carbonate and its relationship to climate. Earth and Planetary Science Letters 71:229–240.

Chapin, F. S., P. A. Matson, and P. M. Vitousek. 2011. Principles of Terrestrial Ecosystem Ecology. 2nd ed. Springer, New York.

Chen, C.-C., H.-W. Lin, J.-Y. Yu, and M.-H. Lo. 2016. The 2015 Borneo fires: What have we learned from the 1997 and 2006 El Niños? Environmental Research Letters 11:104003.

Chen, X., X. Ye, W. Chu, D. C. Olk, X. Cao, K. Schmidt-Rohr, L. Zhang, M. L. Thompson, J. Mao, and H. Gao. 2020. Formation of char-like, fused-ring aromatic structures from a nonpyrogenic pathway during decomposition of wheat straw. Journal of Agricultural and Food Chemistry 68:2607–2614.

Chen, Y., J. T. Randerson, D. C. Morton, R. S. DeFries, G. J. Collatz, P. S. Kasibhatla, L. Giglio, Y. Jin, and M. E. Marlier. 2011. Forecasting fire season severity in south america using sea surface temperature anomalies. Science 334:787–791.

Cobb, K. M., J. F. Adkins, J. W. Partin, and B. Clark. 2007. Regional-scale climate influences on temporal variations of rainwater and cave dripwater oxygen isotopes in northern Borneo. Earth and Planetary Science Letters 263:207–220.

Cobb, K. M., C. D. Charles, H. Cheng, and R. L. Edwards. 2003. El Niño/Southern Oscillation and tropical Pacific climate during the last millennium. Nature 424:271–276.

Cochrane, M. A. 2003. Fire science for rainforests. Nature 421:913–919.

Cochrane, M. A. 2009. Fire in the Tropics. Pages 1–18 Tropical Fire Ecology: Climate Change, Land Use, and Ecosystem Dynamics. Praxis Publishing Ltd., Chichester, UK.

Cochrane, M. A. 2011. The past, present, and future importance of fire in tropical rainforests. Pages 213–240 *in* M. Bush, J. Flenley, and W. Gosling, editors. Tropical Rainforest Responses to Climatic Change. Springer Berlin Heidelberg, Berlin, Heidelberg.

Cochrane, M. A., A. Alencar, M. D. Schulze, C. M. Souza, D. C. Nepstad, P. Lefebvre, and E. A. Davidson. 1999. Positive feedbacks in the fire dynamic of closed canopy tropical forests. Science 284:1832–1835.

Cochrane, M. A., and W. F. Laurance. 2002. Fire as a large-scale edge effect in Amazonian forests. Journal of Tropical Ecology 18:311–325.

Cochrane, M. A., and K. C. Ryan. 2009. Fire and fire ecology: Concepts and principles. Pages 25–62 Tropical Fire Ecology: Climate Change, Land Use, and Ecosystem Dynamics. Praxis Publishing Ltd., Chichester, UK.

Cole, L. E. S., S. A. Bhagwat, and K. J. Willis. 2019. Fire in the swamp forest: Palaeoecological insights into natural and human-induced burning in intact tropical peatlands. Frontiers in Forests and Global Change 2:48.

Conedera, M., W. Tinner, C. Neff, M. Meurer, A. F. Dickens, and P. Krebs. 2009. Reconstructing past fire regimes: methods, applications, and relevance to fire management and conservation. Quaternary Science Reviews 28:555–576.

Conyers, M. K., G. J. Poile, A. A. Oates, D. Waters, and K. Y. Chan. 2011. Comparison of three carbon determination methods on naturally occurring substrates and the implication for the quantification of "soil carbon." Soil Research 49:27–33.

Cotrufo, M. F., C. M. Boot, S. Kampf, P. A. Nelson, D. J. Brogan, T. Covino, M. L. Haddix, L. H. MacDonald, S. Rathburn, S. Ryan-Bukett, S. Schmeer, and E. Hall. 2016. Redistribution of pyrogenic carbon from hillslopes to stream corridors following a large montane wildfire. Global Biogeochemical Cycles 30:1348–1355.

Crausbay, S. D., J. M. Russell, and D. W. Schnurrenberger. 2006. A ca. 800-Year lithologic record of drought from sub-annually laminated lake sediment, East Java. Journal of Paleolimnology 35:641–659.

Curran, L. M., and M. Leighton. 2000. Vertebrate responses to spatiotemporal variation in seed production of mast-fruiting Dipterocarpaceae. Ecological Monographs 70:101–128.

Delgado-Baquerizo, M., D. J. Eldridge, F. T. Maestre, S. B. Karunaratne, P. Trivedi, P. B. Reich, and B. K. Singh. 2017. Climate legacies drive global soil carbon stocks in terrestrial ecosystems. Science Advances 3:e1602008.

Delignette-Muller, M. L., and C. Dutang. 2015. fitdistrplus: An R Package for Fitting Distributions. Journal of Statistical Software 64:1–34.

Dommain, R., A. R. Cobb, H. Joosten, P. H. Glaser, A. F. L. Chua, L. Gandois, F.-M. Kai, A. Noren, K. A. Salim, N. S. H. Su'ut, and C. F. Harvey. 2015. Forest dynamics and tip-up pools drive pulses of high carbon accumulation rates in a tropical peat dome in Borneo (Southeast Asia): Carbon accumulation in tip-up pools. Journal of Geophysical Research: Biogeosciences 120:617–640.

Duarte-Guardia, S., P. L. Peri, W. Amelung, D. Sheil, S. W. Laffan, N. Borchard, M. I. Bird, W. Dieleman, D. A. Pepper, B. Zutta, E. Jobbagy, L. C. R. Silva, S. P. Bonser, G. Berhongaray, G. Piñeiro, M.-J. Martinez, A. L. Cowie, and B. Ladd. 2019. Better estimates of soil carbon from geographical data: a revised global approach. Mitigation and Adaptation Strategies for Global Change 24:355–372.

Eckmeier, E., K. van der Borg, U. Tegtmeier, M. W. I. Schmidt, and R. Gerlach. 2011. Dating charred soil organic matter: comparison of radiocarbon ages from macrocharcoals and chemically separated charcoal carbon. Radiocarbon 51:437–443.

Eltahir, E. A. B., and R. L. Bras. 1996. Precipitation recycling. Reviews of Geophysics 34:367–378.

Finney, M. 1995. The missing tail and other considerations for the use of fire history models. International Journal of Wildland Fire 5:197.

Foereid, B., J. Lehmann, and J. Major. 2011. Modeling black carbon degradation and movement in soil. Plant and Soil 345:223–236.

Fukumoto, Y., X. Li, Y. Yasuda, M. Okamura, K. Yamada, and K. Kashima. 2015. The Holocene environmental changes in southern Indonesia reconstructed from highland caldera lake sediment in Bali Island. Quaternary International 374:15–33.

Gaston, K. J. 2000. Global patterns in biodiversity. Nature 405:220–227.

Gaveau, D. L. A., B. Locatelli, M. A. Salim, H. Yaen, P. Pacheco, and D. Sheil. 2018. Rise and fall of forest loss and industrial plantations in Borneo (2000-2017). Conservation Letters:e12622.

Gaveau, D. L. A., S. Sloan, E. Molidena, H. Yaen, D. Sheil, N. K. Abram, M. Ancrenaz, R. Nasi, M. Quinones, N. Wielaard, and E. Meijaard. 2014. Four decades of forest persistence, clearance and logging on Borneo. PLoS ONE 9:e101654.

Gavin, D. G. 2001. Estimation of inbuilt age in radiocarbon ages of soil charcoal for fire history studies. Radiocarbon 43:27–44.

Gavin, D. G., A. White, P. T. Sanborn, and R. J. Hebda. 2020. Deglacial landforms and Holocene vegetation trajectories in the northern interior cedar-hemlock forests of British Columbia. Page *in* R. B. Waitt, G. D. Thackray, and A. R. Gillespie, editors. Untangling the Quaternary Period: A Legacy of Stephen C. Porter. Geological Society of America.

Glaser, B., J. Lehmann, and W. Zech. 2002. Ameliorating physical and chemical properties of highly weathered soils in the tropics with charcoal - a review. Biology and Fertility of Soils 35:219–230.

Goldammer, J. G., and B. Seibert. 1989. Natural rain forest fires in Eastern Borneo during the Pleistocene and Holocene. The Science of Nature 76:518–520.

González-Pérez, J. A., F. J. González-Vila, G. Almendros, and H. Knicker. 2004. The effect of fire on soil organic matter—a review. Environment International 30:855–870.

Gosling, W. D., H. L. Cornelissen, and C. N. H. McMichael. 2019. Reconstructing past fire temperatures from ancient charcoal material. Palaeogeography, Palaeoclimatology, Palaeoecology 520:128–137.

Goulart, A. C., K. D. Macario, R. Scheel-Ybert, E. Q. Alves, C. Bachelet, B. B. Pereira, C. Levis, B. H. Marimon Junior, B. S. Marimon, C. A. Quesada, and T. R. Feldpausch. 2017. Charcoal chronology of the Amazon forest: A record of biodiversity preserved by ancient fires. Quaternary Geochronology 41:180–186.

Haberle, S. G., G. S. Hope, and S. van der Kaars. 2001. Biomass burning in Indonesia and Papua New Guinea: natural and human induced fire events in the fossil record. Palaeogeography, Palaeoclimatology, Palaeoecology 171:259–268.

Hammes, K., M. W. I. Schmidt, R. J. Smernik, L. A. Currie, W. P. Ball, T. H. Nguyen, P. Louchouarn, S. Houel, Ö. Gustafsson, M. Elmquist, G. Cornelissen, J. O. Skjemstad, C. A. Masiello, J. Song, P. Peng, S. Mitra, J. C. Dunn, P. G. Hatcher, W. C. Hockaday, D. M. Smith, C. Hartkopf-Fröder, A. Böhmer, B. Lüer, B. J. Huebert, W. Amelung, S. Brodowski, L. Huang, W. Zhang, P. M. Gschwend, D. X. Flores-Cervantes, C. Largeau, J.-N. Rouzaud, C. Rumpel, G. Guggenberger, K. Kaiser, A. Rodionov, F. J. Gonzalez-Vila, J. A. Gonzalez-Perez, J. M. de la Rosa, D. A. C. Manning, E. López-Capél, and L. Ding. 2007. Comparison of quantification methods to measure fire-derived (black/elemental) carbon in soils and sediments using reference materials from soil, water, sediment and the atmosphere. Global Biogeochemical Cycles 21:GB3016.

Hammes, K., R. J. Smernik, J. O. Skjemstad, A. Herzog, U. F. Vogt, and M. W. I. Schmidt. 2006. Synthesis and characterisation of laboratory-charred grass straw (Oryza sativa) and chestnut wood (Castanea sativa) as reference materials for black carbon quantification. Organic Geochemistry 37:1629–1633.

Hammes, K., M. S. Torn, A. G. Lapenas, and M. W. I. Schmidt. 2008. Centennial black carbon turnover observed in a Russian steppe soil. Biogeosciences 5:1339–1350.

Hansen, M. C., P. V. Potapov, R. Moore, M. Hancher, S. A. Turubanova, A. Tyukavina, D. Thau, S. V. Stehman, S. J. Goetz, T. R. Loveland, A. Kommareddy, A. Egorov, L. Chini, C. O. Justice, and J. R. G. Townshend. 2013. High-resolution global maps of 21st-century forest cover change. Science 342:850–853.

Hardy, B., and J. E. Dufey. 2017. The resistance of centennial soil charcoal to the "Walkley-Black" oxidation. Geoderma 303:37–43.

Harrison, M. E., S. E. Page, and S. H. Limin. 2009. The global impact of Indonesian forest fires. Biologist 56:156–163.

Heaney, L. R. 1991. A synopsis of climatic and vegetational change in Southeast Asia. Climatic Change 19:53–61.

Hébert-Dufresne Laurent, Pellegrini Adam F. A., Bhat Uttam, Redner Sidney, Pacala Stephen W., Berdahl Andrew M., and Coulson Tim. 2018. Edge fires drive the shape and stability of tropical forests. Ecology Letters 0.

Hendon, H. H. 2003. Indonesian rainfall variability: Impacts of ENSO and local air–sea interaction. Journal of Climate 16:1775–1790.

Hoffmann, W. A., E. L. Geiger, S. G. Gotsch, D. R. Rossatto, L. C. R. Silva, O. L. Lau, M. Haridasan, and A. C. Franco. 2012. Ecological thresholds at the savanna-forest boundary: how plant traits, resources and fire govern the distribution of tropical biomes. Ecology Letters 15:759–768.

Hogg, A. G., Q. Hua, P. G. Blackwell, M. Niu, C. E. Buck, T. P. Guilderson, T. J. Heaton, J. G. Palmer, P. J. Reimer, R. W. Reimer, C. S. M. Turney, and S. R. H. Zimmerman. 2013. SHCal13 Southern Hemisphere calibration, 0–50,000 years cal BP. Radiocarbon 55:1889–1903.

Holm, S. 1979. A simple sequentially rejective multiple test procedure. Scandinavian Journal of Statistics 6:65–70.

Hope, G., U. Chokkalingam, and S. Anwar. 2005. The stratigraphy and fire history of the Kutai Peatlands, Kalimantan, Indonesia. Quaternary Research 64:407–417.

Hope, G., A. P. Kershaw, S. van der Kaars, S. Xiangjun, P.-M. Liew, L. E. Heusser, H. Takahara, M. McGlone, N. Miyoshi, and P. T. Moss. 2004. History of vegetation and habitat change in the Austral-Asian region. Quaternary International 118–119:103–126.

Hua, Q., M. Barbetti, and A. Z. Rakowski. 2013. Atmospheric radiocarbon for the period 1950–2010. Radiocarbon 55:2059–2072.

Hubau, W., J. V. den Bulcke, J. V. Acker, and H. Beeckman. 2015. Charcoal-inferred Holocene fire and vegetation history linked to drought periods in the Democratic Republic of Congo. Global Change Biology 21:2296–2308.

Hubau, W., J. Van den Bulcke, P. Kitin, F. Mees, J. Van Acker, and H. Beeckman. 2012. Charcoal identification in species-rich biomes: A protocol for Central Africa optimised for the Mayumbe forest. Review of Palaeobotany and Palynology 171:164–178.

Hunt, C. O., D. D. Gilbertson, and G. Rushworth. 2012. A 50,000-year record of late Pleistocene tropical vegetation and human impact in lowland Borneo. Quaternary Science Reviews 37:61–80.

Hunt, C. O., and R. Premathilake. 2012. Early Holocene vegetation, human activity and climate from Sarawak, Malaysian Borneo. Quaternary International 249:105–119.

Iglesias, V., G. I. Yospin, and C. Whitlock. 2015. Reconstruction of fire regimes through integrated paleoecological proxy data and ecological modeling. Frontiers in Plant Science 5.

Jarvis, P. G., and K. G. McNaughton. 1986. Stomatal control of transpiration: scaling up from leaf to region. Advances in Ecological Research 15:49.

Jobbágy, E. G., and R. B. Jackson. 2000. The vertical distribution of soil organic carbon and its relation to climate and vegetation. Ecological Applications 10:423–436.

Jones, M. W., C. Santín, G. R. van der Werf, and S. H. Doerr. 2019. Global fire emissions buffered by the production of pyrogenic carbon. Nature Geoscience 12:742–747.

Keeley, J. E., J. G. Pausas, P. W. Rundel, W. J. Bond, and R. A. Bradstock. 2011. Fire as an evolutionary pressure shaping plant traits. Trends in Plant Science 16:406–411.

Kershaw, A. P., M. B. Bush, G. S. Hope, K.-F. Weiss, J. G. Goldammer, and R. Sanford. 1997. The contribution of humans to past biomass burning in the tropics. Pages 413–442 *in* J. S. Clark, H. Cachier, J. G. Goldammer, and B. Stocks, editors. Sediment Records of Biomass Burning and Global Change. Springer Berlin Heidelberg, Berlin, Heidelberg.

Kershaw, A. P., S. van der Kaars, and J. R. Flenley. 2007. The Quaternary history of far eastern rainforests. Pages 77–115 Tropical Rainforest Responses to Climatic Change. Springer, Berlin, Heidelberg.

King, V. T. 1993. The Peoples of Borneo. Blackwell Publishing Ltd., Cambridge, Massachusetts, USA.

Knicker, H. 2011. Pyrogenic organic matter in soil: Its origin and occurrence, its chemistry and survival in soil environments. Quaternary International 243:251–263.

Koele, N., M. Bird, J. Haig, B. H. Marimon-Junior, B. S. Marimon, O. L. Phillips, E. A. de Oliveira, C. A. Quesada, and T. R. Feldpausch. 2017. Amazon Basin forest pyrogenic carbon stocks: First estimate of deep storage. Geoderma 306:237–243.

Koenker, R. 2020. quantreg: Quantile Regression.

Konecky, B. L., J. M. Russell, J. R. Rodysill, M. Vuille, S. Bijaksana, and Y. Huang. 2013. Intensification of southwestern Indonesian rainfall over the past millennium. Geophysical Research Letters 40:386–391.

Koplitz, S. N., L. J. Mickley, M. E. Marlier, J. J. Buonocore, P. S. Kim, Tianjia Liu, M. P. Sulprizio, R. S. DeFries, D. J. Jacob, J. Schwartz, M. Pongsiri, and S. S. Myers. 2016. Public health impacts of the severe haze in Equatorial Asia in September–October 2015: demonstration of a new framework for informing fire management strategies to reduce downwind smoke exposure. Environmental Research Letters 11:094023.

Krull, E. S., C. W. Swanston, J. O. Skjemstad, and J. A. McGowan. 2006. Importance of charcoal in determining the age and chemistry of organic carbon in surface soils. Journal of Geophysical Research: Biogeosciences 111.

Kumagai, T., T. M. Saitoh, Y. Sato, T. Morooka, O. J. Manfroi, K. Kuraji, and M. Suzuki. 2004. Transpiration, canopy conductance and the decoupling coefficient of a lowland mixed dipterocarp forest in Sarawak, Borneo: Dry spell effects. Journal of Hydrology 287:237–251.

Kurth, V. J. 2004. Charcoal in ponderosa pine ecosystems of western Montana| decomposition, mineralization, and quantification. University of Montana, Missoula, Montana.

Kurth, V. J., M. D. MacKenzie, and T. H. DeLuca. 2006. Estimating charcoal content in forest mineral soils. Geoderma 137:135–139.

Lal, R. 2005. Forest soils and carbon sequestration. Forest Ecology and Management 220:242–258.

Lal, R. 2008. Carbon Sequestration. Philosophical Transactions: Biological Sciences 363:815–830.

Langner, A., J. Miettinen, and F. Siegert. 2007. Land cover change 2002–2005 in Borneo and the role of fire derived from MODIS imagery. Global Change Biology 13:2329–2340.

Lavallee, J. M., R. T. Conant, M. L. Haddix, R. F. Follett, M. I. Bird, and E. A. Paul. 2019. Selective preservation of pyrogenic carbon across soil organic matter fractions and its influence on calculations of carbon mean residence times. Geoderma 354:113866.

Lawrence, D. 2004. Erosion of tree diversity during 200 years of shifting cultivation in Bornean rain forest. Ecological Applications 14:1855–1869.

Lawrence, D., D. R. Peart, and M. Leighton. 1998. The impact of shifting cultivation on a rainforest landscape in West Kalimantan: spatial and temporal dynamics. Landscape Ecology 13:135–148.

Lewis, S. L., D. P. Edwards, and D. Galbraith. 2015. Increasing human dominance of tropical forests. Science 349:827–832.

Licata, C., and R. Sanford. 2012. Charcoal and total carbon in soils from foothills shrublands to subalpine forests in the Colorado Front Range. Forests 3:944–958.

Liles, G. C., D. E. Beaudette, A. T. O'Geen, and W. R. Horwath. 2013. Developing predictive soil C models for soils using quantitative color measurements. Soil Science Society of America Journal 77:2173.

MacKenzie, M. D., E. J. B. McIntire, S. A. Quideau, and R. C. Graham. 2008. Charcoal distribution affects carbon and nitrogen contents in forest soils of California. Soil Science Society of America Journal 72:1774–1785.

Maestrini, B., and J. R. Miesel. 2017. Modification of the weak nitric acid digestion method for the quantification of black carbon in organic matrices. Organic Geochemistry 103:136–139.

Malhi, Y., T. A. Gardner, G. R. Goldsmith, M. R. Silman, and P. Zelazowski. 2014. Tropical forests in the Anthropocene. Annual Review of Environment and Resources 39:125–159.

Malhi, Y., J. T. Roberts, R. A. Betts, T. J. Killeen, W. Li, and C. A. Nobre. 2008. Climate change, deforestation, and the fate of the Amazon. Science 319:169–172.

Marlon, J. R., P. J. Bartlein, A.-L. Daniau, S. P. Harrison, S. Y. Maezumi, M. J. Power, W. Tinner, and B. Vanniére. 2013. Global biomass burning: a synthesis and review of Holocene paleofire records and their controls. Quaternary Science Reviews 65:5–25.

McAlpine, C. A., A. Johnson, A. Salazar, J. Syktus, K. Wilson, E. Meijaard, L. Seabrook, P. Dargusch, H. Nordin, and D. Sheil. 2018. Forest loss and Borneo's climate. Environmental Research Letters 13:044009.

McBeath, A. V., R. J. Smernik, M. P. W. Schneider, M. W. I. Schmidt, and E. L. Plant. 2011. Determination of the aromaticity and the degree of aromatic condensation of a thermosequence of wood charcoal using NMR. Organic Geochemistry 42:1194–1202.

McBeath, A. V., C. M. Wurster, and M. I. Bird. 2015. Influence of feedstock properties and pyrolysis conditions on biochar carbon stability as determined by hydrogen pyrolysis. Biomass and Bioenergy 73:155–173.

Meister, K., M. S. Ashton, D. Craven, and H. Griscom. 2012. Carbon Dynamics of Tropical Forests. Pages 51–75 *in* M. S. Ashton, M. L. Tyrrell, D. Spalding, and B. Gentry, editors. Managing Forest Carbon in a Changing Climate. Springer Netherlands, Dordrecht.

Miller, W. P., and D. M. Miller. 1987. A micro-pipette method for soil mechanical analysis. Communications in Soil Science and Plant Analysis 18:1–15.

Morin-Rivat, J., A. Biwolé, A.-P. Gorel, J. Vleminckx, J.-F. Gillet, N. Bourland, O. J. Hardy, A. L. Smith, K. Daïnou, L. Dedry, H. Beeckman, and J.-L. Doucet. 2016. High spatial resolution of late-Holocene human activities in the moist forests of central Africa using soil charcoal and charred botanical remains. The Holocene:1–14.

Murphy, B. P., and D. M. J. S. Bowman. 2012. What controls the distribution of tropical forest and savanna? Ecology Letters 15:748–758.

Noorduyn, J. 1978. Majapahit in the fifteenth century. Bijdragen tot de taal-, land- en volkenkunde / Journal of the Humanities and Social Sciences of Southeast Asia 134:207–274.

Ohlson, M., and E. Tryterud. 2000. Interpretation of the charcoal record in forest soils: forest fires and their production and deposition of macroscopic charcoal. The Holocene 10:519–525.

Pan, Y., R. A. Birdsey, J. Fang, R. Houghton, P. E. Kauppi, W. A. Kurz, O. L. Phillips, A. Shvidenko, S. L. Lewis, J. G. Canadell, P. Ciais, R. B. Jackson, S. W. Pacala, A. D. McGuire, S. Piao, A. Rautiainen, S. Sitch, and D. Hayes. 2011. A Large and Persistent Carbon Sink in the World's Forests. Science 333:988–993.

Pan, Y., R. A. Birdsey, O. L. Phillips, and R. B. Jackson. 2013. The structure, distribution, and biomass of the world's forests. Annual Review of Ecology, Evolution, and Systematics 44:593–622.

Paoli, G. D., L. M. Curran, and J. W. F. Slik. 2007. Soil nutrients affect spatial patterns of aboveground biomass and emergent tree density in southwestern Borneo. Oecologia 155:287–299.

Paoli, G. D., L. M. Curran, and J. W. F. Slik. 2008. Soil nutrients affect spatial patterns of aboveground biomass and emergent tree density in southwestern Borneo. Oecologia 155:287–299.

Paoli, G. D., L. M. Curran, and D. R. Zak. 2006. Soil nutrients and beta diversity in the Bornean Dipterocarpaceae: evidence for niche partitioning by tropical rain forest trees. Journal of Ecology 94:157–170.

Partin, J. W., K. M. Cobb, J. F. Adkins, B. Clark, and D. P. Fernandez. 2007. Millennial-scale trends in west Pacific warm pool hydrology since the Last Glacial Maximum. Nature 449:452–455.

Pessenda, L. R., S. M. Gouveia, R. Aravena, B. M. Gomes, R. Boulet, and A. S. Ribeiro. 2006. 14C dating and stable carbon isotopes of soil organic matter in forest-savanna boundary areas in the southern Brazilian Amazon region. Radiocarbon 40:1013–1022.

Petersen, L. 1991. Soils of Kalimantan, Indonesia. Pages 173–187 Folia Geographica Danica.

Pierre-Louis, K. 2019, August 28. The Amazon, Siberia, Indonesia: A World of Fire. The New York Times.

Pingree, M. R. A. 2011, May. The first pre- and post-wildfire charcoal quantification using peroxide-acid digestion. Master of Science Thesis, Western Washington University, Bellingham, WA.

Preston, C. M., and M. W. I. Schmidt. 2006. Black (pyrogenic) carbon: a synthesis of current knowledge and uncertainties with special consideration of boreal regions. Biogeosciences 3:397–420.

Quinn, W. H., D. O. Zopf, K. S. Short, and R. T. W. K. Yang. 1978. Historical trends and statistics of Southern Oscillation, El Nino, and Indonesian droughts. Fishery Bulletin 76:663–678.

R Core Team. 2019. R: A language and environment for statistical computing. R Foundation for Statistical Computing, Vienna, Austria.

Razafimbelo, T., T. Chevallier, A. Albrecht, L. Chapuis-Lardy, F. N. Rakotondrasolo, R. Michellon, L. Rabeharisoa, and M. Bernoux. 2013. Texture and organic carbon contents do not impact amount of carbon protected in Malagasy soils. Scientia Agricola 70:204–208.

Reed, W. J., C. P. S. Larsen, E. A. Johnson, and G. M. MacDonald. 1998. Estimation of temporal variations in historical fire frequency from time-since-fire map data. Forest Science 44:465–475.

Reeves, J. M., H. C. Bostock, L. K. Ayliffe, T. T. Barrows, P. De Deckker, L. S. Devriendt, G. B. Dunbar, R. N. Drysdale, K. E. Fitzsimmons, M. K. Gagan, M. L. Griffiths, S. G. Haberle, J. D. Jansen, C. Krause, S. Lewis, H. V. McGregor, S. D. Mooney, P. Moss, G. C. Nanson, A. Purcell, and S. van der Kaars. 2013. Palaeoenvironmental change in tropical Australasia over the last 30,000 years – a synthesis by the OZ-INTIMATE group. Quaternary Science Reviews 74:97–114.

Reimer, P. J., E. Bard, A. Bayliss, J. W. Beck, P. G. Blackwell, C. B. Ramsey, C. E. Buck, H. Cheng, R. L. Edwards, M. Friedrich, P. M. Grootes, T. P. Guilderson, H. Haflidason, I. Hajdas, C. Hatté, T. J. Heaton, D. L. Hoffmann, A. G. Hogg, K. A. Hughen, K. F. Kaiser, B. Kromer, S. W. Manning, M. Niu, R. W. Reimer, D. A. Richards, E. M. Scott, J. R. Southon, R. A. Staff, C. S. M. Turney, and J. van der Plicht. 2013. IntCal13 and Marine13 radiocarbon age calibration curves 0–50,000 Years cal BP. Radiocarbon 55:1869–1887.

Reisser, M., R. S. Purves, M. W. I. Schmidt, and S. Abiven. 2016. Pyrogenic carbon in soils: A literature-based inventory and a global estimation of its content in soil organic carbon and stocks. Frontiers in Earth Science 4.

Rick, J. W. 1987. Dates as data: An examination of the Peruvian preceramic radiocarbon record. American Antiquity 52:55–73.

Roberts, P., N. Boivin, and J. O. Kaplan. 2018. Finding the anthropocene in tropical forests. Anthropocene 23:5–16.

Roberts, P., C. Hunt, M. Arroyo-Kalin, D. Evans, and N. Boivin. 2017. The deep human prehistory of global tropical forests and its relevance for modern conservation. Nature Plants 3:17093.

Rodysill, J. R., J. M. Russell, S. Bijaksana, E. T. Brown, L. O. Safiuddin, and H. Eggermont. 2012. A paleolimnological record of rainfall and drought from East Java, Indonesia during the last 1,400 years. Journal of Paleolimnology 47:125–139.

Rodysill, J. R., J. M. Russell, S. D. Crausbay, S. Bijaksana, M. Vuille, R. L. Edwards, and H. Cheng. 2013. A severe drought during the last millennium in East Java, Indonesia. Quaternary Science Reviews 80:102–111.

Rumpel, C., A. Ba, F. Darboux, V. Chaplot, and O. Planchon. 2009. Erosion budget and process selectivity of black carbon at meter scale. Geoderma 154:131–137.

Rumpel, C., V. Chaplot, O. Planchon, J. Bernadou, C. Valentin, and A. Mariotti. 2006. Preferential erosion of black carbon on steep slopes with slash and burn agriculture. Catena 65:30–40.

Saatchi, S. S., N. L. Harris, S. Brown, M. Lefsky, E. T. A. Mitchard, W. Salas, B. R. Zutta, W. Buermann, S. L. Lewis, S. Hagen, S. Petrova, L. White, M. Silman, and A. Morel. 2011. Benchmark map of forest carbon stocks in tropical regions across three continents. Proceedings of the National Academy of Sciences 108:9899–9904.

Sachs, J. P., D. Sachse, R. H. Smittenberg, Z. Zhang, D. S. Battisti, and S. Golubic. 2009. Southward movement of the Pacific intertropical convergence zone AD 1400–1850. Nature Geoscience 2:519–525.

Saner, P., Y. Y. Loh, R. C. Ong, and A. Hector. 2012. Carbon stocks and fluxes in tropical lowland Dipterocarp rainforests in Sabah, Malaysian Borneo. PLOS ONE 7:e29642.

Santín, C., S. H. Doerr, E. S. Kane, C. A. Masiello, M. Ohlson, J. M. de la Rosa, C. M. Preston, and T. Dittmar. 2016. Towards a global assessment of pyrogenic carbon from vegetation fires. Global Change Biology 22:76–91.

Santín, C., S. H. Doerr, C. M. Preston, and G. González-Rodríguez. 2015. Pyrogenic organic matter production from wildfires: a missing sink in the global carbon cycle. Global Change Biology 21:1621–1633.

Santos, G. M., P. R. S. Gomes, R. M. Anjos, R. C. Cordeiro, and B. J. Turcq. 2000. 14C AMS dating of fires in the central Amazon rain forest. Nuclear Instruments and Methods in Physics Research B 172:761–766.

Scharlemann, J. P., E. V. Tanner, R. Hiederer, and V. Kapos. 2014. Global soil carbon: understanding and managing the largest terrestrial carbon pool. Carbon Management 5:81–91.

Schmidt, M. W. I., and A. G. Noack. 2000a. Black carbon in soils and sediments: Analysis, distribution, implications, and current challenges. Global Biogeochemical Cycles 14:777–793.

Schmidt, M. W. I., and A. G. Noack. 2000b. Black carbon in soils and sediments: Analysis, distribution, implications, and current challenges. Global Biogeochemical Cycles 14:777–793.

Scott, A. C., D. M. J. S. Bowman, W. J. Bond, S. J. Pyne, and M. E. Alexander. 2013. Fire on Earth: An Introduction. Chichester, West Sussex : Wiley Blackwell, Inc., Chichester, West Sussex.

Sedjo, R., and B. Sohngen. 2012. Carbon sequestration in forests and soils. The Annual Review of Resource Economics.

Sellato, B. 1999. The kingdom of Ulu are in Borneo's history: a comment. Borneo Research Bulletin 30:110–112.

Sheil, D., I. Basuki, L. German, T. W. Kuyper, G. Limberg, R. K. Puri, B. Sellato, M. Van Noordwijk, and E. Wollenberg. 2012. Do Anthropogenic Dark Earths occur in the interior of Borneo? Some initial observations from East Kalimantan. Forests 3:207–229.

Shrestha, G., S. Traina, and C. Swanston. 2010. Black carbon's properties and role in the environment: A comprehensive review. Sustainability 2:294–320.

Siegert, F., G. Ruecker, A. Hinrichs, and A. A. Hoffmann. 2001. Increased damage from fires in logged forests during droughts caused by El Niño 414:4.

da Silva Carvalho, L. C., P. M. Fearnside, M. T. Nascimento, and R. I. Barbosa. 2018. Amazon soil charcoal: Pyrogenic carbon stock depends of ignition source distance and forest type in Roraima, Brazil. Global Change Biology 24:4122–4130.

Silva, L. C. R. 2017. Carbon sequestration beyond tree longevity. Science 355:1141–1141.

Singh, N., S. Abiven, M. S. Torn, and M. W. I. Schmidt. 2012. Fire-derived organic carbon in soil turns over on a centennial scale. Biogeosciences 9:2847–2857.

Skjemstad, J. O., and J. A. Taylor. 1999. Does the Walkley-Black method determine soil charcoal? Communications in Soil Science and Plant Analysis 30:2299–2310.

Slik, J. W. F., E. Breman, C. Bernard, M. van Beek, C. H. Cannon, K. A. O. Eichhorn, and K. Sidiyasa. 2010. Fire as a selective force in a Bornean tropical everwet forest. Oecologia 164:841–849.

Smith, F. A. 2016. Indianization in west Borneo: The elephant in the room. Borneo Research Bulletin 47:63–83.

Smith, F. A., and H. F. Smith. 2011. A shadowy state in Borneo: where was Tanjungpura? Borneo Research Bulletin 42:89–103.

Soil Survey Staff. 2014. Kellogg Soil Survey Laboratory Methods Manual. United States.

Soucémarianadin, L. N., S. A. Quideau, and M. D. MacKenzie. 2014. Pyrogenic carbon stocks and storage mechanisms in podzolic soils of fire-affected Quebec black spruce forests. Geoderma 217–218:118–128.

Soucémarianadin, L. N., S. A. Quideau, M. D. MacKenzie, G. M. Bernard, and R. E. Wasylishen. 2013. Laboratory charring conditions affect black carbon properties: A case study from Quebec black spruce forests. Organic Geochemistry 62:46–55.

Stibig, H.-J., F. Achard, S. Carboni, R. Raši, and J. Miettinen. 2013. Change in tropical forest cover of Southeast Asia from 1990 to 2010. Biogeosciences Discussions 10:12625–12653.

Timpson, A., S. Colledge, E. Crema, K. Edinborough, T. Kerig, K. Manning, M. G. Thomas, and S. Shennan. 2014. Reconstructing regional population fluctuations in the European Neolithic using radiocarbon dates: a new case-study using an improved method. Journal of Archaeological Science 52:549–557.

Topographisch Bureau, Batavia. 1989, 1941. Blad IX Soekadana.

Tovar, C., E. Breman, T. Brncic, D. J. Harris, R. Bailey, and K. J. Willis. 2014. Influence of 1100 years of burning on the central African rainforest. Ecography:1139–1148.

Trumbore, S. E. 1993. Comparison of carbon dynamics in tropical and temperate soils using radiocarbon measurements. Global Biogeochemical Cycles 7:275–290.

Trumbore, S. E., and S. Zheng. 2006. Comparison of fractionation methods for soil organic matter 14C analysis. Radiocarbon 38:219–229.

Tsing, A. L. 1993. In the Realm of the Diamond Queen: Marginality in an Out-of-the-Way Place. Princeton University Press, Princeton, New Jersey.

Turcios, M. M., M. M. A. Jaramillo, J. F. do Vale, P. M. Fearnside, and R. I. Barbosa. 2016. Soil charcoal as long-term pyrogenic carbon storage in Amazonian seasonal forests. Global Change Biology 22:190–197.

Van Der Werf, G. R., J. T. Randerson, G. J. Collatz, and L. Giglio. 2003. Carbon emissions from fires in tropical and subtropical ecosystems. Global Change Biology 9:547–562.

Vleminckx, J., J. Morin-Rivat, A. B. Biwolé, K. Daïnou, J.-F. Gillet, J.-L. Doucet, T. Drouet, and O. J. Hardy. 2014. Soil charcoal to assess the impacts of past human disturbances on tropical forests. PLoS ONE 9:e108121.

Wang, X., X. Sun, P. Wang, and K. Stattegger. 2009. Vegetation on the Sunda Shelf, South China Sea, during the Last Glacial Maximum. Palaeogeography, Palaeoclimatology, Palaeoecology 278:88–97.

Webb, C. O., and D. R. Peart. 2000. Habitat associations of trees and seedlings in a Bornean rain forest. Journal of Ecology 88:464–478.

Weninger, B., L. Clare, O. Jöris, R. Jung, and K. Edinborough. 2015. Quantum theory of radiocarbon calibration. World Archaeology 47:543–566.

Whitlock, C., and C. Larsen. 2001. Charcoal as a Fire Proxy. Pages 75–97 *in* J. P. Smol, H. J. B. Birks, W. M. Last, R. S. Bradley, and K. Alverson, editors. Tracking Environmental Change Using Lake Sediments: Terrestrial, Algal, and Siliceous Indicators. Springer Netherlands, Dordrecht.

Wieder, W. R., G. B. Bonan, and S. D. Allison. 2013. Global soil carbon projections are improved by modelling microbial processes. Nature Climate Change 3:909–912.

Wieder, W. R., M. D. Hartman, B. N. Sulman, Y.-P. Wang, C. D. Koven, and G. B. Bonan. 2017. Carbon cycle confidence and uncertainty: Exploring variation among soil biogeochemical models. Global Change Biology 24:1563–1579.

Williams, A. N. 2012. The use of summed radiocarbon probability distributions in archaeology: a review of methods. Journal of Archaeological Science 39:578–589.

Wilson, R. 1994. A Cargo of Spice, or Exploring Borneo. Radcliffe Press, London, United Kingdom.

Wondzell, S. M., and J. G. King. 2003. Postfire erosional processes in the Pacific Northwest and Rocky Mountain regions. Forest Ecology and Management 178:75–87.

Wooster, M. J., G. L. W. Perry, and A. Zoumas. 2012. Fire, drought and El Niño relationships on Borneo (Southeast Asia) in the pre-MODIS era (1980–2000). Biogeosciences 9:317–340.

Wündsch, M., S. Biagioni, H. Behling, B. Reinwarth, S. Franz, P. Bierbaß, G. Daut, R. Mäusbacher, and T. Haberzettl. 2014. ENSO and monsoon variability during the past 1.5 kyr as reflected in sediments from Lake Kalimpaa, Central Sulawesi (Indonesia). The Holocene 24:1743–1756.

Zimmerman, A. R., and S. Mitra. 2017. Trial by fire: On the terminology and methods used in pyrogenic organic carbon research. Frontiers in Earth Science 5:95.